

Effect of Aspirin and Salicylic acid on LPA
induced differentiation of P19 stem cells
into cardiomyocytes

KEVIN GEORGE FARIA

SUBMITTED TO THE UNIVERSITY OF HERTFORDSHIRE IN PARTIAL
FULFILMENT OF THE REQUIREMENTS FOR THE DEGREE OF MSC
BY RESEARCH

FEBRUARY 2019

Abstract

The use of stem cell-based therapy in conjunction with existing medical interventions, to target complications caused by coronary artery disease (CAD) is not fully examined. In parallel, the role of lysophosphatidic acid (LPA); an important endogenous bioactive phospholipid, has shown cardioprotective characteristics at low physiological concentrations, providing a potential for future treatment plans. In addition, studies have indicated the promise of aspirin (ASA)/ salicylic acid (SA) or LPA to induce and promote cardiac differentiation of SCs in various models. Therefore, in this project, we investigated the effects of ASA/SA in the presence or absence of LPA to induce the differentiation of the murine P19 teratocarcinoma stem cell line into cardiomyocytes.

Routine cell culture was undertaken using P19 stem cells cultured in complete α -minimal essential medium (α -MEM). In the first instance, the protocol was optimised to ensure that efficient and reproducible differentiation was achieved. Embryoid bodies (EB) were formed by seeding cells and left to aggregate over a period of 2 days in ultra-low attachment 96-well plates, to establish differentiation. P19 stem cells were pre-incubated for 1 hour with ASA and SA at varying concentrations (0.1mM, 0.3mM, 1mM and 3mM) and selective NF κ B inhibitor (0.1nM CAY10470) were pre-incubated 1 hour prior to adding LPA (5 μ M). Control cells were cultured in complete α -MEM alone. 6-8 EBs were isolated and seeded into 12-well tissue culture plates and cultured for 6 days. Western blotting was used to confirm differentiation, examining for the expression of ventricular myosin light chain (MLC-1v), relative to β -actin. To determine the potential mechanism through which differentiation may be induced, changes in phosphorylation of activated NF κ B and I κ B were determined.

Optimisation of the differentiation protocol revealed that 1×10^4 cells grown for 2 days, produced consistent EBs sizes which ranged between 350-450 μ m in diameter. These EBs efficiently differentiated into cardiomyocytes. Differentiation was consistently achieved using LPA (5 μ M) and at selected concentrations of ASA (0.3 -

1mM, at day 3) and SA (1mM, at day 3). Maximal expression of MLC-1v in ASA/SA conditions was seen at 1mM. However, LPA induced differentiation was inhibited by both in combination treatment with ASA and SA, despite both inducing differentiation independently. Analysis of phosphorylated and native proteins associated with the NFκB complex was successfully detected. These initial studies indicated substantial expression of phospho NFκB in LPA, SA and ASA treated cells and increases were seen at the 6-9-hour time points. The expression of phospho IκB in LPA treated cells peaked at 10-15 mins, while ASA/SA treated cells showed phospho IκB peaking at a later time point (3 hours).

In conclusion, the experiments conducted in this thesis have shown that both ASA/SA and LPA induced cardiomyocyte differentiation. However, when ASA or SA are used in combination with LPA, an antagonistic effect is seen, preventing LPA to induce differentiation.

Acknowledgements

First and foremost, I would like to thank God Almighty for giving me the strength, knowledge, ability and opportunity to undertake this research study and to persevere and complete it satisfactorily. Without his blessings, this achievement would not have been possible.

I would like to dedicate this thesis to my parents for their continuous support, motivation and belief throughout the duration of this research and my life. The research conducted in this thesis would not have been possible to accomplish without the guidance and support shown by many individuals. I would like to thank my principal supervisor **Professor Anwar Baydoun** for giving me the opportunity to undertake this research and for his help support and guidance with the issues I had to overcome. I extend my thanks also to my second supervisor **Dr Shori Thakur** for all the help and support given through the course of this degree. I would like to show my gratitude towards members of the supervisory team **Dr Nidhin Raj** and **Dr Jessal Patel**, for their continued advice and daily support. Furthermore, I would like to extend my appreciation towards all the technicians in the Life Science Department; my colleagues and friends **Komal Patel**, **Yugal Kalaskar**, **Abdul-Azim Hassan** and **Rakhi Marwaha**.

Furthermore, I also would like to thank the University of Hertfordshire, for providing the opportunity to conduct my studies and providing the resources to complete my thesis.

Contents

<u>ABSTRACT</u>	<u>1</u>
<u>ACKNOWLEDGEMENTS</u>	<u>3</u>
<u>LIST OF FIGURES</u>	<u>7</u>
<u>LIST OF TABLES</u>	<u>9</u>
<u>LIST OF ABBREVIATIONS</u>	<u>10</u>
<u>1. INTRODUCTION</u>	<u>13</u>
1.1 Coronary artery disease	14
1.1.1 Pathophysiology of atherosclerosis	14
1.1.2 Myocardial Infarction	15
1.1.3 Current treatments of coronary artery disease	16
1.2 Stem cells for heart diseases	19
1.2.1 Stem cells	21
1.2.2 Clinically relevant inducers of stem cell differentiation	23
1.3 Lysophosphatidic acid (LPA):	24
1.3.1 LPA Synthesis	25
1.3.2 LPA Receptors	25
1.3.3 Role of LPA in the vascular system	28
1.4 Signal Transduction	29
1.4.1 Transcription Factors	29
1.4.2 Nuclear factor-kappa B	31
1.5 Aspirin in stem cell therapy	33
1.5.1 Cellular mechanism of action of aspirin	34
1.6 Aims of the project:	36
<u>2. MATERIALS AND METHODS</u>	<u>37</u>
2.1 Cell Culture	38
2.1.1 Resuscitation of P19 stem cells	38
2.1.2 Culture and maintenance of P19 stem cell	38
2.1.3 Cryopreservation of P19 Stem cells	39
2.2 Antibodies and Reagents	39

2.3	Determination of drug concentrations.....	39
2.4	Differentiation and Embryoid Body formation of P19 stem cells.....	40
2.4.1	Lysophosphatidic acid stock preparation	40
2.4.2	Cell counting and plating for EB formation	40
2.4.3	Differentiation of P19 stem cells into cardiomyocytes	41
2.5	Protein determination and quantification	42
2.5.1	Cell lysate generation for MLC-1v protein expression	42
2.5.2	Cell lysate generation for phosphorylated protein expression	43
2.5.3	Protein quantification using bicinchoninic acid (BCA) assay	43
2.6	Protein analysis using western blotting and SDS-PAGE	45
2.6.1	Sodium dodecyl sulphate-polyacrylamide gel electrophoresis (SDS-PAGE)	45
2.6.2	Western Blotting	46
2.7	Cell Viability Assay	49
2.7.1	MTT (3-(4, 5-dimethyl thiazolyl-2)-2, 5-diphenyltetrazolium bromide) assay	49
2.8	Statistical analysis	51
3.	<u>RESULTS</u>.....	<u>52</u>
3.1	Development and characterization of P19 stem cell differentiation model	53
3.2	Establishing embryoid bodies from monolayers of P19 cells	57
3.2.1	Establishing embryoid bodies using Petri dish cell suspension	57
3.2.2	Embryoid body differentiation into cardiomyocytes	59
3.2.3	Establishing embryoid bodies using low-attachment 96 well-plate cell suspension	60
3.2.4	Effects of SA and ASA on EB formation in Petri dishes and ultra-low attachment	
	96-well plates in the presence and absence of LPA.	65
3.3	Examining the effect of LPA on MLC-1v expression.	68
3.3.1	Effect of SA on MLC-1v expression in the presence and absence of LPA.	69
3.3.2	Effect of ASA on MLC-1v expression in the presence and absence of LPA.	71
3.4	Cell viability assay	73
3.4.1	MTT assay determining the toxicity of SA	73
3.4.2	MTT assay determining the toxicity of ASA	77
3.5	Effect of LPA, SA and ASA on p65-NFκB expression.	81

3.5.1	Effect of LPA, SA and ASA on phospho NFκB expression.	85
3.5.2	Effect of LPA, SA and ASA on IκB expression.	89
3.5.3	Effect of LPA, SA and ASA on phospho IκB expression.....	93
3.5.4	Effect of CAY10470 on LPA-induced MLC-1v expression.	97
4.	<u>DISCUSSION</u>	<u>99</u>
5.	<u>CONCLUSION</u>	<u>111</u>
6.	<u>FUTURE WORKS</u>	<u>113</u>
7.	<u>REFERENCES</u>	<u>115</u>

List of Figures

Figure 1.1. Stem cell potency	22
Figure 1.2: Overview of LPAR expression.	28
Figure 1.3: Canonical and alternative NFκB pathways.....	33
Figure 1.4: Biosynthesis of prostaglandins and thromboxane enzyme cascade.....	35
Figure 2.1: Differentiation of P19 stem cells into cardiomyocytes	42
Figure 2.2. BCA protein standard curve.	45
Figure 2.3. Cell number standard curve for MTT assay.	50
Figure 3.1: Growth pattern of P19 stem cells at different confluency	54
Figure 3.2: Morphology of P19 stem cells in culture.	55
Figure 3.3: Morphology of confluent P19 stem cell monolayer.....	56
Figure 3.4: Morphology of EB in Petri dish culture, grown over 4 days.	58
Figure 3.5: Growth of cells from EBs in culture	59
Figure 3.6: Determination of optimum EB size and growth period in 96 well-plates.	61
Figure 3.7: Comparison of EB morphology during growth in Petri dish and 96 well plates.....	62
Figure 3.8: Beating cardiomyocyte generated from EBs grown in Petri dish and 96 well plates.....	64
Figure 3.9: Effects of SA and ASA on EB formation and growth in Petri dishes.....	66
Figure 3.10: Diameter study on EB's treated with SA and ASA, grown in 96 well plates.	67
Figure 3.11: LPA concentration-dependent induction of MLC-1v expression.	68
Figure 3.12: Effect of SA on differentiation of P19 SCs.	70
Figure 3.13: Effect of ASA on differentiation of P19 SCs.....	72
Figure 3.14: Effect of SA on cell viability in the absence and presence of LPA (day 3).	74
Figure 3.15: Effect of SA on cell viability in the absence and presence of LPA (day 6).	76
Figure 3.16: Effect of ASA on cell viability in the absence and presence of LPA (day 3).	78
Figure 3.17: Effect of ASA on cell viability in the absence and presence of LPA (day 6).	80

Figure 3.18: Densitometric data for total p65-NFκB protein expression.....	82
Figure 3.19: Control p65-NFκB densitometric data compared with LPA, SA and ASA p65-NFκB.	83
Figure 3.20: LPA p65-NFκB densitometric data compared with SA and ASA p65-NFκB.	84
Figure 3.21: Densitometric data for total phospho NFκB protein expression.	86
Figure 3.22: Control phospho NFκB densitometric data compared with LPA, SA and ASA phospho NFκB.	87
Figure 3.23: Phospho NFκB expression in LPA treated cells compared to SA or ASA treated cells.....	88
Figure 3.24: Densitometric data for total IκB protein expression.	90
Figure 3.25: Control IκB densitometric data compared with LPA, SA and ASA IκB.....	91
Figure 3.26: IκB expression in LPA treated cells compared to SA or ASA treated cells.	92
Figure 3.27: Densitometric data for total phospho IκB protein expression.	94
Figure 3.28: Control phospho IκB densitometric data compared with LPA, SA and ASA phospho IκB.....	95
Figure 3.29: Phospho IκB expression in LPA treated cells compared to SA or ASA treated cells.	96
Figure 3.30: Concentration-dependent effects of CAY10470 on MLC-1V expression in LPA activated P19 SCs.....	97
Figure 3.31: Effect of CAY10470 on P19 SC viability.	98

List of Tables

Table 1-1. Transcription factors mediating cardiac hypertrophy. Adapted from (Kohli <i>et al.</i> , 2011)	30
Table 2-1: Cell seeding calculations for EB formation.....	41
Table 2-2: RadiolmmunoPrecipitation Assay (RIPA) Buffer- 200mL.....	43
Table 2-3. Preparation of diluted BSA standards.....	44
Table 2-4. 96-well plate layout for preparation for BCA.....	44
Table 2-5. Gel recipe for SDS-PAGE (4 Gels)	47
Table 2-6. Recipe for 2x Sample Buffer (10 mL)	48
Table 2-7. Recipe for 10x Tank Buffer (2 Litres).....	48
Table 2-8. Recipe for 10x Transfer Buffer (2 Litres)	48
Table 2-9. Recipe for 10x TBS (Wash Buffer) (1 Litre).....	49
Table 2-10. Recipe for blocking buffer	49
Table 2-11. Preparation of diluted cell densities	51

List of Abbreviations

α-MEM	Alpha minimum essential medium
ASA	Aspirin/acetylsalicylic acid
ASC	Adult stem cells
ATL	Aspirin-triggered lipoxin
ATX	Autotaxin
BCA	Bicinchoninic acid
bFGF	Basic fibroblast growth factor
BMSC	Bone marrow mesenchymal stem cells
CAD	Coronary artery disease
CAM	Chorioallantoic membrane
cAMP	Cyclic adenosine monophosphate
CBSC	Cortical bone stem cells
CD40	Cluster of differentiation 40
C_{max}	Maximum (or peak) serum concentration
COX1	Cyclooxygenase 1
DDW	Double distilled water
DMSO	Dimethyl sulfoxide
EB	Embryoid body
EC	Embryonic carcinoma
EDCs	Explant-derived cells
EDG	Endothelial Differentiation Gene
EGF	Epidermal growth factor
ERK	Extracellular signal-regulated kinase
ESCs	Embryonic stem cells
FGF	Fibroblast growth factor
GPAT	Glycerophosphate acyltransferase
GPCRs	G protein-coupled receptors
hASC	Human adipose-derived stem cells
HB-EGF	Heparin-binding EGF-like growth factor

HD	Heart disease
hESC	Human embryonic stem cell
hESC-CMs	hESC-derived cardiomyocytes
HGF	Hepatocyte growth factor
HMG-CoA	3-Hydroxy-3-methylglutaryl-coenzyme A
ICAM-1	Intercellular adhesion molecule 1
IGF-1	Insulin-like growth factor 1
IκB-α	Inhibitor of kappa B-alpha
IκB-β	Inhibitor of kappa B-beta
iPSCs	Induced pluripotent stem cells
LDH	Lactate dehydrogenase
LDL	Low-density lipoprotein
LPA	Lysophosphatidic acid
LPAR1	Cognate high-affinity receptor of LPA
LPC	Lysophosphatidylcholine
LTBR	Lymphotoxin beta receptor
LV	Left ventricular
LVEF	Left ventricular ejection fraction
MAPK	Mitogen-activated protein kinase
mECSC	Murine embryonic carcinoma stem cells
mESC	Murine embryonic stem cells
MI	Myocardial infarction
MSCs	Mesenchymal stem cells
MTT	3-(4, 5-dimethylthiazolyl-2)-2, 5-diphenyltetrazolium bromide
NFκB	Nuclear factor kappa B
NSAIDs	Nonsteroidal anti-inflammatory drugs
OxLDL	Oxidised LDL
PA	Phosphatidic acid
PBS	Phosphate buffered saline
PCI	Percutaneous coronary intervention
PDGF-A-B	Platelet-derived growth factor

PDLSCs	Periodontal ligament stem cells
PG	Prostaglandins
PKC	Phosphoinositide 3-kinase
PSCs	Pluripotent stem cells
PVDF	Polyvinylidene difluoride
RCF	Relative centrifugal force
RIPA	Radioimmunoprecipitation assay
ROCK	Rho-associated protein kinase
S.E.M.	Standard error mean
SA	Salicylic acid
SC	Stem cell
SDS-PAGE	Sodium dodecyl sulfate polyacrylamide gel electrophoresis
TF	Transcription factor
TX	Thromboxane
TXA₂	Thromboxane A ₂
VCAM-1	Vascular cell adhesion protein
VEGF	Vascular endothelial growth factor
VSMC	Vascular smooth muscle cell

1. Introduction

1.1 Coronary artery disease

Coronary artery disease (CAD) is reported to cause over 17.3 million deaths worldwide, accounting for 31.5% of all deaths (Townsend *et al.*, 2016). Atherosclerosis is caused by the build-up of fatty deposits within the coronary arterial walls and over time, can lead to the narrowing of arterial walls causing restricted blood flow to the heart; this results in angina, arrhythmia, myocardial infarction (MI), and other cardiovascular events (Leon & Maddox, 2015). Atherosclerosis may also enhance the expression of other supplementary mediators such as adipokines, adhesion molecules, selectins and inflammatory markers present at the site of the lesion (Hochrainer *et al.*, 2013). Risk factors for CAD (or atherosclerosis) include age, sex, cigarette smoke, family history of CAD, hypertension, hypercholesterolemia, diabetes, obesity, physical inactivity and may also be linked to the accretion of fibrinogen, lipoproteins and triglycerides levels (Assmann *et al.*, 1999).

1.1.1 Pathophysiology of atherosclerosis

Atherosclerosis is an underlying pathology associated with CAD; defined as an inflammatory-fibroproliferative response to multiple forms of endothelial injury and chronic inflammatory stimulus, ultimately leading to stenosis and thrombosis within the major conduit arteries. Atherosclerosis is a progressive development, as continued morphological changes within the arterial wall lesions, results in the accumulation of cholesterol-rich lipids and inflammatory cytokines. The initiation of atherosclerosis occurs upon damage caused to the endothelium by various factors including high blood pressure, viruses, cigarette toxins, resulting in high concentrations of plasma cholesterol, more specifically low-density lipoprotein (LDL) entering the arterial intima from the blood, which accumulates within the arterial wall. Once in the vessel wall, LDL particles undergo chemical modification resulting in oxidised LDL (OxLDL), which can induce pro-atherogenic genes such as intercellular adhesion molecule 1 (ICAM-1), vascular cell adhesion protein (VCAM-1), heparin-binding EGF-like growth factor (HB-EGF) and platelet-derived growth factor (PDGF-A–B) (L.-F. Chen & Greene, 2004).

Inflammation is initiated when chemoattractant and chemokines are expressed by activated intimal smooth muscle cells and activated endothelial cells that secrete adhesion molecules, consequently enrolling circulating neutrophils, monocytes, lymphocytes and mast cells within the intimal layer. Once in the intimal layer, monocytes differentiate into macrophages which express scavenger receptors that bind to oxidised LDL (Takase *et al.*, 2013). Macrophages laden with engulfed oxidised LDL become foam cells and are the first early signs of atherosclerosis which appears as yellow fatty streaks. In addition, plaque formation is associated with the increasing accumulation of extracellular lipids that coalesces into pools, forming lipid-rich necrotic cores in the intimal layer. As a result, fibrous tissues are formed over these lipid-rich necrotic cores, encasing them under the endothelium producing a fibrous cap (Takase *et al.*, 2013). The resulting thrombus formation associated with the pathophysiology of atherosclerosis leads to life-threatening complications such as myocardial infarction (MI).

1.1.2 Myocardial Infarction

Myocardial ischaemia arises from blockage of the coronary artery, resulting from either lipid deposition in the coronary arteries or from a blood clot that is formed in response to atherosclerotic plaque. The formation of atheroma causes occlusion of blood vessels, consequently hardening and narrowing the coronary artery. Subsequently, the reduction in oxygen supply to the surrounding heart muscles leads to myocardial infarction, which in turn give rise to various necrosis and pathological characteristics such as myocyte necrosis, coagulation necrosis, contraction band necrosis and specific areas expressing myocytolysis are also denoted. Furthermore, myocardial infarction is distinguished into type 1 (spontaneous myocardial infarction) and type 2 (myocardial infarction secondary to ischaemic imbalance). Type 1 myocardial infarction associated with events resulting from atherothrombosis, ulceration, plaque rupture, fissuring and erosion, leading to coronary thrombus formation in one or more of the coronary arteries. Type 2 myocardial infarction occurs

as a result of inadequate myocardial oxygen supply and demand associated by factors other than CAD such as arrhythmia, severe anaemia, respiratory failure, bradycardia, and hypotension (Kohli *et al.*, 2011). Therefore, the severity of myocardial infarction has led to a broad range of pharmacological interventions being adopted for clinical use as mentioned below.

1.1.3 Current treatments of coronary artery disease

Contemporary treatment for CAD uses approaches to reduce the risk of adverse cardiovascular events, improve and recover the functional capacity of the myocardium and re-establish normal working blood flow throughout the coronary arteries (X. Chen *et al.*, 2003; Martinez-Agosto *et al.*, 2007). One of the first course of action for acute MI consist of undertaking the detection of the blockage, to plan the next course of treatments. To accommodate these test X-rays, electrocardiogram and coronary angiography would be conducted. Consequently, the first line of treatments consists of administering patients under appropriate medications such as anticoagulant, antiplatelet and thrombolytic agents, etc. In addition to these treatments, percutaneous coronary intervention (PCI) procedures are followed, such as angioplasty, in which a balloon-tipped catheter is inserted at the target location (plaque formed area) and pushed against the endothelial wall, thus initiating an increase in blood flow by widening the blood vessel walls. Furthermore, coronary stenting often accompanies angioplasty, in which a small wire-mesh tube structure is inserted into the narrowed/damaged blood vessel, providing a scaffold that increases structural integrity and diameter (Michaels & Chatterjee, 2002). In severe cases, coronary artery bypass surgery is considered, whereby the surgery involves re-establishing blood flow to the heart by bypassing the occluded or narrowed coronary artery using grafted blood vessel.

In prolonged cases of oxygen deprivation to the cardiac muscles, resulting from severe myocardial infarction (MI), the cardiac tissues undergo necrosis and subsequently, heart failure develops. In such cases, heart transplantations are undertaken and may

be the only effective choice of treatment. However, this method of treatment is hurdled by several challenges, examples of these include transplant rejection of the donor's heart, due to the host's immune system targeting foreign tissue. This can result in stem cell (SC) graft failure and may increase infection susceptibility, as the medications are taken post-transplant weakening the patient's immune system, leaving them vulnerable to infections (Cha *et al.*, 2015). Furthermore, the combination of these treatments associated with heart transplant does not guarantee success or indeed survival of the patient. Consequently, the combination of these factors calls for an alternative and effective form of therapy.

Physiologically, a small degree of innate regenerative capacity (pre-existing vessels and vascular progenitor cells contributing to angiogenesis) and cardioproliferative effects of the heart are seen following MI and ischaemic injury (Bertero & Murry, 2018). However, the limited rate of regeneration is not sufficient for functional restoration. Furthermore, the inability of the heart to functionally repair itself results in its limited capacity to function adequately. This is further hampered by the lack of treatment to target the loss of cardiomyocytes resulting from MI. Cardiac tissue regeneration using stem cells has however been the focus over the past decade. The success of using stem cells clinically has also shown limited progress. This is due to several barriers that are yet to be overcome and include cell death due to the hostile microenvironment presented as a direct result of MI. The hypoxic condition presented by restricted blood flow to the affected areas and acidosis caused by the increase in pH due to the increase in carbon dioxide content, all contribute to cell death (Zhao *et al.*, 2016). Conclusively, regeneration of patient's cardiac tissue could negate the underlying issues listed previously, for example, such as the lack of survivability seen in grafted SCs. One way forward is the use of stem cell therapy, as there has been extensive research in this field in recent years. One such example is fusing rat cardiomyocytes and human stem cells obtained from adipose tissue, that were capable of beating and replacing damaged heart tissue following MI (Metzele *et al.*, 2011) and the transplantation of cardiac muscle cells derived from human embryonic

stem cells, into primate monkey cardiac muscle, showing 40% repair in cardiac muscle damage (Chong *et al.*, 2014).

Although these studies initially provided a promising innovation in using stem cells therapy for cardiac treatment, it is still considered a highly controversial area. Over 31 scientific papers have been redacted in the field of cardiac cell therapy (recently *Circulation Research and Circulation*, have listed 13 redactions); independent evidence has disproved claims that c-kit⁺ cell is a cardiac muscle progenitor (Sultana *et al.*, 2015); studies have shown a lack of rigour and positive bias, reporting a significant amount of technical errors within their research (Nowbar *et al.*, 2014). In conclusion, the translational relevance of stem cell therapy to the clinical application could lie anywhere from 5-25 years and to overcome the previously mentioned issues, rigorous studies should be carried out, fully recognising the multiple challenges and complexities of cardiac cell therapy (Chien *et al.*, 2019).

Subsequently, the use of prophylactic treatments has been undertaken in regulating the progression of MI and further maintaining the symptoms imposed by CAD. One of the pharmacological agents used for this is aspirin, an antiplatelet agent that targets the generation of thromboxane A₂ (TXA₂), by irreversibly inhibiting the function of platelet cyclooxygenase (COX1) pathway. As a result, platelet activation and aggregation are prevented due to the inability of TXA₂ to form (Schrör, 2016). In addition, fibrinolytic drugs such as reteplase and streptokinase that target the stimulation of plasminogen, resulting in fibrin disintegration are yet another example of pharmacological interventions prescribed for patients with CAD. Lipid-lowering drugs such as atorvastatin, fluvastatin, and lovastatin are also used to control hypercholesterolemia by reducing the levels of circulating LDL levels. Their mechanism of action includes targeting the rate-limiting step in cholesterol synthesis by competitively inhibiting the enzyme 3-Hydroxy-3-methylglutaryl-coenzyme A (HMG-CoA) reductase, resulting in the increase of LDL receptors expression, leading to the increase of LDL reuptake (Willey *et al.*, 2006). In conclusion, the pharmacological

interventions described above govern the regulation of heart disease (HD) symptoms and prevent further progression of risks and consequences associated HD.

1.2 Stem cells for heart diseases

Recently, studies have examined the use of cortical bone stem cells (CBSCs), isolated from Gottingen minipig or transgenic C57/BL6 mice, in improving cardiac function after MI. The data suggested an increase in cardiac lineage commitment, increased proliferation and migration of the transplanted stem cells that produce functional gap junctions (connexin 43) between the transplanted and pre-existing cells. As a result, CBSCs have the potential to enhance protective effects after cardiac injury (Mohsin *et al.*, 2015). Stem cell injection delivery studies have also been conducted on human patients, demonstrating the potential for stem cell in improving damaged cardiac structures and function. Mesenchymal stem cells (MSCs) have been proposed to improve left ventricular (LV) structure by enhancing left ventricular ejection fraction (LVEF). To test this hypothesis, patients were injected with autologous MSCs into akinetic/hypokinetic myocardial territories. The results implicated there was comprehensive restitution of regional function that could contribute to successful cell-based therapy (Karantalis *et al.*, 2014).

From these previous studies, research undertaking the potential use of human embryonic stem cell (hESC)-derived cardiomyocytes (hESC-CMs) were conducted, which examined the generation of highly vascularised cardiac tissues *in vitro*, to improve the survivability of transplanted myocytes. The results demonstrated cardiac-specific tissues with functional properties could be achieved by generating highly vascularized human engineered cardiac tissue, thereby establishing an increase in functional cardiac benefit and graft survival (Caspi *et al.*, 2007). Furthermore, the use of autologous human cells, such as human adipose-derived stem cells (hASC) has been proposed to be a potential source for stem cell-based therapy. This was investigated through the trans-differentiation of the human adult stem cells mentioned above, by

exposing these cells to human atrial extracts. In conclusion, the reprogramming of adult stem cells could be used in treating cardiac diseases (Perán *et al.*, 2010).

To address pre-existing concerns associated with SC therapy, a study conducted by Zhao *et al* aimed to implant pre-differentiated pluripotent stem cells (PSCs) into the early cardiac stage, as the rate of survivability was significantly lower when using mature cardiomyocytes. The native chemical, mechanical and electrical cues pre-existing within the heart, would provide a foundation to ensure the prolonged survival of pre-differentiated cardiac cells into a mature cardiomyocyte. Furthermore, this theory was supported by the bioengineering of an injectable encapsulated aggregates of PSC (Zhao *et al.*, 2016). Firstly, a semi-permeable alginate hydrogel was constructed using co-axial electrospray to mimic the pre-hatching embryo physical configuration. This was subsequently used to micro-encapsulate murine embryonic stem cells (mESC) within the permissive liquid core of hydrogel, leading to the formation of one single aggregate of mESC's. These were then pre-differentiated into early cardiomyocytes inside the microcapsules. Using sodium citrate as an isotonic solution, the encasing microcapsule was dissolved to release the pre-differentiated aggregates. Finally, mESC aggregates were re-encapsulated within a micromatrix, preparing them for implantation in the desired location (Zhao *et al.*, 2016).

Alternatively, research has examined the use of paracrine mediators to ensure the improvement of post-ischaemic cardiac function and stem cell-mediated cardiac repair (Jackson *et al.*, 2015). A key cardioprotective cytokine; insulin-like growth factor 1 (IGF-1) activates pro-survival of cardiac function via the protein kinase B and extracellular signal-regulated kinase/ mitogen-activated protein kinase (ERK/MAPK) pathways. The overexpression of IGF-1 was achieved using a third-generation lentiviral vector system to facilitate the integration of the transfer plasmid sequences into the host genome. The results of this study showed an enhancement in paracrine signals by the transplanted explant-derived cells (EDCs), resulting in the recruitment of

progenitor cells, increase in survival and of the generation of new cardiomyocytes and salvage of the reversibly damaged tissue (Jackson *et al.*, 2015).

1.2.1 Stem cells

Stem cells are unspecialized cells with the ability to present themselves in asymmetric divisions, existing in a mitotically quiescent form that employ the capacity to extensively self-renew; generating daughter cells identical to their parent cell and leading to the production of a progeny with more restricted potential of multiple cell lineages through these self-renewing capabilities, known as differentiation (Lanza, 2006; Vartiainen *et al.*, 2003). The multitude of characteristics expressed by stem cells enables them to govern the development and the regeneration of tissues within the body lost through normal wear and tear, injury, or diseases (Eroles *et al.*, 2014).

1.2.1.1 Stem cell Potency

Potency is referred by the ability of stem cells to differentiate into specialized cell types, with the capacity to form any mature cell type. Furthermore, these differentiation potentials are categorised as totipotent, pluripotent, multipotent, oligopotent and unipotent. Totipotent SCs are derived from the first few divisions of fertilised eggs (zygote), these cells have the potential to differentiate into embryonic, extraembryonic cell types and give rise to primitive-germ-line, somatic stem/progenitor SCs. Pluripotent SCs, are obtained from the inner cell mass of blastocysts and are descendants of totipotent SCs. These cells have the ability to differentiate into nearly all cells and tissues, e.g. germ layer derived cells (endoderm, ectoderm and the mesoderm) (De Luna-Bertos *et al.*, 2012; Evans & Kaufman, 1981). In contrast, multipotent SCs have the ability to differentiate into a number of limited forms of cell types; those closely related to the tissues they reside in. Examples of such SCs are adult haematopoietic stem cells, which give rise to multiple blood cell lineages. In contrast, oligopotent SCs can give rise to a few but specific lineage of cells seen in Figure 1.1. Examples include myeloid and lymphoid SCs. Finally, unipotent being the

latter in SC potency have the potential to differentiate along into only one lineage, with the ability to renew (Lanza, 2006).

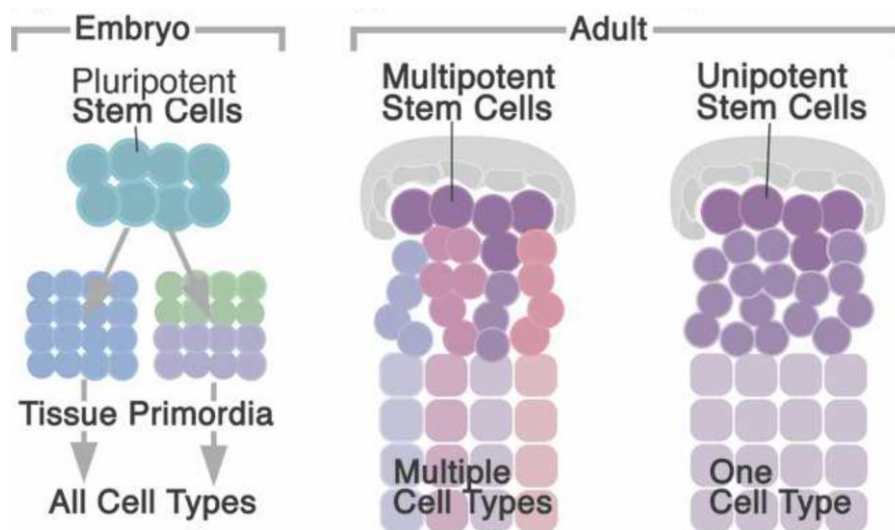


Figure 1.1. Stem cell potency

EC cells of mammalian embryos are pluripotent, giving rise to all types of cells. Whereas, multipotent adult stem cells can give rise to multiple different lineages and unipotent adult stem cells produce a single cell type (Martinez-Agosto *et al.*, 2007).

1.2.1.2 Adult Stem cells

Adult stem cells (ASC) can be found in differentiated tissue and have the ability to renew the specific cell type of that tissue. Examples of such sources of tissue include skeletal muscle, dental pulp, bone marrow, liver, blood, eye, skin and brain (Eaves, 2002). In addition, SC from the mesodermal tissue, including bone marrow, have shown to give rise to the three major types of ectodermal derivative brain cells (Mezey *et al.*, 2000). A limited number of cell lineages present themselves as multipotent or oligopotent. However, some ASCs are only able to differentiate into a singular cell line, thereby they are categorized as monopotent SCs (Gudjonsson & Magnusson, 2005).

1.2.1.3 Embryonic Stem cells

Embryonic stem cells (ESCs) are derived from an early-stage embryo originating from a zygote; initiated through the fertilization of an ovum by a sperm, leading to the

systematic formulation of a morula and resulting in a specialized spherical formation known as a blastocyst. The blastocyst consists of an outer layer (trophoblast) and a cluster of cellular mass known as the inner cell mass. The inner cell mass ability to give rise to the majority of the germline (ectoderm, mesoderm, and endoderm) (Eaves, 2002). Moreover, a singular ESC could potentially differentiate into 200 cell lineages leading to tissue and organ formations. Thereby, ESC presents themselves as totipotent, due to their differentiating capacity. These characteristics portrayed above enable ESC to be used as homogeneous stem cell cultures without an apparent limit (Marshak *et al.*, 2008). Embryonic carcinoma (EC) cell lines were the first pluripotent cell lines to be established from human germ cell tumours. They have the ability to differentiate into derivatives of all three embryonic germ layers; endoderm, ectoderm and mesoderm (Yu & Thomson, 2008).

1.2.1.4 Induced Pluripotent Stem Cells

A novel approach to achieving pluripotent stem cell line characteristics was developed by Yamanaka and colleagues (Takahashi & Yamanaka, 2006), generating from normal adult mouse somatic cells (skin fibroblasts) and later in human somatic cells. Consequently, these cells were termed as induced pluripotent stem cells (iPSCs). These somatic cells were reprogrammed, presenting pluripotent characteristics through overexpression of four transcription factors: c-Myc; Oct4; Klf4; and Sox2 (Takahashi & Yamanaka, 2006). The reprogrammed cells displayed many features of embryonic stem cells such as teratoma formations, morphology, proliferation and functions. Using this technique, the sacrifice of embryos was negated, enabling patient-specific pluripotent stem cell lines to be obtained and programmed for therapeutic applications of stem cells (Mummery *et al.*, 2011).

1.2.2 Clinically relevant inducers of stem cell differentiation

The use of extrinsic factors mediating SC differentiation into cardiomyocytes has proven to be successful in this field of research, however, the implication of these mediators in clinical applications and relevance are yet to be represented successfully.

Although experimental studies previously undertaken have used organic solvents such as dimethyl sulfoxide (DMSO), and growth factors such as epidermal growth factor (EGF), fibroblast growth factor (FGF), hepatocyte growth factor (HGF), drug-related chemicals (cyclosporine, and 5-azacytidine) and active vitamin derivatives (retinoic acid), these regulators create challenges for clinical use and most are not readily expressed endogenously (Metzele *et al.*, 2011). Consequently, the use of a more sustainable endogenous molecule was considered for this research. One such molecule is lysophosphatidic acid (LPA), an independent predictor of peripheral arterial disease and atherosclerotic cardiovascular disease. Lysophosphatidic acid is an endogenous bioactive phospholipid that is elevated in plasma concentrations and produced by various stress-inducing stimuli (Orsó & Schmitz, 2017). Lysophosphatidic acid may, therefore, be an ideal candidate and may show promising clinical relevance in cardiac regeneration. The interactions of these inducers initiating cellular differentiation are further understood when examining the signal transduction mechanism and their interactions with these molecules.

1.3 Lysophosphatidic acid (LPA):

Lysophosphatidic acid is a ubiquitous glycerophospholipid with a molecular weight of 430-480 Da, found at low concentrations in the blood plasma of many eukaryotic species. Discovered to be an essential extracellular signalling molecule, it activates five known rhodopsin-like G protein-coupled receptors (GPCRs). Lysophosphatidic acid's structure is constituted with a fatty acid chain at the sn-1 (or sn-2), the hydroxyl group at the sn-2 (or sn-1), and a phosphate group at sn-3 (Hopper *et al.*, 1999). Furthermore, LPA has been noted to exist in body fluids as long chains of saturated and the more biologically active unsaturated fatty acids (Xiao *et al.*, 2000). Lysophosphatidic acid has been linked to the control of various cellular functions (cell proliferation, cell migration, cell survival, cell transformation, platelet aggregation and smooth muscle contraction) through the interactions with specific G-protein coupled receptors

(GPCR), associated with endothelial differentiation gene (EDG2, EDG4 and EDG7) families (Pagès *et al.*, 2001)

1.3.1 LPA Synthesis

Lysophosphatidic acid is actively present, both intracellularly and extracellularly and found in various organ systems and tissues. Intracellular LPA, acting as an intermediate for the synthesis of other glycerolipids can be synthesised enzymatically from mitochondria and endoplasmic reticulum (Pagès *et al.*, 2001). In which, membrane-bound glycerophosphate acyltransferase (GPAT) located within the mitochondria, converts phosphatidic acid (PA) into LPA. Whereas, extracellular LPA can also be synthesised enzymatically through the conversion of autotaxin (ATX), resulting in the reduction of lysophosphatidylcholine (LPC) into LPA (Sheng *et al.*, 2015).

1.3.2 LPA Receptors

Lysophosphatidic acid's signalling orchestrates many biological effects, from normal physiological functions and tissue development to tissue repair and vascular remodelling (Lin *et al.*, 2010; Orsó & Schmitz, 2017). The first cognate high-affinity receptor of LPA (LPA₁) was noted in 1996, subsequently leading to the identifications of two additionally related receptors LPA₂ LPA₃ and more notably the recent determination of two more divergent LPA receptors (LPA₄ & LPA₅). These receptors were denoted the distinct genes *LPAR1–LPAR5* in humans and *Lpar1–Lpar5* in mice, the functions of these receptors are further illustrated in Figure 1.2 (Choi *et al.*, 2010).

1.3.2.1 LPA₁:

The mammalian *LPAR1* gene attributed to the LPA₁ high-affinity receptor, encodes for approximately 364 amino acids, putative transmembrane domains (7), resulting in molecular weight of approximately 41-kDa. LPA₁ mediates a variety of cellular response ranging from cell migration, proliferation, survival and cytoskeletal changes to the activation of the Rho pathways, mitogen-activated protein kinase Akt and phospholipase pathways. These biological activities are mediated through Gα_{i/o},

$G\alpha_{12/13}$ and $G\alpha_{11/q}$ G proteins. Additionally, the inhibition of the adenylyl cyclase and modulation of Ca^{2+} were also observed as a cellular response to LPA_1 (Choi *et al.*, 2010).

1.3.2.2 LPA_2 :

The second LPA receptor (LPA_2) is encoded by the *LPAR2* gene, which is similar to *LPAR1* and can be determined, due to the mutual structure of amino acids (60%) and a predicted amino acid residue of 348, thus presenting a molecular mass of 38 kDa. However, *LPAR2* varies spatiotemporally as compared to *LPAR1* for expression patterns. The activation of LPA_2 has denoted behaviours mediating cell survival, cell migration and interactions with adhesion molecules. In contrast, LPA_2 had proven to provide inhibitory actions such as effects on the epidermal growth factor-induced migration mechanisms of cancerous cells and therefore resulting in a potential factor in cancer metastasis. This occurs similar to LPA_1 , through the coupling in heterotrimeric regions of a family of G proteins $G\alpha_{i/o}$, $G\alpha_{11/q}$, and $G\alpha_{12/13}$. These interactions activate complimentary pathways such as the mitogen-activated protein kinase, phosphatidylinositol 3-kinase, Ras, Rho, Rac, diacylglycerol and phospholipase C (Choi *et al.*, 2010).

1.3.2.3 LPA_3 :

The likenesses of these receptors are further seen when examining the structure of *LPAR3* gene encoding for LPA_3 , sharing an approximately 50% of GPCRs expressed in LPA_1 and LPA_2 , substantiating in an overall molecular weight of ~40-kDa. *LPAR3* is able to couple with $G\alpha_{i/o}$ and $G\alpha_q$ G protein receptors, inducing the activation of mitogen-activated protein kinase, phospholipase C activation, Ca^{2+} mobilization and preventing the inhibition of the adenylyl cyclase pathway. However, LPA_3 is unable to couple to $G\alpha_{12/13}$. Furthermore, LPA_3 is distinct in comparison to LPA_1 and LPA_2 's affinity to saturated acyl chains, due to the lack of responsivity, it expresses a high affinity to 2-acyl-LPA containing unsaturated fatty acids (Choi *et al.*, 2010).

1.3.2.4 LPA₄:

LPA₄ is encoded by the *LPAR4* gene and is the fourth receptor gene located on the X chromosome in humans and structurally different from the previously mentioned LPA receptors in the classical structural sense. The structure consists of 1113 base pairs encoding an intronless open reading frame, calculated at a molecular mass of to ~42 kDa. The morphological changes associated with LPA₄ induces neurite retraction, stress fibre formation and cell rounding, as a result of G $\alpha_{12/13}$ and Rho/Rho-kinase pathways activations. Following this, the mobilization of Ca²⁺ through the induction of G $\alpha_{q/11}$ and G α_s mediated signalling, resulting in intracellular cyclic adenosine monophosphate (cAMP) accumulation. Additionally, cell adhesion, through the interactions of the N-cadherin-dependent and cell aggregation mediated through Rho-kinase pathways are further expressed (Choi *et al.*, 2010).

1.3.2.5 LPA₅:

Although structurally different to LPA receptors 1-3, LPA₅ belongs to the identical rhodopsin-GPCR family, sharing 35% homology to the other LPA receptors. Encoded by the *LPAR5* gene, LPA₅ has approximately 372 amino acids and with a molecular mass of ~42 kDa. It is widely expressed in a range of embryonic tissues, such as embryonic stem cells, lung, heart, brain, thymus, spleen, stomach, skin, intestine, liver and small intestines. More specifically LPA₅ increases intracellular calcium levels, cAMP levels and inositol phosphate production through the activation of G-proteins G α_q and coupling of G $\alpha_{12/13}$ (Choi *et al.*, 2010).

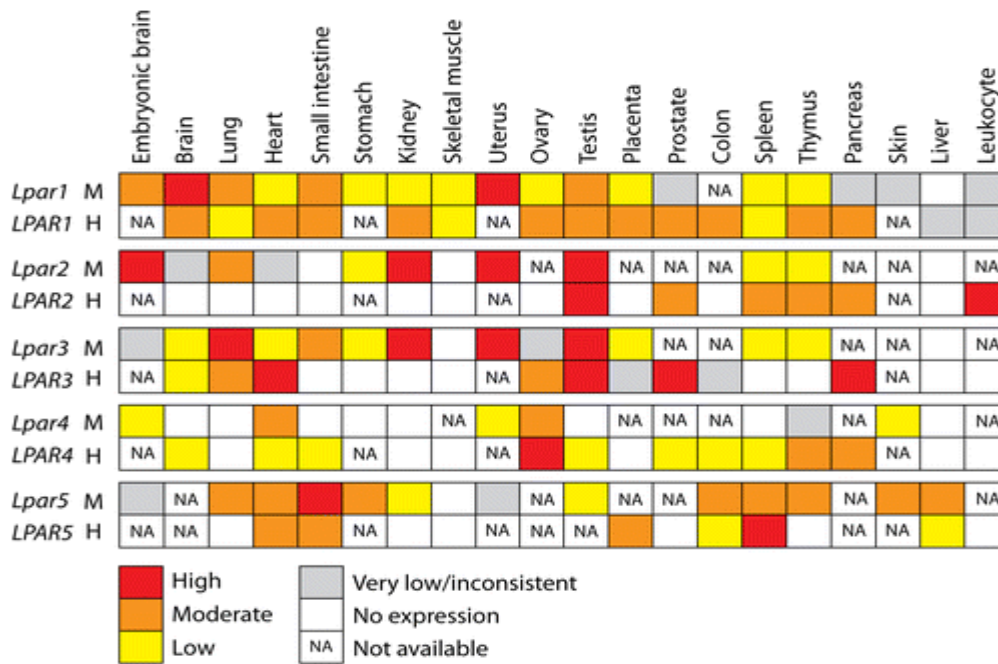


Figure 1.2: Overview of LPAR expression.

The tissue distribution and main function of these LPA receptors are highly expressed in the heart, lung and stomach in humans, whereas in mouse species they are more expressed in lungs and kidneys, an image adapted from (Choi *et al.*, 2010).

1.3.3 Role of LPA in the vascular system

Within the cardiovascular system, LPA exerts numerous roles ranging from myocardial hypertrophy and protection against ischaemic injury, regulating the cardiovascular function of cardiac myocytes, endothelial and smooth muscle cells and platelets. In contrast to these physiological effects, LPA has been implicated in pathophysiologic vascular responses by promoting migration of vascular smooth muscle cells (VSMCs) and growth through signalling of $G\alpha_q$ subunits. These two factors are key in the development of intimal hyperplasia after vascular injury (Lim *et al.*, 2013). Furthermore, studies have shown LPA induces a chemotactic response in pulmonary artery endothelial cells of bovine species with a similar intensity to vascular endothelial growth factor (VEGF) and basic fibroblast growth factor (bFGF) (Kattman *et al.*, 2006). In addition, studies examining angiogenic characteristics, LPA has been shown to evoke the formation of new blood vessels in chicken chorioallantoic membrane (CAM)

assays. This angiogenic trait is further supported by the evidence seen in a multitude of cancer cells (prostate, ovarian and lymphoma), where the induction of VEGF-A expression via HIF-1 α activation was presented (Kattman *et al.*, 2006).

An increase in LPA activity and production is attributed to an increase in response to cellular stimuli and agonists, resulting from wound healing, inflammation and thrombus formations. Under normal biological conditions, serum concentrations of LPA at 1.66 mg/L are seen, whereas patients who have suffered an acute myocardial infarction, showed serum concentrations of LPA to increase by 6.3 fold to 10.46 mg/L, after a 72 hour period (X. Chen *et al.*, 2003). Additionally, studies have shown LPA concentration levels are elevated in cardiac injury and ischaemic conditions, evoking their cardioprotective characteristics that protect cardiomyocytes from hypoxia-induced apoptosis and similar events. (Isao Ishii *et al.*, 2004).

1.4 Signal Transduction

Signal transduction is a major aspect in the regulation of key functions in multicellular organisms, mediating the intracellular machinery that directs cellular responses such as cell proliferation, migration, differentiation and apoptosis. These effects are normally initiated by various stimulants including growth factors, hormones and chemical/physiological stress. These agents could act through signal transduction cascades which eventually result in activation of transcription factors such as nuclear factor-kappa B (NF κ B), which can then go onto activate targeted gene transcription.

1.4.1 Transcription Factors

Transcription factors (TFs) are a large subset of proteins involved in regulating gene expression through transcriptional control consisting of short non-coding RNA. The regulation of RNA synthesis and the subsequent interaction binding to specific regulatory sites in DNA initiate gene expression or repression with varying groups or complexes; forming multiple interactions that lead to the cellular responses

mentioned above, including differentiation (Phillips & Hoopes, 2008). There is a multitude of TFs families that regulate cardiomyocyte differentiation such as GATA, myocyte enhancer factors (MEF2), Homeobox protein Nkx-2.5, mesoderm posterior 1 (MESP1) and nuclear factor kappa B (NFκB). Further examples of TFs are seen in Table 1-1.

Table 1-1. Transcription factors mediating cardiac hypertrophy. Adapted from (Kohli *et al.*, 2011)

Transcription Factor	Type of domain	Physiological Significance
Pro-Hypertrophic Transcription Factors		
GATA-Family	Double Zinc Finger	Hematopoiesis and Cardiac Development
MEF-2	MADS-domain	Embryonic Development, differentiation and stress response
Csx-Nkx-2.5	Helix-turn-helix	Cardiogenesis
SRF & Myocardin	MADS-box	Cell cycle regulation, Cardiac and smooth muscle gene expression
HAND	Helix-loop-helix	Cardiac and Vascular Development
TEAD	Helix-loop-Helix	Foetal heart development and cardiac remodelling
NFAT	Rel homology region	Immune response, Cardiac and skeletal muscle development
Anti-Hypertrophic Transcription Factors		
FoxO	Forkhead box	Cell growth, proliferation and differentiation
MITF	Helix-loop-helix Leucine Zipper	Melanocyte and osteoclast development
YY1	Zinc Finger	Histone modification for promoter regulation
CHF1/Hey2	Basic helix-loop-helix	Cardiac Development and ventricular function

Lysophosphatidic acid, being the target biomolecule in our research has raised interest to examine how TFs direct the expressions of a gene that is directly activated by LPA, leading to cardiomyocyte differentiation of P19 mouse embryonic carcinoma stem cells (mECs). As mentioned previously, NFκB has shown to be a critical inducible TF that is involved in various pathological and physiological functions including proliferation, survival, and differentiation. Studies have shown protein level of NFκB p65 are increased upon differentiation of mouse ES cells as opposed to

undifferentiated EC cells (Young-Eun *et al.*, 2008). This is also expressed in a study conducted by Norman *et al.*, in which NFκB subunits p65, p50, inhibitor of kappa alpha (IκB-α) and inhibitor kappa beta (IκB-β) were actively present through development and the NFκB complex participated in myocardial gene regulation in response to cytokine interactions, activating cardiac myocytes (Norman *et al.*, 1998). The essential role of NFκB in the process of differentiation has further shown to extend into the maintenance of pluripotency in human IPCs, by which the augmentation of NFκB activity was proportional to the state of cellular differentiation, resulting in the increased expression of pluripotency-associated transcription factors (Oct3/4 and Nanog), and the up-regulation of the differentiated markers (WT-1 and Pax-2) (Takase *et al.*, 2013).

1.4.2 Nuclear factor-kappa B

Nuclear factor kappa B (NFκB) is a transcription factor complex, discovered almost 20 years ago, and was originally regarded as an immunoglobulin gene. However, due to research interest over the years, it has been established as a ubiquitously expressed TF. The NFκB transcription factor family in mammals consists of 5 distinct transcriptionally active homo/heterodimeric complex proteins: p65/RelA, RelB, c-Rel, p105/p50 (NF-κB1), and p100/p52 (NF-κB2) (Takase *et al.*, 2013). A conserved N-terminal Rel homology domain within each member of NFκB enables homo- and heterodimerization nuclear localization and, more importantly, DNA binding. This results in the signalling through two major pathways, the canonical and the non-canonical pathways (Rinkenbaugh & Baldwin, 2016).

In basal conditions, NFκB exists as an inactive p65-p50 dimer bound to κB proteins (IκBs), which readily enable nucleocytoplasmic shuttling by shifting the steady-state localization of NFκB to the cytosol. However, upon exposure towards many stimuli, including LPS and pro-inflammatory cytokines (TNF, IL-1), results in the downstream activation via the canonical pathway. The restrictive κB proteins complex (IKK), constituting of regulatory subunit IKKγ (NEMO) and kinase subunits IKKα and IKKβ;

phosphorylate I κ B α , which results in the proteasomal degradation and ubiquitination of the complex (Rinkenbaugh & Baldwin, 2016). The bound NF κ B is released, leading to an accumulation of resident NF κ B; an increase in DNA binding and inevitably enabling the transcription of proliferation factors (cyclin D1) and various target genes. However, the degradation of I κ B α alone is not sufficient enough to enable maximal NF κ B transcriptional activity (L.-F. Chen & Greene, 2004). To maintain the control of NF κ B, a group of the target gene (A20, I κ B α) acts as a negative feedback loop and negatively regulates the levels of NF κ B. In contrast, within the non-canonical pathway, the bound p100 of the p100/p52 NF κ B acts as the inhibitory I κ B molecule mentioned earlier and retains Rel B within the cytoplasm. During activation of this pathway from developmental stimuli such as tumour necrosis factor receptor superfamily members (B-cell activating factor receptor, BAFF-R), lymphotoxin beta receptor (LTBR) or cluster of differentiation 40 (CD40); the stabilization of NF κ B-inducing kinase (NIK) occurs, this is further represented in Figure 1.3. This activates the phosphorylation of p100 and IKK α dimers, leading to p100 cleaving into p50 and actively producing Rel B-p52. Similar to the canonical pathway, NF κ B is subsequently free to move into the nucleus and enable the transcription of various target genes (Rinkenbaugh & Baldwin, 2016). An aspect of our research examined how NF κ B signalling could be involved in LPA-induced differentiation of P19 SCs into cardiomyocytes.

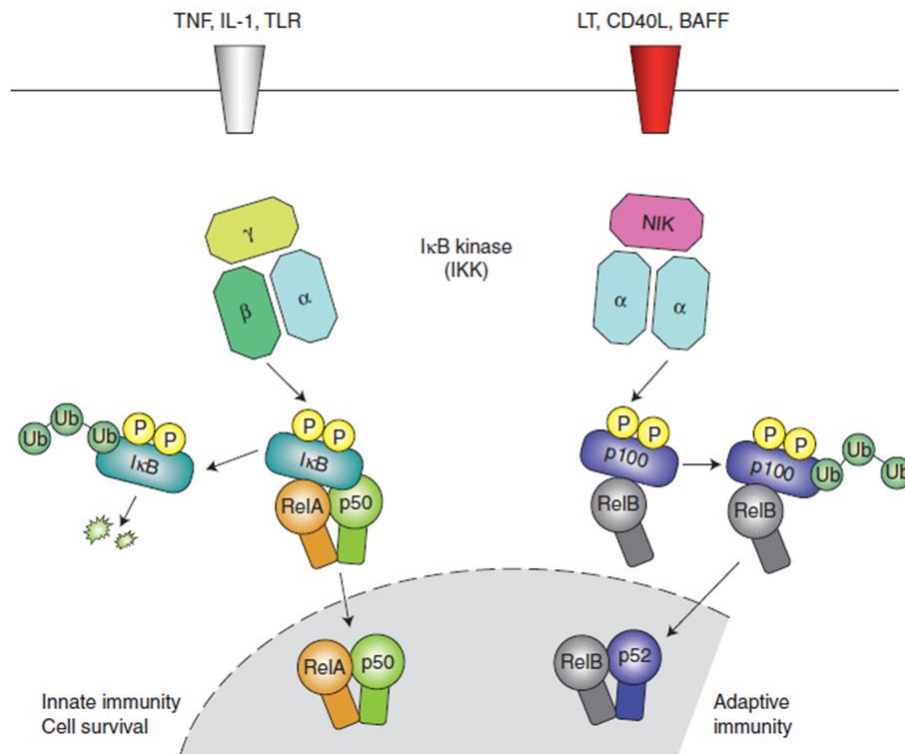


Figure 1.3: Canonical and alternative NFκB pathways.

The stimulation of the canonical pathway is triggered by proinflammatory cytokines and TLRs, leading to activation of RelA that regulates expression of cell proliferation, proinflammatory and cell survival genes. The alternative NF-κB pathway is stimulated by BAFF-R, LTBR and CD40L, causing the activation of RelB/p52 complexes within the nucleus. An image adapted from (Lawrence, 2009).

1.5 Aspirin in stem cell therapy

The use of aspirin and its capability of accelerating regenerative potential in stem cells has been the topic of research over the past decade. Research has examined the effect of aspirin on the bone marrow mesenchymal stem (BMSC) in a mini swine calvarial bone defect model. The authors showed that aspirin promoted osteogenic characteristic of BMSCs. Furthermore, BMSCs treated with aspirin significantly decreased the cell signalling protein TNF-α and IFN-γ involved in apoptotic cell death. Consequently, the improvement of BMSC-mediated calvarial bone regeneration can be regulated through the administration of aspirin. This has promoted the idea of

using aspirin in other MSC-based therapies (Cao *et al.*, 2015). Similarly, research on the potential of periodontal ligament stem cells (PDLSCs) was also undertaken, examining the osteogenic potential, proliferative capacity and expression of growth factor-associated genes enhanced by site-specific aspirin treatment. These results have shown aspirin modulates the expression of growth factors and the upregulation of specific genes leading to the activation of canonical pathways. Consequently, aspirin imposed a modulatory effect on cell proliferation, tissue regeneration, and differentiation, enhancing PDLSC function (Abd Rahman *et al.*, 2016). However, there have not been any studies conducted to establish the effect of aspirin on cardiac regeneration/ differentiation of SCs. Our research, therefore, aims to address this missing niche within the area of cardiac stem cell therapy research.

1.5.1 Cellular mechanism of action of aspirin

It was not until 1970 when the mechanism of action of aspirin was first published by the group led by John Vane. Three articles were then published in *Nature* describing the multiple biological activities of aspirin which were all related to inhibition of prostaglandin biosynthesis (Massimi *et al.*, 2014). The latter explains the anti-inflammatory and analgesic properties observed with aspirin. The trans-acetylation of the COX-1 target protein was noted to be a factor in the inhibition of platelet function, consequently, aspirin has been widely used as an anticoagulant. The acetylation of COX-2 resulted in the generation of anti-inflammatory mediators such as aspirin-triggered lipoxin (ATL), thus leading to the inhibition of leukocyte recruitment, whereby the facilitation of inflammation was negated (Schrör, 2016).

Aspirin's primary mechanism of action suppresses the production of prostaglandins (PG) and thromboxane (TX) as it acts as an acetylating agent which subsequently irreversibly inactivates cyclooxygenases (COX-1 & COX-2), the initiating enzyme in the synthesis of PG and TX, as seen in Figure 1.4. Furthermore, aspirin has shown secondary modes of action expressing anti-inflammatory, antipyretic and analgesic effects. Moreover, aspirin acts on the enzymes cyclooxygenase 1 (COX-1) on Ser 530

and cyclooxygenase 2 (COX2) on Ser 516, consequently inhibiting their function to transform arachidonic acid into prostaglandins, by adding an acetyl group ($-C(O)CH_3$) to an amino acid residue (Dang *et al.*, 2002).

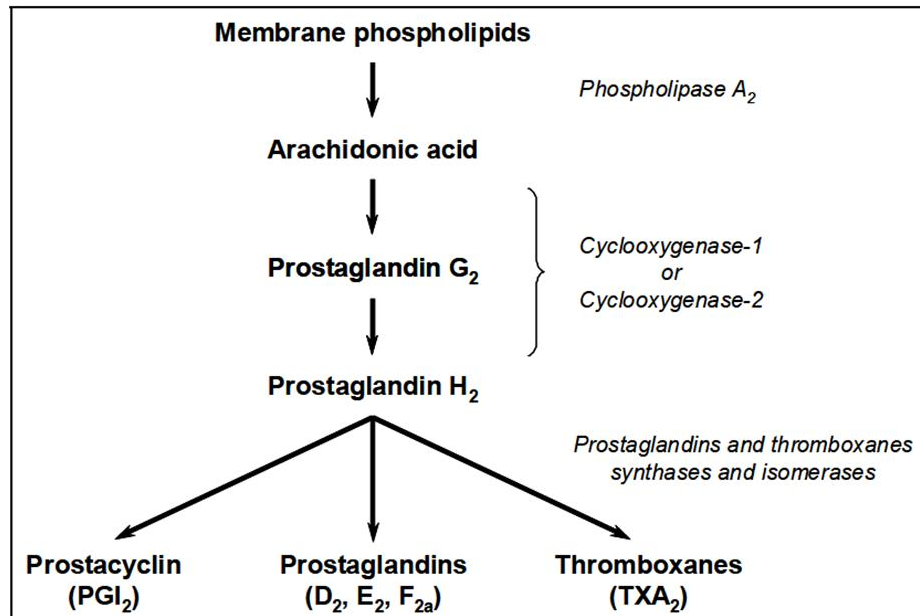


Figure 1.4: Biosynthesis of prostaglandins and thromboxane enzyme cascade.

Enzyme cascade representing the production of Prostacyclin (PGI₂), prostaglandin (D₂, E₂, F_{2A}) and thromboxane (TXA₂) from arachidonic acid by the conversion of two COX isoenzymes (COX-1 and COX-2). An image adapted from (Novella & Hermenegildo, 2011).

Furthermore, aspirin's mechanism of action on platelet COX-1 works by mediating the inhibition of the enzyme active site, thus leading to irreversible acetylation and subsequent blockade of downstream TXA₂ synthesis. Moreover, the arachidonic cascade is disrupted, resulting in arachidonic acid being unable to enter the enzyme active site. Consequently, the production of prostaglandins synthesis is prevented. However, to overcome this reduction in prostaglandin synthesis, the formation of new COX enzymes is required which are not affected by aspirin to continue their function. Similarly to COX-1, aspirin inhibits COX-2 through irreversible acetylation and reversible salicylate blockade, in turn, the active site on the enzyme is blocked, preventing the synthesis of prostaglandins, resulting in the reduction of inflammation, fever and pain (Drier *et al.*, 1999; Zhang *et al.*, 2012).

1.6 Aims of the project:

The aim of this thesis is to investigate the effects of aspirin (ASA) and salicylic acid (SA) on P19 embryonic carcinoma SCs differentiation into cardiomyocytes in the absence and presence of LPA. LPA has been utilised here as it has been used extensively in our laboratory to induce differentiation of SCs to cardiomyocytes, thus providing a useful tool in developing a differentiation model. If this model using LPA is to be exploited clinically, in the future, understanding how it might be regulated by drugs commonly prescribed to patients with or at risk of MI is critical. The focus will also be on understanding whether ASA/SA either on its own or in the presence of LPA regulates the ability of SCs to differentiate into cardiomyocytes. In addition, ASA was chosen as it has an extensive pharmacological background, providing a firm foundation to conduct our research under, in the limited time available. Furthermore, the ability of ASA to regulate the actions of LPA either directly or indirectly will also be investigated. Lastly, the underlying signalling pathways involved in the actions of ASA and/or SA will be investigated, however, these studies may be restricted in their scope due to time constraints.

2. Materials and Methods

2.1 Cell Culture

Cryopreserved ampoules of mouse P19 (ATCC® CRL-1825™) embryonal carcinoma cells, were purchased at passage 2 and experiments were carried out at passages 7-20. These cells were cultured in complete culture medium consisting of alpha minimum essential medium (α -MEM), constituting of 10% heat-inactivated foetal calf serum (FCS), penicillin (100 unit/mL) and streptomycin (100 μ g/mL) and maintained at 37°C and at 5% CO₂. Cells were sub-cultured using 0.05% trypsin-EDTA at a ratio of 1:10 every 2-3 days, depending on the expected confluency (~75-85 %).

2.1.1 Resuscitation of P19 stem cells

Vials containing frozen cells were thawed and transferred into 15 mL Falcon tubes, in which 9 mL of complete α -MEM was added, and the cell suspension was centrifuged, leaving a pellet. The supernatant was aspirated, and 7 mL of complete α -MEM was added and gently mixed to disperse the cell pellet. Following this, the cell suspension was transferred into T25 flasks. Cells were grown to a confluency of ~75-85 %, complete α -MEM was changed every other day.

2.1.2 Culture and maintenance of P19 stem cell

The culture of P19 cells was developed and maintained routinely at a set seeding density of 3.5×10^5 cells per mL. The prime confluency of ~75-85% was sustained through the duration of the experiments, in which the cells were washed twice with 1X phosphate buffered saline (PBS). To dissociate adherent cells, 1-6 mL of 0.05% trypsin-EDTA, respective of the flask volume was added for a duration of 1-3 mins. To inactivate the trypsin, complete α -MEM was added to the flasks at a ratio of 1:1. The cell suspension was mixed thoroughly and transferred to 15 mL or 50 mL Falcon tubes and centrifuged. The supernatant was aspirated, leaving a cell pellet which was then disassociated in 6-9 mL of complete α -MEM. Cell counting was undertaken to establish the appropriate volume to achieve a seeding density of 3.5×10^5 in the required final volume for sub-culture, embryoid body (EB) formation or cryopreservation.

2.1.3 Cryopreservation of P19 Stem cells

Cells were trypsinised as mentioned above and the remaining cell pellet was resuspended in 1mL of a freezing medium consisting of 10% glycerol and 90% FCS. To prevent cell damage resulting from rapid crystallization in -80°C , the solution containing the cells were placed into a Thermo Scientific NALGENE Mr. Frosty, with a controlled freezing rate of $1^{\circ}\text{C}/\text{min}$ for a period of 24 hours. Subsequently, the cells were transferred from Mr Frosty into liquid nitrogen containers for storage.

2.2 Antibodies and Reagents

General cell culture reagents were purchased from Gibco (Life Technologies, UK) and Invitrogen (UK). DMSO was from Fisher scientific and glycerol from Sigma-Aldrich. Lysophosphatidic acid (Oleoyl-L- α -lysophosphatidic acid sodium salt), acetylsalicylic acid and salicylic were purchased from Sigma-Aldrich. Primary antibodies used in these studies: NF κ B p65, β -Actin and MLC-Iv were purchased from Abcam, (UK); Phospho-NF κ B p65, Phospho-p44/42 MAPK (Erk1/2), Phospho-IKK α and I κ B α from Cell Signalling technologies (UK); CAY10470 (selective NF κ B inhibitor) (from (Merck Chemicals)); Acetylsalicylic acid and salicylic acid from Sigma-Aldrich (UK). Secondary antibodies used in these studies: goat anti-mouse IgG-HRP antibodies were purchased from Santa Cruz Biotechnology, (United States); anti-rabbit IgG HRP-linked and anti-mouse IgG HRP-linked from Cell Signalling Technologies (UK); goat anti-rabbit IgG H&L HRP and goat anti-rabbit IgG H&L HRP from Abcam (UK). Salts and chemical compounds used for molecular biology were purchased from Sigma-Aldrich (UK), Fisher Scientific (UK) and Invitrogen (UK). Pierce BCA protein assay kits were purchased from Thermo Scientific (UK).

2.3 Determination of drug concentrations

Cell culture-based experiments examining the effects of aspirin used a concentration range of 0–10 mM, which provided an appropriate working index to achieve the maximum effect relative to cytotoxicity (Campregher *et al.*, 2007; Castaño *et al.*, 1999;

Luciani *et al.*, 2007). Furthermore, the selected concentrations used in this experiment are similar to that of used in the research conducted by Hao *et al.*, concluding a concentration of 2 mM aspirin is the most effective, as lower concentrations failed to elicit a response and higher concentrations induced high cellular toxicity. Therefore, the concentrations were modelled on these findings (Hao *et al.*, 2018). Initial EB optimisation of the P19 stem cell differentiation model was carried out using a concentrations range of 0.01 mM, 0.03 mM, 0.1 mM, 0.3 mM and 1 mM for both ASA and SA compounds. These concentrations listed above were further revised to a range of 0.1 mM, 0.3 mM, 1 mM and 3mM for both compounds in subsequent cell culture experiments.

When comparing clinical relevance it is worth noting that these concentrations are well above plasma concentrations, as the C_{max} (maximum /or peak serum concentration) of a 500 mg ASA dose given intravenously versus is seen at 54.25 mg/L, (~0.3 mM) and 4.84 mg/L (~0.03mM) with ASA 500 mg given orally (Nagelschmitz *et al.*, 2014). However, there are varying factors to consider in cell culture conditions, which justify the use of higher concentrations of ASA and SA in our experiments.

2.4 Differentiation and Embryoid Body formation of P19 stem cells

2.4.1 Lysophosphatidic acid stock preparation

To induce differentiation, LPA was dissolved at a final stock concentration of 5 mM, in 1x PBS and 0.01% fatty acid-free bovine serum albumin (BSA). Aliquots of 50 μ L were stored at -80°C and upon use, the stock concentration of LPA was diluted to 5 μ M in complete α -MEM.

2.4.2 Cell counting and plating for EB formation

Cell count was achieved by detaching monolayers of P19 stem cells with 0.05% trypsin-EDTA, to which complete α -MEM was added to inactivate trypsin-EDTA, forming single-cells in suspension. An equal volume of cell suspension was mixed with 0.4 %

trypan blue (20 μL) and counted on a Countess electronic cell counter. The following formula is shown below (Table 2-1) was used to achieve the desired seeding density of 1.4×10^4 in 96-well cell culture plates.

Table 2-1: Cell seeding calculations for EB formation.

Total cells: $2.86 \times 10^6/\text{mL}$
 Cell Viability: 81%
 Live Cells: $2.32 \times 10^6/\text{mL}$
 Final volume per 96-well: 0.290 mL
 Seeding density: $1.4 \times 10^4/\text{mL}$

E.g. volume of suspension (X) plated= $\frac{\text{Desired concentration of cells} \times \text{Final volume}}{\text{Viable cell concentration (1 mL)}}$

$$\frac{1.4 \times 10^4 \times 0.290 \text{ mL}}{2.32 \times 10^6} = 0.00175 \text{ mL}$$

In 289 μL of complete α -MEM

2.4.3 Differentiation of P19 stem cells into cardiomyocytes

Differentiation was induced using a differentiation medium consisting of 0.8% DMSO in complete α -MEM as a positive control or 5 μM of LPA. Post trypsinisation, the cell suspension was incubated with α -MEM alone or with LPA either at 5 μM or varying concentrations as required. Embryoid bodies were allowed to form at 37°C and at 5% CO_2 for a period of 48 hours as seen in Figure 2.1. 6-8 EBs were then plated per well in a 12-well tissue culture plates in 3 mL of complete α -MEM for selected time points. Media was intermittently changed every other day with complete α -MEM.

To establish the effects of ASA and SA on differentiation of P19 cells into cardiomyocytes, trypsinised cell suspensions were pre-treated for 60 minutes with either ASA (0.1, 0.3, 1, 3 mM) or SA (0.1, 0.3, 1, 3 mM) before being incubated with α -MEM alone or with α -MEM in the presence of LPA (5 μM).

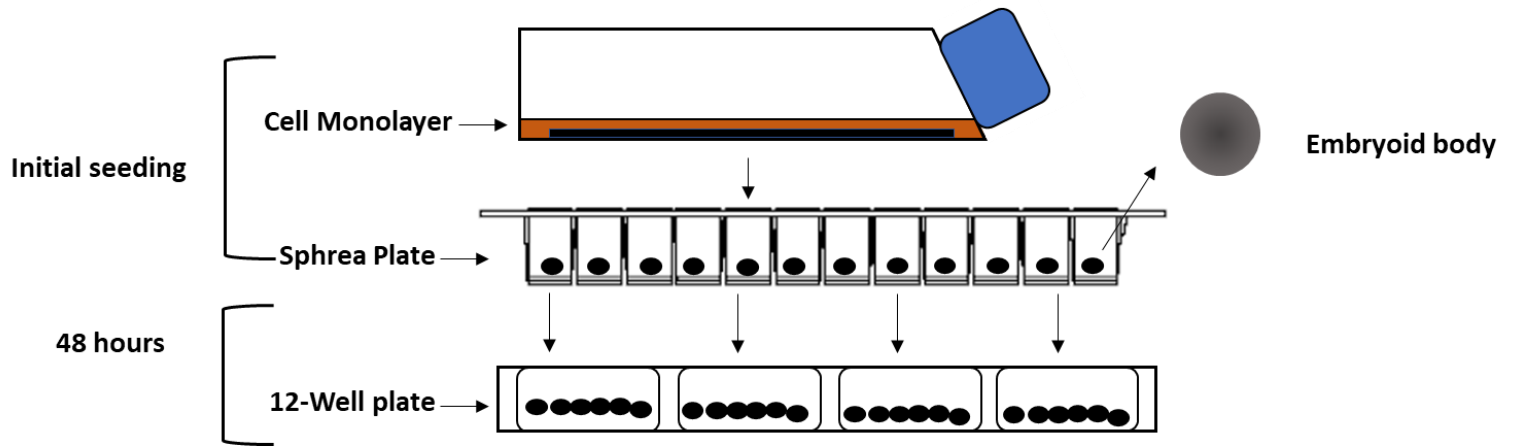


Figure 2.1: Differentiation of P19 stem cells into cardiomyocytes

Cells monolayers were grown to a confluency of ~75-85% trypsinised and seeded into ultra-low attachment 96-well plates, with and without 5 μ M LPA over a period of 48 hours. Embryoid bodies were then seeded into 12-well tissue culture grade plates and allowed to differentiate into cardiomyocyte monolayers.

2.5 Protein determination and quantification

2.5.1 Cell lysate generation for MLC-1v protein expression

Cell lysates were obtained at specific time points ranging from days 3, 6, 9, and 12 and probed for myosin light chain 3 (MLC-1v). Plates were transferred onto the ice at the end of specific incubation periods and existing culture media was aspirated and the cells were washed twice with ice-cold 1x PBS. Whilst on the ice, radioimmunoprecipitation assay (RIPA) buffer (Figure 2.2) (at a volume of 80-150 μ L was added to each well and cells were scraped using a fine pipette tip and transferred to ice-cold 1.5 mL microcentrifuge tubes in an ice box. The lysates were sonicated in an ice-filled sonication bath for a period of 90 seconds with 15-second intervals and centrifuged at the max relative centrifugal force (RCF) or 13,000 rpm for 10 mins at 4°C. Cells lysates were then immediately stored at -80°C to prevent protein degradation.

Table 2-2: RadioImmunoPrecipitation Assay (RIPA) Buffer- 200mL

Vials	Volume of Diluent (μL)
50mM Tris-HCL (pH 8)	1.211g
150 mM NaCl	1.753 g
0.1% Triton x-100	200 μL
10% sodium deoxycholate	1000 μL
0.1% SDS	200 μL
(1%) Inhibitor Cocktails	10uL/mL
50mM Tris-HCL (pH 8)	1.211g

2.5.2 Cell lysate generation for phosphorylated protein expression

Lysates were obtained by conducting early time point studies. Post trypsinisation, the single-cell suspension treated with varying concentrations of ASA (0.1, 0.3, 1, 3 mM) or SA (0.1, 0.3, 1, 3 mM) and/or LPA (5 μM) were seeded into Gosselin square Petri dishes and incubated for specific time points. At the allocated time point, 2-3 mL of cell suspensions were transferred into Falcon tubes, centrifuged for 30 seconds and cells were washed with 1 mL of 1x PBS and transferred into ice-cold 1.5 mL microcentrifuge tubes in an ice box. As mentioned above, the same methodology was followed by adding RIPA, sonicating and centrifuging the samples to obtain cell lysates. Cells lysates were they immediately stored at -80°C to prevent protein degradation.

2.5.3 Protein quantification using bicinchoninic acid (BCA) assay

To determine the total protein content of the cell lysates the Pierce BCA protein kit was used. Using 2 mg/mL ampoules of BSA stock, a standard curve was prepared using double distilled water (DDW) with a set of working standards and layout as seen in Table 2-3. The 96 well plate containing the samples and standards was then placed onto an orbital shaker for 30 mins, followed by incubating at room temperature for 15 mins. The plates were read at a wavelength of 620 nm using the CLARIOstar plate reader. Using the standard curve equation $y=mx+c$ (seen in Figure 2.2), the unknown protein absorbance readings were replaced for y in the rearranged formula $x= (y-c)/m$

and this values were further used to calculate for a loading volume of 20 $\mu\text{g}/\mu\text{L}$ for sodium dodecyl sulfate-polyacrylamide gel electrophoresis (SDS-PAGE). In this equation X was the unknown concentration to be determined, Y was the absorbance value at 620nm, C is the intercept and m is the slope.

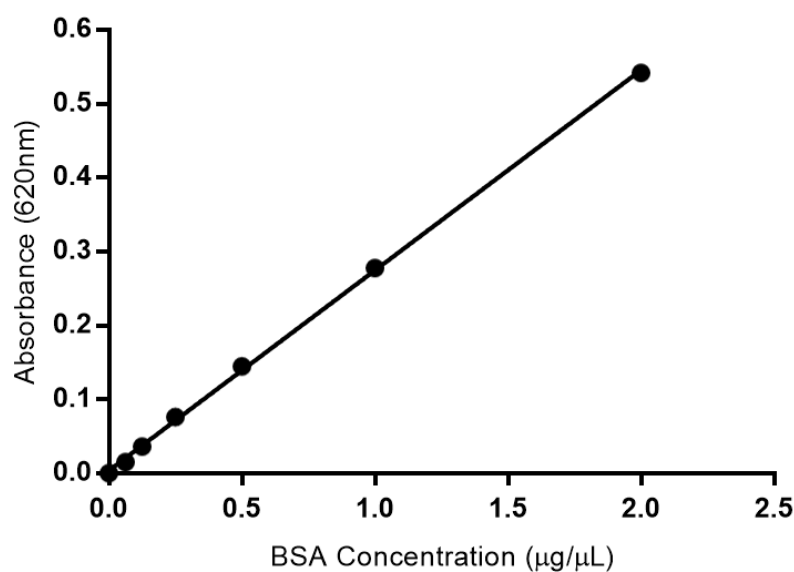
Table 2-3. Preparation of diluted BSA standards

Working stock concentration of BSA 2 mg/mL and Diluent (DDW)

Vials	Volume of Diluent (μL)	Volume and Source of BSA (μL)	Final concentration ($\mu\text{g}/\mu\text{L}$)
A	0	50 of Stock	2
B	25	25 of vial A dilution	1
C	25	25 of vial B dilution	0.5
D	25	25 of vial C dilution	0.25
E	25	25 of vial D dilution	0.125
F	25	25 of vial E dilution	0.063
G	50	0	0 = Blank

Table 2-4. 96-well plate layout for preparation for BCA

Samples	DDW (μL)	Cell Lysates (μL)	Standards (μL)	RIPA Buffer (μL)	BCA (μL)
Control	5	-	-	5	100
Cell Lysates	5	5	-	-	100
Standards	-	-	5	5	100



R^2 Value= 0.9995

$$y = 0.2709x + 0.003727$$

Figure 2.2. BCA protein standard curve.

Graph representing the BCA standard curve of bovine serum albumin at 620nm absorbance, with a standard regression coefficient of $R^2 = 0.9995$ and the line equation of $y=0.27x + 0.01$.

2.6 Protein analysis using western blotting and SDS-PAGE

Sodium dodecyl sulphate-polyacrylamide gel electrophoresis (SDS-PAGE) was used to resolve and separate proteins in cell lysates according to their molecular weight and size. Subsequently, the gels were then transferred using enhanced chemiluminescence and immunoblotting for proteins of interest.

2.6.1 Sodium dodecyl sulphate-polyacrylamide gel electrophoresis (SDS-PAGE)

2.6.1.1 Gel Preparation

Resolving gel at 12% and stacking gel at 4% was prepared following the recipe in Table 2-5. Resolving gel (4 mL) solution was pipetted into BIO-RAD glass sandwich plates and allowed to polymerise. Double distilled water (DDW) (150-200µL) was layered on top

of the gel to prevent the dehydration and to prevent bubble formation. Following polymerisation, the layer of distilled water was removed using a filter paper and stacking gel (1.5-3 mL) solution was pipetted and set with the addition of a 10 well loading comb and left to polymerize appropriately. Using the buffer recipes in Table 2-7, the electrode/tank buffer was loaded into electrophoresis tanks, in which the gels were placed.

2.6.1.2 Sample Preparation

Calculations were carried out determining the loading volume for 20 µg of cell protein lysates in the 2x sample buffer (Table 2-6). The samples were then heated at 95°C for 3-5 mins, allowed to cool and then loaded into each well. The gels were run at 150mA, 200 V for 45 mins.

2.6.1.3 Protein transfer

The gels were placed into 1X transfer buffer (seen in Table 2-8) for 5 mins. Polyvinylidene difluoride (PVDF) membranes were cut prior and then transferred into 100% methanol for 30 seconds activating the membrane and immediately placed into distilled water for 2 mins, as PVDF membranes are hydrophobic, prior to use. The membrane was equilibrated in the 1X transfer buffer for 5 mins. A PVDF membrane sandwich was constructed, consisting of pre-soaked filter papers, membrane and gels. Air bubbles in the sandwich were removed using a rolling pin and the semi-dry transfer carried out on a Pierce Power Blotter at 25 V, 2.5mA for 7 mins.

2.6.2 Western Blotting

2.6.2.1 Blocking and antibody probing of membranes

The membranes were blocked with 5% non-fat semi-skimmed milk using the recipe in Table 2-10 and placed on an oscillating shaker for 1-2 hours at room temperature. Polythene bags were used to probe membranes with primary antibody overnight at 4°C. A dilution of 1:1000 in blocking buffer was used to dilute the antibodies for primary and secondary antibodies from Abcam and a dilution of 1:5000 for primary

and secondary antibodies purchased from Cell Signalling Technologies. Following primary antibody probing, membranes were washed with 1x TBST 3 times for 30 mins with 10 min intervals on an oscillating shaker. Secondary antibodies were used at 1:5000 dilution and probed similarly at room temperature for 2 hours and washed again. For chemiluminescence, Thermo ECL reagents were used at a ratio of 1:1. Membranes were incubated with the reagent for 5 mins and analysed using the Thermo ECL imager.

2.6.2.2 Membrane Stripping and re-probing

Membranes were washed in 1x TBS as mentioned above, following ECL imaging and placed into 20 mL of Thermo Restore stripping buffer for 15 mins on an oscillating shaker. Membranes were rewashed, blocked and re-probed with the appropriate antibodies.

2.6.2.3 Analysis of western blot images

A housekeeping protein such as β -actin was used to normalise the protein loading and protein expression with the accompanying primary antibodies. Raw image files of the selected membranes derived from the ThermoECL imager were analysed using Bio-Rad Image Lab software to plot the expression of proteins.

Table 2-5. Gel recipe for SDS-PAGE (4 Gels)

Reagents	Resolving Gel (12%)	Stacking Gel (4%)
DDW	6.6 mL	6.1 mL
Acrylamide (30%)	8 mL	1.3 mL
Tris-HCL (1.5 mM, pH 8.0)	5 mL	-
Tris-HCL (0.5 mM, pH 6.8)	-	2.5 mL
Ammonium Persulfate (10%)	200 μ L	200 μ L
SDS (10%)	200 μ L	100 μ L
TEMED	12 μ L	20 μ L

Table 2-6. Recipe for 2x Sample Buffer (10 mL)

Reagents	Volume (mL)
0.5 M Tris-HCL (6.8pH)	2.5
Glycerol	2
SDS 10%	4
Bromophenol Blue 1%	0.4
Dithiothreitol (DTT) 2M	0.1
DDW	1

Table 2-7. Recipe for 10x Tank Buffer (2 Litres)

Buffers were diluted to 1x before use.

Reagents	Constituent
Glycine	288 g
Tris base	60.4 g
SDS	20 g
DDW	1.8 L

Table 2-8. Recipe for 10x Transfer Buffer (2 Litres)

Buffers were diluted to 1x before use with 10% Ethanol added last.

Reagents	Weight (g)
glycine	288 g
Tris base	60.4 g
Methanol	200 mL
DDW	1.8 L

Table 2-9. Recipe for 10x TBS (Wash Buffer) (1 Litre)

Stock pH was adjusted to 7.6 with HCl and buffers were diluted to 1x before use.

Reagents	Weight (g)
Tris base	24 g
Sodium Chloride	88 g
DDW	1 L

Table 2-10. Recipe for blocking buffer

Blocking buffers were also used to dilute and immunoprobe antibodies on PVDF membranes.

Reagents	Constituent
Non-fat semi skimmed milk powder	5g
Tween- 20	100 µL
Transfer Buffer 10X	10 mL
DDW	90 mL

2.7 Cell Viability Assay

2.7.1 MTT (3-(4, 5-dimethyl thiazolyl-2)-2, 5-diphenyltetrazolium bromide) assay

The MTT cell metabolism assay was performed to determine the viability of cells under different experimental conditions. Mitochondrial dehydrogenases of viable cells cleave the MTT dye into insoluble purple formazan crystals, resulting from NAD (P) H-dependent cellular oxidoreductase enzymes present in viable cells. Therefore, the absorbance present is proportional to viable cells (Liu *et al.*, 1997).

Cells were seeded at 1.0×10^5 cells in a final volume of 200 µL into each Falcon 96-well tissue culture plate. Cells were cultured for the selected time points and serum-free media was used to replace the existing media (50µL) and 50µL of MTT solution (5 mg/mL). Cells were incubated for 4 hours at 37°C and at 5% CO₂. Media was then discarded and 100µL of isopropanol was added to dissolve the formazan crystals

formed. The plates were placed onto an orbital shaker for 10 mins and the absorbance was read at 540nm on a CLARIOstar plate reader. Cell number was determined using a standard curve of known cell densities. This was prepared with known cell densities of cells seeded into serum-free media filled 96-well plates (seen in Table 2-11) and incubated overnight, to enable cells adhered without proliferating and then assayed as mentioned above. Using the line of the equation, cell number and cell cytotoxicity were analysed respectively.

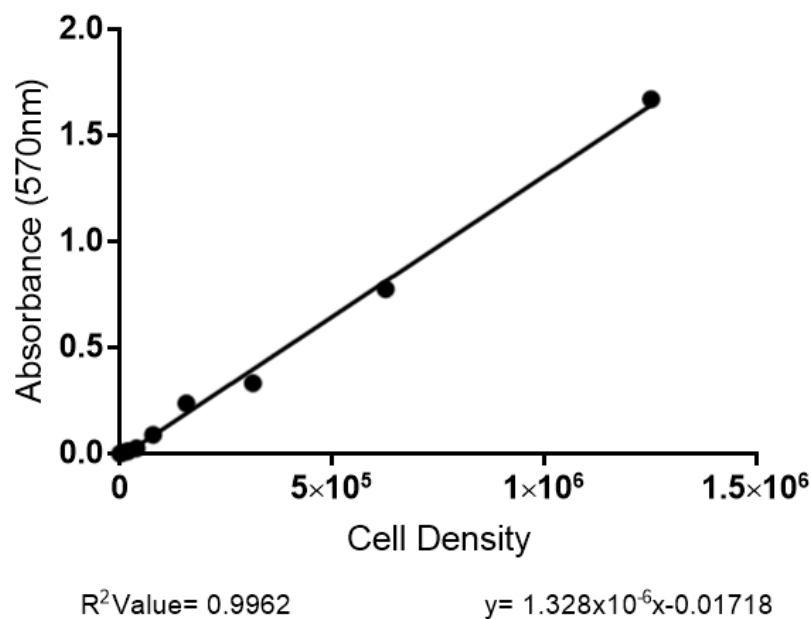


Figure 2.3. Cell number standard curve for MTT assay.

Graph representing cell number standard curve read at an absorbance of 570nm, with a standard regression coefficient of $R^2 = 0.9962$ and line equation of $y = 1.328 \times 10^{-6}x - 0.01718$.

Table 2-11. Preparation of diluted cell densities

Working stock concentration of 1.0×10^7 cells and Diluent (serum-free α -MEM)

Vials	Volume of Diluent (μ L)	Volume and Source of cells (μ L)	Final concentration of cells
A	0	400 of Stock	1.25×10^6
B	400	400 of vial A dilution	6.25×10^5
C	400	400 of vial B dilution	3.13×10^5
D	400	400 of vial C dilution	1.56×10^5
E	400	400 of vial D dilution	7.81×10^4
F	400	400 of vial E dilution	3.91×10^4
G	400	400 of vial F dilution	1.95×10^4
H	400	400 of vial G dilution	9.77×10^3
I	400	0	Blank

2.8 Statistical analysis

The results were subjected to the statistical software on GraphPad Prism 7 and presented as means \pm standard error means (S.E.M.). Using a one-way and two-way ANOVA with the Dunnett's post Hoc test analysis of variance, multiple comparisons of significance was analysed. A significance value of $p < 0.05$ (95% confidence interval) was used to compare the effects of ASA and SA conditions, in the presence and absence of LPA. Independent experiments exceeding $n=3$ were carried out to provide adequate data for these statistical tests carried out.

3. Results

3.1 Development and characterization of P19 stem cell differentiation model

To conduct a routine cell culture of P19 ECS, the cells were systematically cultured over a period of 2-3 days, until a confluency rate of 75-85% was achieved. Aseptic techniques were undertaken with the utmost precaution to prevent contamination of SCs and subsequent cultures.

In initiating the studies, the first consideration was to determine the growth pattern of P19 cells in culture and to establish the time period taken for optimal growth and confluency. Trypsinised cells were seeded at a concentration of 3.5×10^5 cells per mL in a T-25/T-75 tissue culture flasks, which were observed daily under an inverted Olympus microscope over a period of 4 days. As shown in Figure 3.1A, the trypsinised cells plated in the flasks appear rounded and sparsely distributed because of the low seeding density. As the cells became established, they attached to the surface of the flask; beginning to grow, changing their morphology as they do so. This is evident 24 hours post cell seeding (Figure 3.1B). The cells continued to grow in small clusters over 48 hours (Figure 3.1C and D) reaching optimal confluency at 72 hours. Full confluency was reached at 96 hours showing a very tightly packed monolayer of cells (Figure 3.1E).

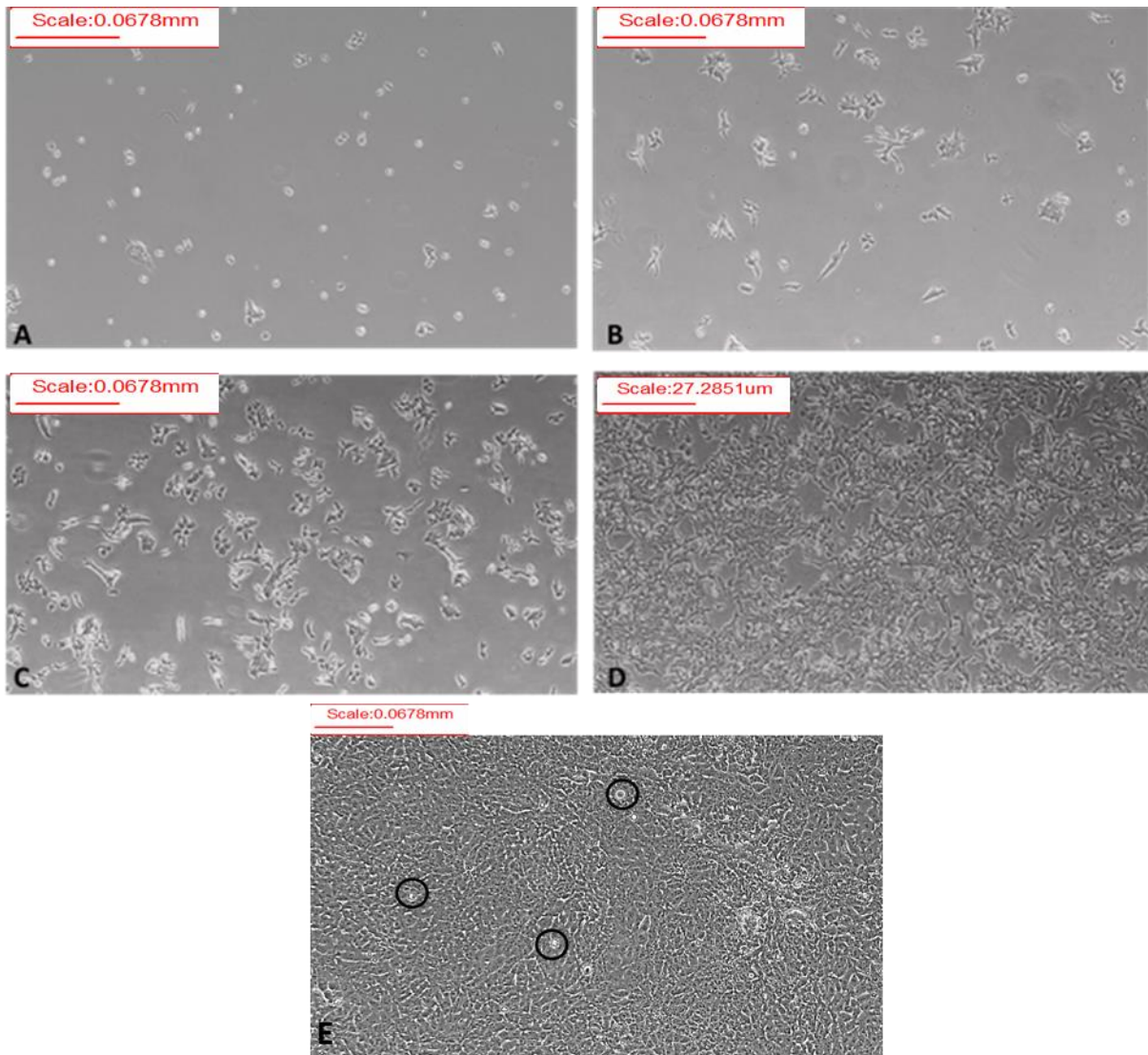


Figure 3.1: Growth pattern of P19 stem cells at different confluency

Passage 19, P19 SCs were trypsinised using 1% trypsin-EDTA and seeded 3.5×10^5 cells/mL. Cells were grown at 37°C, 95% air and 5% CO₂. The cells were cultured in complete α -MEM containing 10% foetal calf serum (FCS) and 100 units/mL penicillin together with 100 μ g/mL streptomycin. Images were taken with an Olympus inverted microscope. (A) Initial seeding of P19 SCs, at 10X magnification. (B) Cells at 5-10% confluency on day 2, at 10X magnification. (C) Cells at 50% confluency on day 3 at 10X magnification. (D) Cells at 90% confluency on day 3 at 4X magnification. (E) Cells at 100% confluency on day 4 at 4X magnification. Free floating cell debris are circled.

Figure 3.2 shows a monolayer of P19 SCs progressing to approximately 70% of confluency under routine culture. The cells appear elongated with a unique stellate shape, as the cells are constantly dividing and reaching optimum confluency to achieve a single monolayer, spreading uniformly throughout the flask. In addition, some cells have fused together as they divide in close proximity, forming clusters which are seen as the beginning of a monolayer formation. Furthermore, unattached SCs and cell debris are evidently seen free floating in the complete medium.

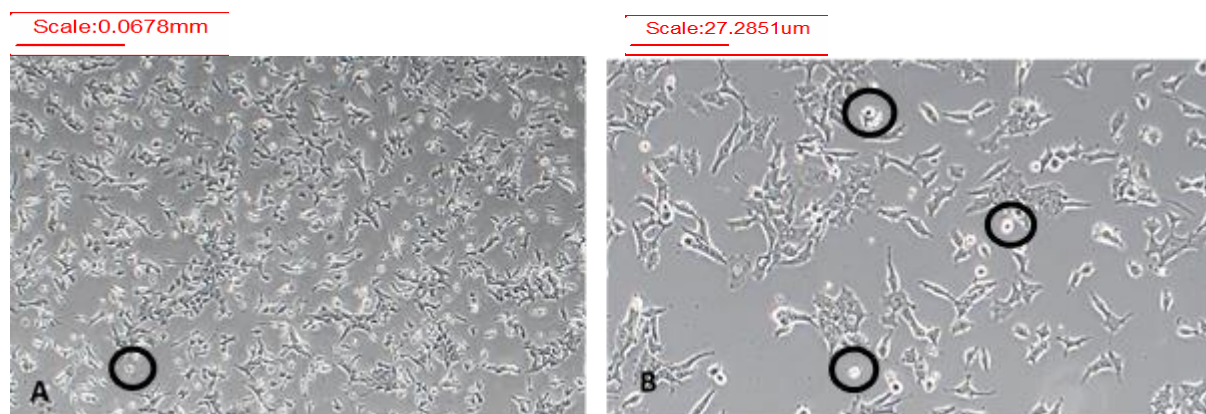


Figure 3.2: Morphology of P19 stem cells in culture.

Passage 21, P19 SCs were trypsinised using 1% trypsin-EDTA and seeded 3.5×10^5 cells/mL. Cells were grown at 37°C, 95% air and 5% CO₂. The cells were cultured in complete α -MEM containing 10% foetal calf serum (FCS) and 100 units/mL penicillin together with 100 μ g/mL streptomycin. Images were taken with an Olympus inverted microscope. (A) Cells at 50-60% confluency of healthy P19 SCs, at 4X magnification. (B) Cells at 10X magnification with the same set of cells. Areas representing free floating unattached cells and cell debris are circled above.

When allowed to grow further, cells reached maximum confluency; saturating the surface area of the flask as shown in Figure 3.3. The cells appear very tightly packed and more cobbled stone in their morphology. There is also evidence of dead cells and cell debris as indicated by translucent structures floating in the medium. It was, therefore, important to ensure that the cells were not allowed to reach super confluency (day 4 growth) in culture as this may affect their viability. All experiments were therefore carried out using cells at 75-85% confluency.

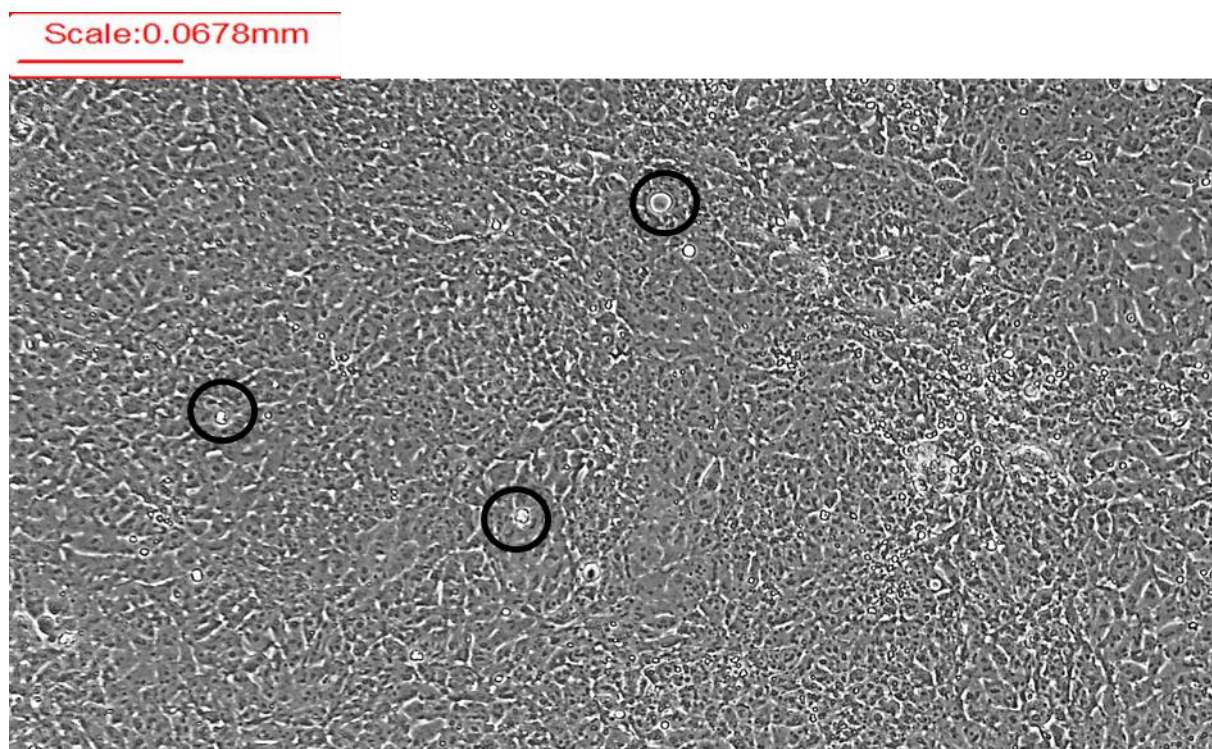


Figure 3.3: Morphology of confluent P19 stem cell monolayer.

Passage 12, P19 SCs were trypsinised using 1% trypsin-EDTA and seeded 3.5×10^5 cells/mL. Cells were grown at 37°C, 95% air and 5% CO₂. The cells were cultured in complete α -MEM containing 10% foetal calf serum (FCS) and 100 units/mL penicillin together with 100 μ g/mL streptomycin. Images were taken with an Olympus inverted microscope. Cells shown at 100% confluency, at 4X magnification. Areas representing free floating unattached cells and cell debris are circled above.

3.2 Establishing embryoid bodies from monolayers of P19 cells

To induce differentiation, monolayers of cells had to initially be grown as three-dimensional aggregates referred to as EBs. These were generated using either cells suspended in non-adherent Petri dishes or in ultra-low attachment 96-well plates in order to determine the efficiency of optimal embryoid bodies (EB) formation.

3.2.1 Establishing embryoid bodies using Petri dish cell suspension

Trypsinised P19 monolayers were seeded at a density of 3.7×10^5 cells/mL in P60 microbiology non-adherent Petri dishes, suspended in 5mL of complete α -MEM. The cultures were routinely maintained at 37°C, 95% air and 5% CO₂ over 4 days. Figure 3.4 below shows representative growth of EBs at varying morphological stages from days 2-4. Embryoid bodies at day 4 were considered morphologically adequate for seeding into cell culture plates and used for experimentation. However, it is clear from Figure 3.4 C & D that the EBs formed varied considerably in size. This has been indicated in other studies to be responsible for the lack of generation of consistent beating clusters of cardiomyocytes.

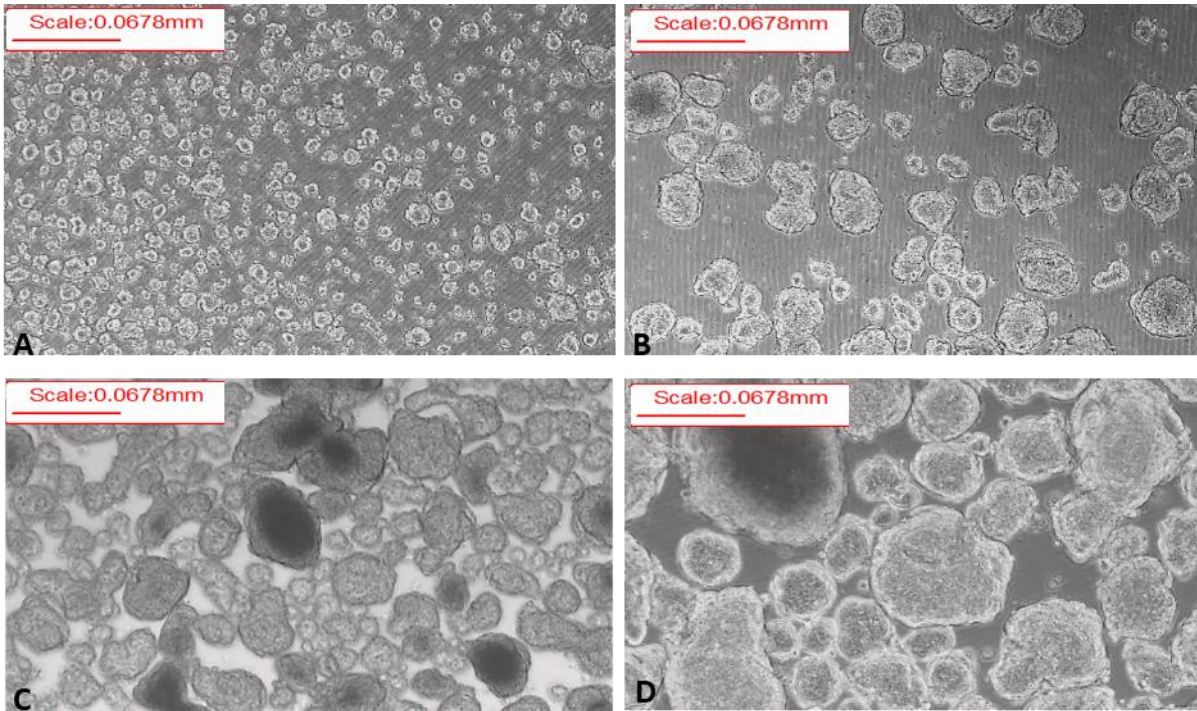


Figure 3.4: Morphology of EB in Petri dish culture, grown over 4 days.

Passage 12, P19 SCs were seeded 3.5×10^5 cells/mL in P60 microbiology Petri dishes. Cells were grown at 37°C, 95% air and 5% CO₂ and cultured in complete α -MEM containing 10% foetal calf serum (FCS) and 100 units/mL penicillin together with 100 μ g/mL streptomycin. Images were taken with an Olympus inverted microscope. (A) EB formation at 24 hours. (B) At 48 hours. (C) At day 72 hours. (D) At 96 hours at 4X magnification of the same set of cells.

3.2.2 Embryoid body differentiation into cardiomyocytes

Four to six EBs were seeded into 24-well tissue culture plates to which the EBs adhered and cells migrated from the EB clusters, growing as single cell monolayers as seen in Figure 3.5. The monolayer showed similar morphology to initial P19 monolayer growth seen in Figure 3.4 above, sharing the distinctive tightly packed cobblestoned-like pattern shown at a higher magnification of 10X (Figure 3.5B) and 20X (Figure 3.5C) at day 12.

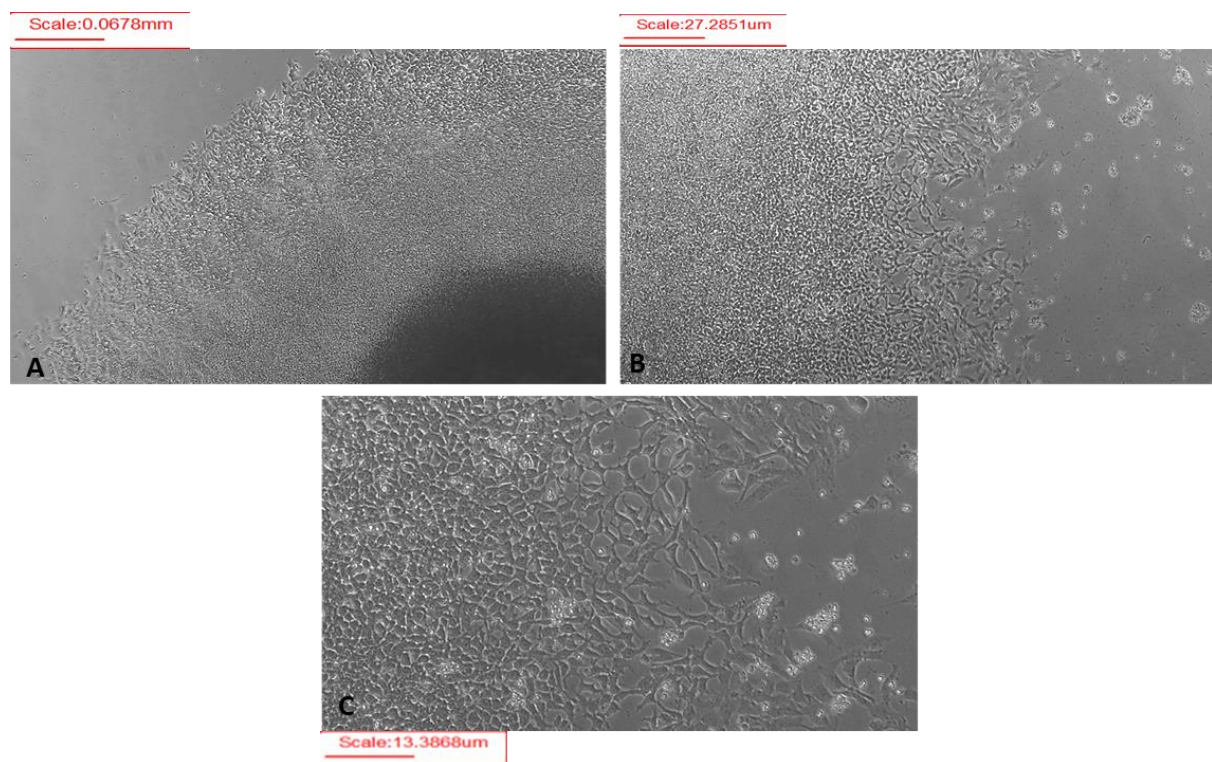


Figure 3.5: Growth of cells from EBs in culture

Embryoid bodies were cultured over a period of 4 days, 3-4 EBs were seeded into individual wells in 12 well plates. Cells were grown at 37°C, 95% air and 5% CO₂ and cultured in complete α -MEM containing 10% foetal calf serum (FCS) and 100 units/mL penicillin together with 100 μ g/mL streptomycin. Images were taken with an Olympus inverted microscope. (A) Growth at 24 hours at 4X magnification. (B) 10X magnification. (C) 20X magnification of the same set of cells.

3.2.3 Establishing embryoid bodies using low-attachment 96 well-plate cell suspension

When seeded in ultra-low attachment 96-well plates, P19 cells aggregated to a more consistent diameter of 350-450 μm , within 48 hours. This is shown in Figure 3.6 where the shape and size of most of the EBs formed were consistent when compared to those seen using the Petri dish method. As opposed to the other conditions (attachment to Petri dishes) in which the sizes of EBs formed varied quite considerably within the same culture.

To determine the optimal size of EBs, parallel experiments were carried out looking at differences in seeding densities and time point, using the ultra-low attachment 96-well plates. Figure 3.6 shows that a seeding density of 10,000 cells incubated for 48 hours produced the required EB diameter of 350-450 μm . However, higher seeding densities produced larger EBs. Incubations for 24 rather than 48 hours, produced masses of EBs with less defined outer borders. These differences are shown more clearly in Figure 3.7 for a better comparison. All experiments were carried out with 10,000 cells seeded for 48 hours for the required EBs to form.

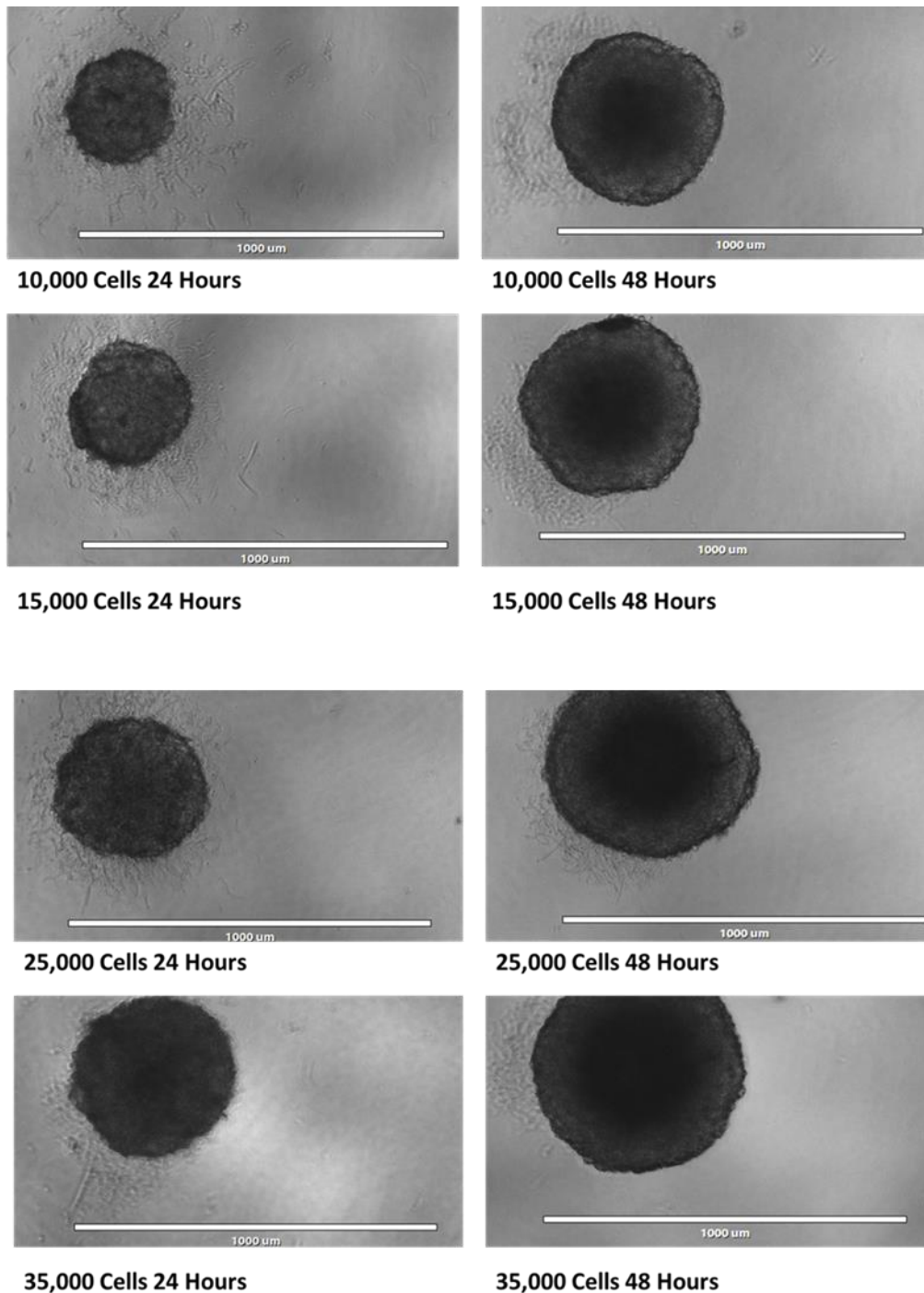


Figure 3.6: Determination of optimum EB size and growth period in 96 well-plates.

Passage 12, P19 SCs were seeded between 1×10^4 – 3.5×10^4 cells/mL in ultra-low attachment 96 well plates. Embryoid bodies were cultured over a period of 2 days. Cells were grown at 37°C, 95% air and 5% CO₂ and were cultured in complete α -MEM containing 10% foetal calf serum (FCS) and 100 units/mL penicillin together with 100 μ g/mL streptomycin. Images were taken with an EVOS® FL Cell Imaging microscope at 10X magnification.

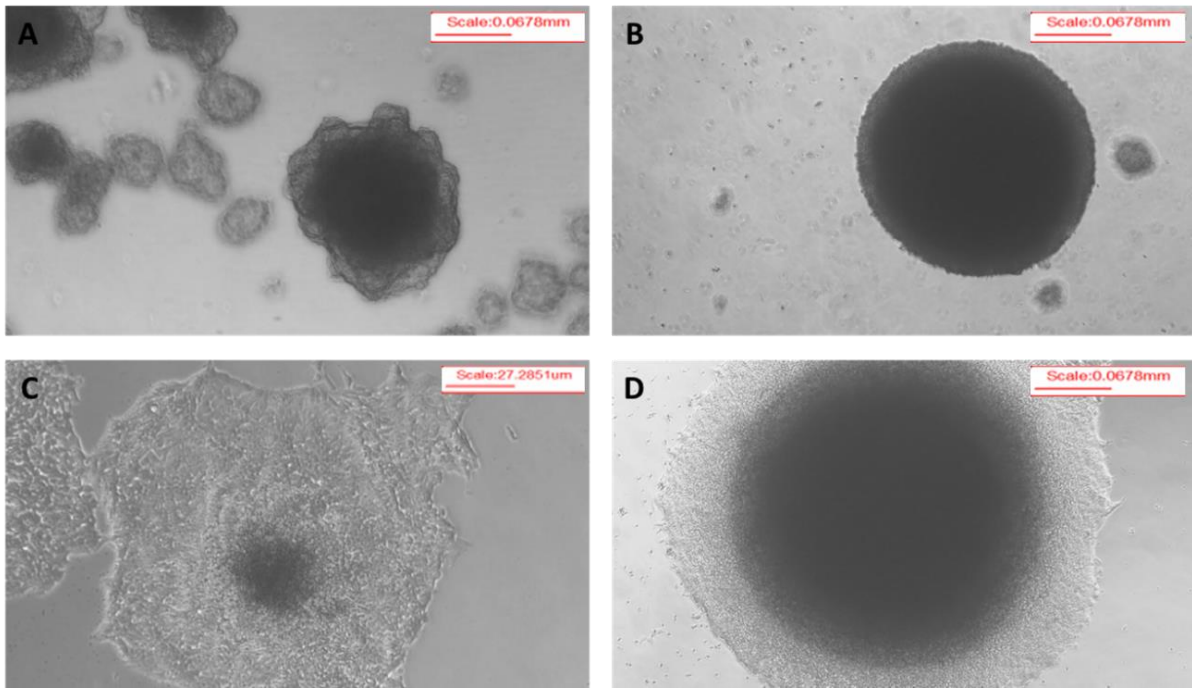


Figure 3.7: Comparison of EB morphology during growth in Petri dish and 96 well plates.

Passage 12, P19 SCs were seeded and formed in P60 microbiology Petri dishes and ultra-low attachment 96 well plates over a period of 2-4 days, then 3-4 EBs were seeded into individual wells in 24 well plates. Cells were grown at 37°C, 95% air and 5% CO₂ and cultured in complete α -MEM containing 10% foetal calf serum (FCS) and 100 units/mL penicillin together with 100 μ g/mL streptomycin. Images were taken with an Olympus inverted and EVOS® FL Cell Imaging microscopes. (A) EBs were seeded in Petri dish. (B) EBs seeded in 96 well plates. (C) EBs grown in Petri dishes, plated. (D) EBs grown in 96 well-plates, plated. Images were taken at 4X magnification.

More importantly, we observed that EBs generated by the Petri dish method produced cardiomyocytes which needed to grow to very high confluency before beating clusters could be identified and this was not always consistent (Figure 3.8A). In contrast, EBs from the ultra-low attachment 96-well plates produced distinct beating cardiomyocytes within 3 days of plating (Figure 3.8B). Very often individual cells are spindle-shaped with an extended length, that are more morphologically associated with actin filaments, which were also seen beating in culture (Figure 3.8B) (Cros *et al.*, 2014)

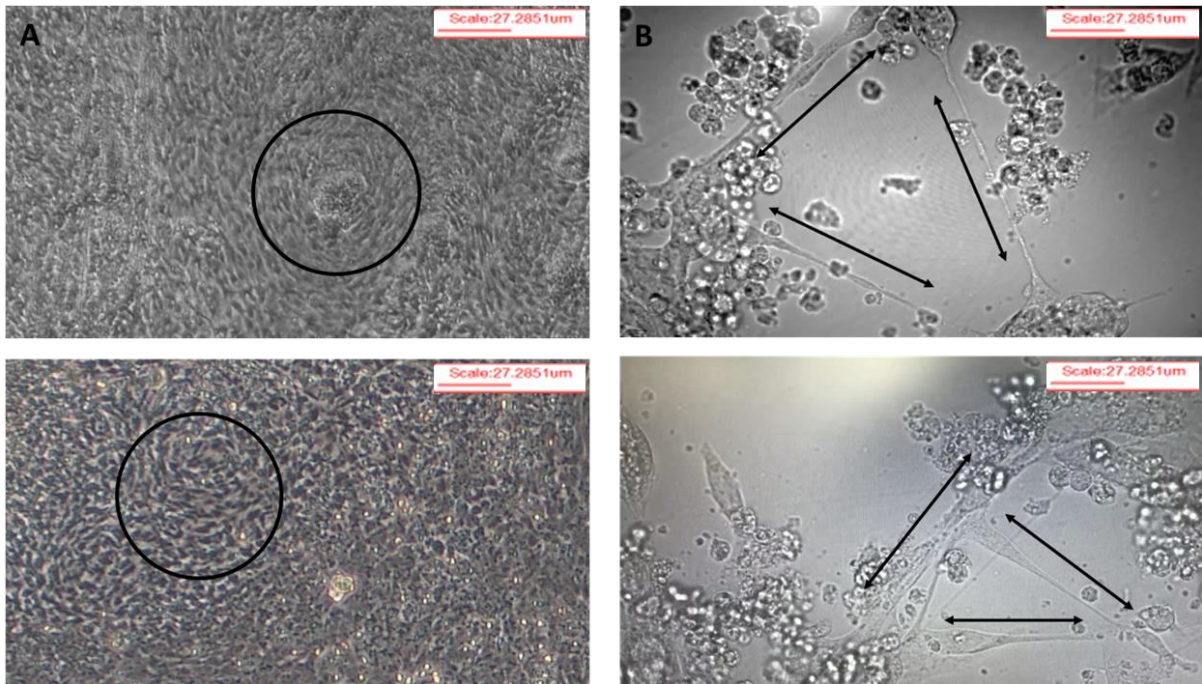


Figure 3.8: Beating cardiomyocyte generated from EBs grown in Petri dish and 96 well plates.

Passage 12, P19 SCs were seeded and formed in P60 microbiology Petri dishes and ultra-low attachment 96 well plates over a period of 2-4 days, then 3-4 EBs were seeded into individual wells in 24 well plates. Cells were grown at 37°C, 95% air and 5% CO₂ and cultured in complete α -MEM containing 10% foetal calf serum (FCS) and 100 units/mL penicillin together with 100 μ g/mL streptomycin. Images were taken with an Olympus inverted microscope. (A) Circles indicate the contractile region of cardiomyocyte from EBs grown in Petri dishes (4X magnification). (B) Arrows indicate contractile direction of individual cardiomyocytes generated from EBs grown using ultra-low attachment 96-well plate (10X magnification).

3.2.4 Effects of SA and ASA on EB formation in Petri dishes and ultra-low attachment 96-well plates in the presence and absence of LPA.

To determine whether our treatment conditions altered the size of EBs formed, studies were carried out examining the effects of increasing concentrations of SA or ASA in the absence and presence of LPA using EBs from either the Petri dish or the ultra-low attachment 96-well plate models. Figure 3.9A shows a concentration-dependent growth inhibition in EBs generated from Petri dishes when SA was used alone. The latter reduced EB size to around 25% at 0.3mM and to more than 50% at 1mM. By comparison, ASA did not appear to significantly alter EB size (Figure 3.9A and B). The reason for this discrepancy is not clear, especially as the data in each case represent an n of at least 8 individual experiments. When combined with SA, LPA appeared to enhance (20-40%) EB size formation in the presence of 0.03-0.3 mM SA. In contrast, EB size was decreased (60-70%) in the presence of LPA and ASA at 0.3-1mM expressed a decrease in overall EB diameter. In contrast to these findings above, parallel studies conducted with EBs grown in ultra-low attachment 96-well plates showed that none of the treatment conditions altered EB size which remained at the optimum diameter of around 350-450 μ m (Figure 3.10A and B). These are indeed important observations and may suggest that the consistency in the sizes of EBs generated with the ultra-low attachment model gives more reproducible data.

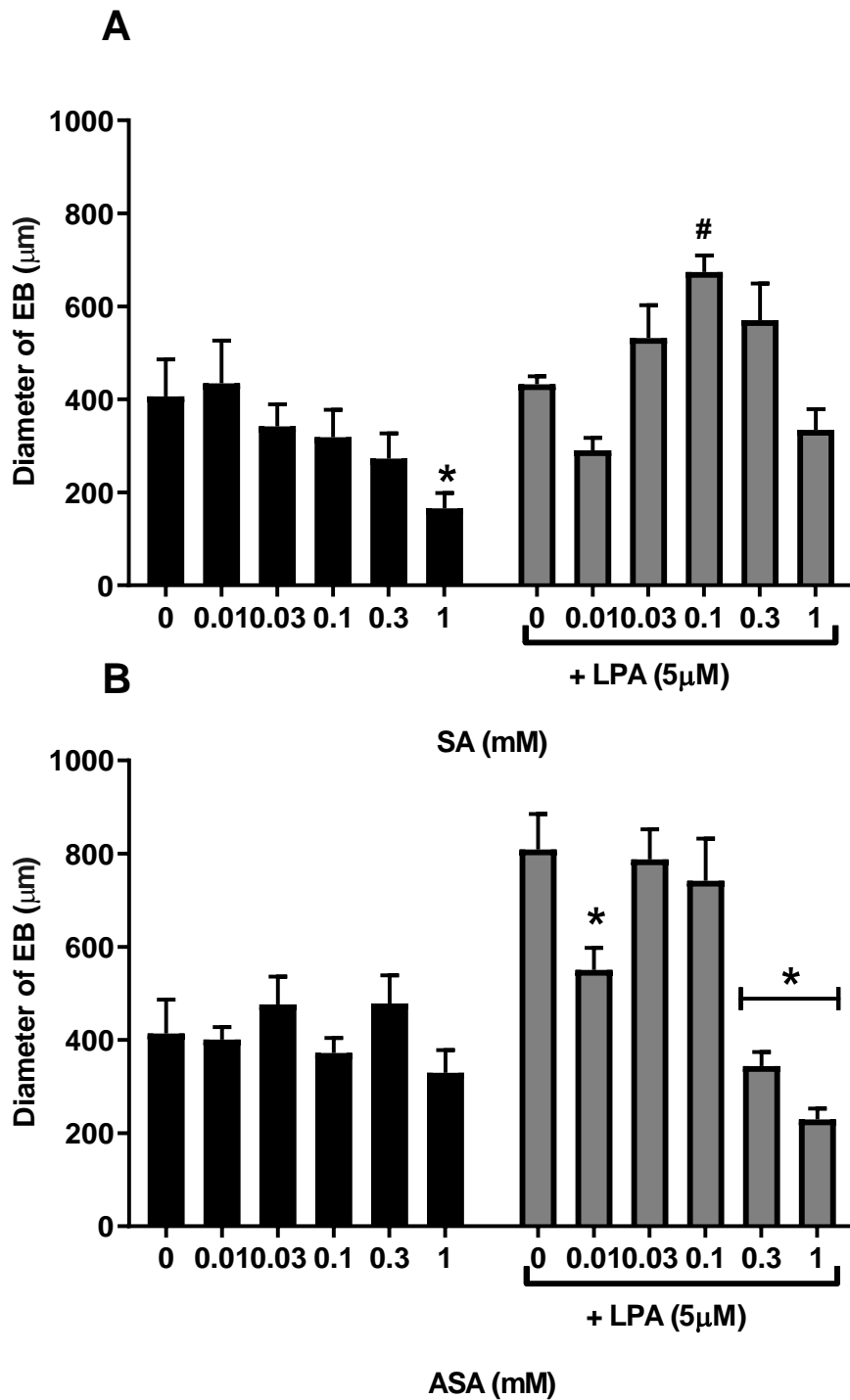


Figure 3.9: Effects of SA and ASA on EB formation and growth in Petri dishes.

Embryoid bodies formed in P60 microbiology Petri dishes and cultured over a period of 4 days. Cells were grown at 37°C, 95% air and 5% CO₂ and cultured in complete α -MEM containing 10% foetal calf serum (FCS) and 100 units/mL penicillin together with 100 μ g/mL streptomycin. (A) SA or SA + LPA (5 μ M) treated cells (B) ASA or ASA + LPA (5 μ M) treated cells. Statistical comparison was performed using two-way ANOVA with Dunnett's post Hoc test ($\alpha=0.05$). 20-30 EBs per microscope field were examined at x3 fields per well. The data represents the means \pm S.E.M. of 8 individual experiments. (A)* Represents statistical comparison between SA relative to control # represents statistical comparison relative to LPA. (B) * denotes statistical comparison relative to LPA.

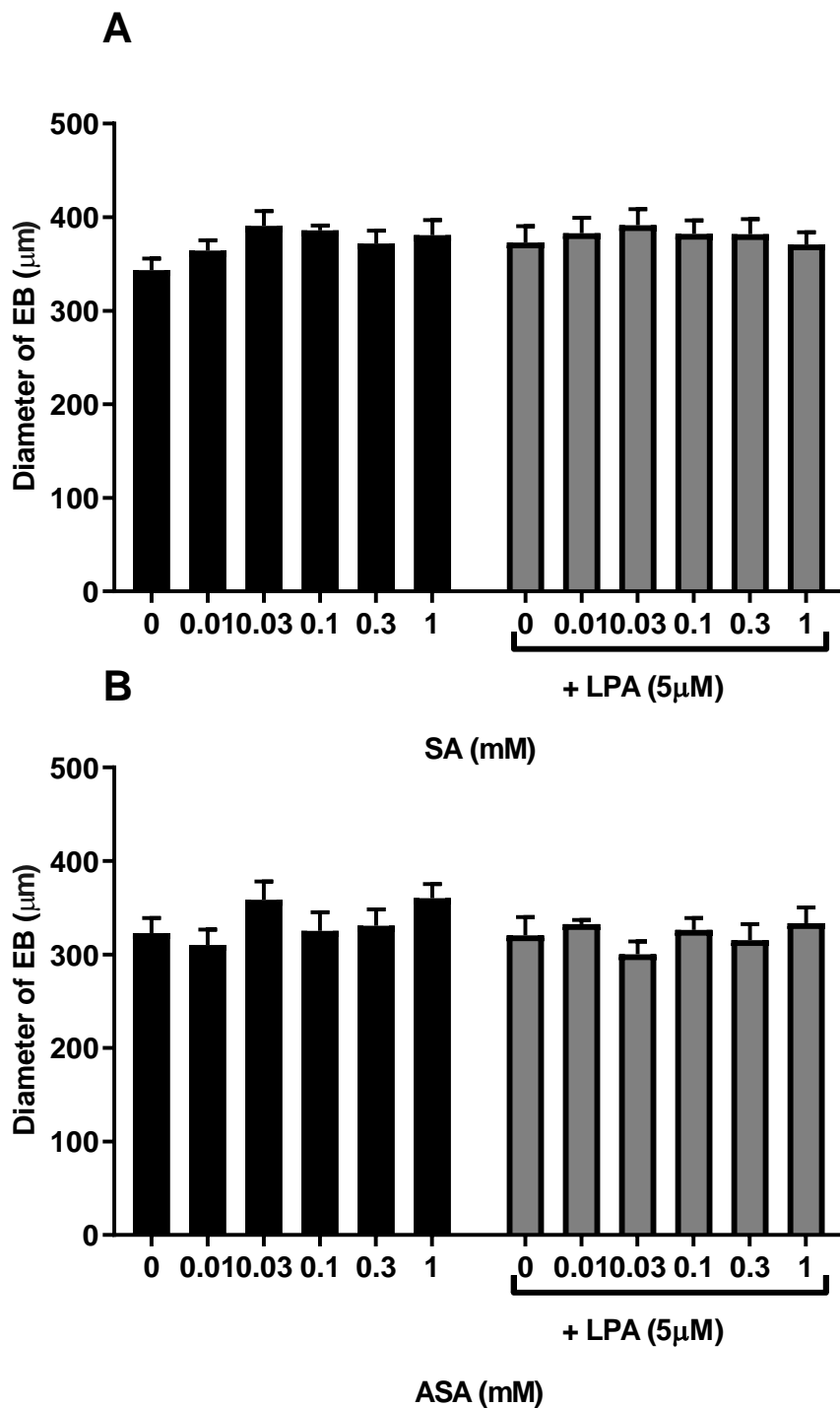


Figure 3.10: Diameter study on EB's treated with SA and ASA, grown in 96 well plates.

Embryoid bodies formed in ultra-low attachment 96 well plates and cultured over a period of 2 days. Cells were grown at 37°C, 95% air and 5% CO₂ and cultured in complete α -MEM containing 10% foetal calf serum (FCS) and 100 units/mL penicillin together with 100 μ g/mL streptomycin. (A) SA or SA + LPA (5 μ M) treated cells (B) ASA or ASA + LPA (5 μ M) treated cells. Statistical comparison was performed using two-way ANOVA with Dunnett's post Hoc test ($\alpha=0.05$). 60 EBs per microscope field were examined at x3 fields. The data represents the means \pm S.E.M. of 8 individual experiments.

3.3 Examining the effect of LPA on MLC-1v expression.

To examine the effects of LPA alone on the differentiation of cardiomyocytes, P19 SCs were seeded with increasing concentrations of LPA ranging from 1 μ M, 5 μ M, 10 μ M, and 20 μ M. To examine the extent of LPA induced differentiation, the treatments were compared to DMSO 1% as a positive control and examined for the expression of the cardiac-specific marker MLC1-v using western blotting, the results in Figure 3.11 showed a concentration-dependent expression of MLC-1v, reaching significant maximal induction of MLC-1v at 10 μ M. The levels of LPA dependent expression of MLC-1v at this concentration exceeded that of DMSO induced differentiation. Expression of MLC-1v in controls was at basal levels (25-30%) seen previously in studies carried out within our group.

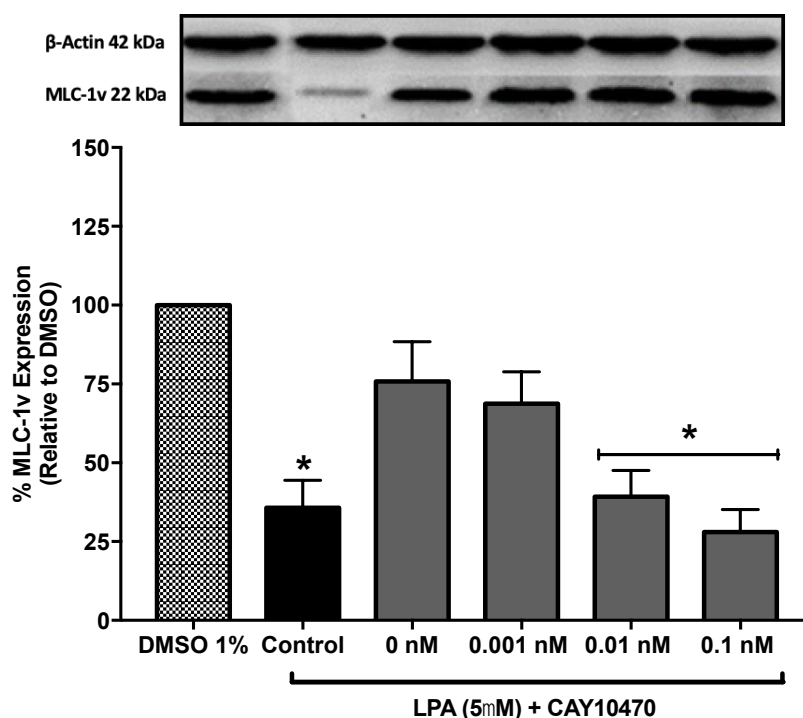


Figure 3.11: LPA concentration-dependent induction of MLC-1v expression.

Passage 9, P19 SCs were seeded at 3.5×10^5 cells/mL in P60 microbiology Petri dishes. The cells were treated in the presence and absence of LPA (5 μ M), 1-hour post treatment and grown at 37°C, 95% air and 5% CO₂. The cells were cultured in complete α -MEM medium and left to form EBs over 2 days. In this study, 6-8 EBs were plated into 24 well-plates and cultured for 3 days and lysed to be probed for β -actin and MLC-1v expression by western blotting as described in the methods. Statistical comparison was performed using two-way ANOVA with Dunnett's post Hoc test ($\alpha=0.05$). The data represents the means \pm S.E.M. of 4 individual experiments.

3.3.1 Effect of SA on MLC-1v expression in the presence and absence of LPA.

To examine the effects of SA on the differentiation process, EBs were seeded in the presence of increasing concentrations of SA (0mM, 0.1mM, 0.3mM and 1mM) in the absence and presence of LPA (5 μ M) and examined for the expression of MLC-1v using western blotting on lysates generated at days 3 and 6. The results in Figure 3.12A showed a concentration-dependent effect on the expression of MLC-1v up to 1mM SA and declining thereafter at day 3. The increase, however, was only statistically significant at 1mM, the rest were marginally above control. When used with LPA, MLC-1v expression was further enhanced by SA but at 0.1mM (30% increase) with 0.3mM showing no difference to the response with LPA alone, whilst 1mM and 3mM inhibited LPA induced MLC-1v to 40 % and 15% respectively (Figure 3.12A). This suggests that while SA may potentiate MLC-1v expression independently it is also capable of suppressing the responses to LPA.

When lysates were generated on day 6 and analysed, a different trend to that described above was observed. In this case, MLC-1v expression was inhibited concentration-dependently by SA alone which also inhibited the induction caused by LPA. In both cases, the maximum inhibition (12%) was obtained with 1-3mM of SA. It is worth noting that MLC-1v expression was relatively high in control in this set of experiments when compared to levels observed previously, suggesting that the batch of cells used in these studies may already have been partially induced to differentiate under basal conditions. In any case, the basal increase in MLC-1v expression was inhibited by SA in a manner similar to that seen when SA was applied with LPA (Figure 3.12B).

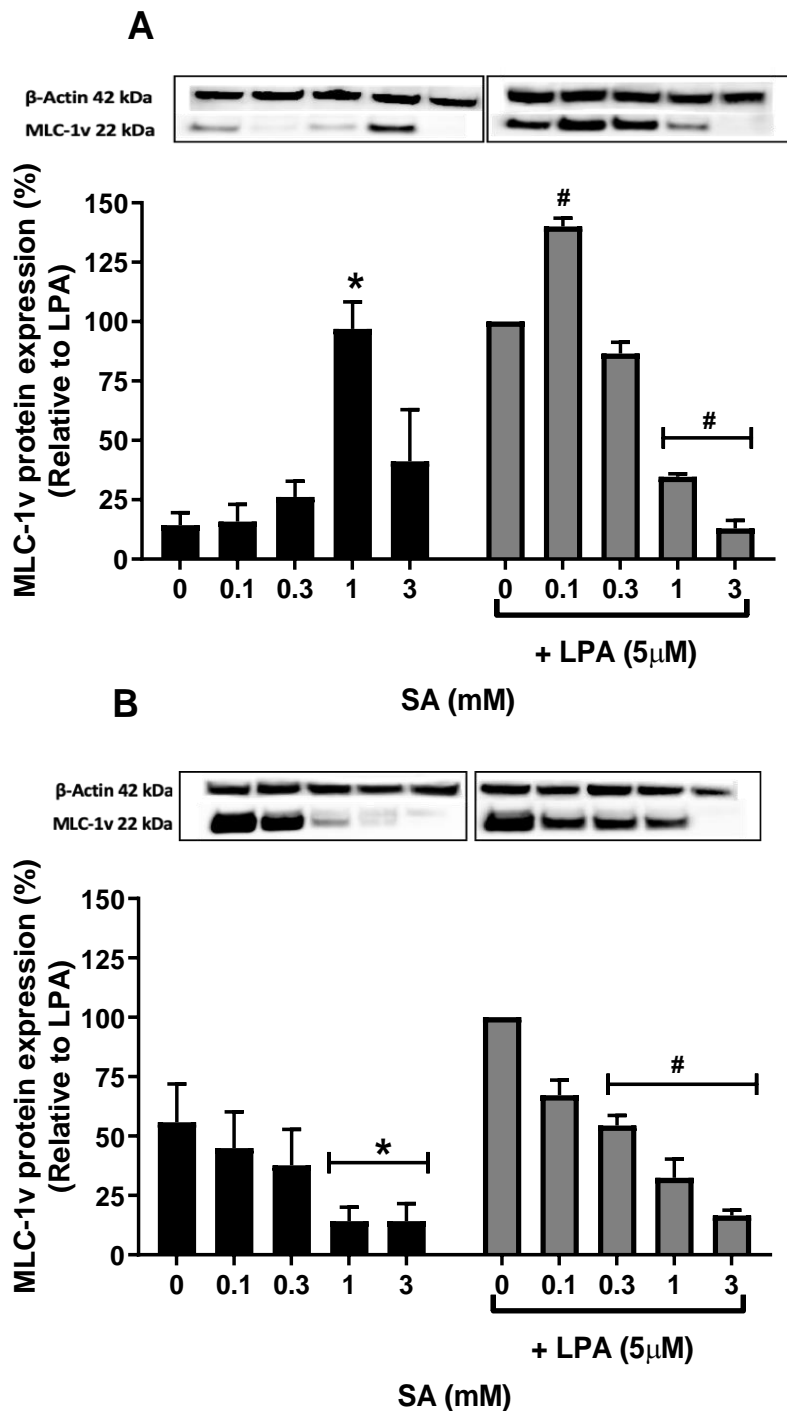


Figure 3.12: Effect of SA on differentiation of P19 SCs.

Embryoid bodies were grown in ultra-low attachment 96 well-plates and cells were treated with increasing concentrations of SA alone or in the presence of LPA (5 μ M). Cells were grown at 37 $^{\circ}$ C, 95% air and 5% CO₂ and cultured in complete α -MEM medium and left to form EBs over 2 days. In this study, 6-8 EBs were plated into 24 well-plates and cultured for 3 and 6 days and lysed to be probed for MLC-1v expression normalised to β -actin by western blotting. (A) Lysates collected at day 3. (B) Lysates collected at day 6. Statistical comparison was performed using two-way ANOVA with Dunnett's post Hoc test ($\alpha=0.05$). The data represents the means \pm S.E.M. of 7 individual experiments. * Represents statistical comparison relative to control # represents statistical comparison relative to LPA.

3.3.2 Effect of ASA on MLC-1v expression in the presence and absence of LPA.

The results in Figure 3.13A shows data for lysates obtained at day 3 and demonstrate that ASA concentration-dependently enhanced expression of MLC-1v up to 1mM, which decreased in the presence of 3mM ASA. When applied in the presence of LPA, ASA concentration-dependently decreased MLC-1v expression induced by LPA, with the maximum inhibition (30%) observed with 3mM ASA.

At day 6, lysates from control cells were found to express high levels of MLC-1v (75% of LPA response). These levels were not significantly affected by ASA, which also failed to alter the induction of MLC-1v by LPA. There was a decrease in the LPA response with 3mM ASA, but this was not statistically significant (Figure 3.13B).

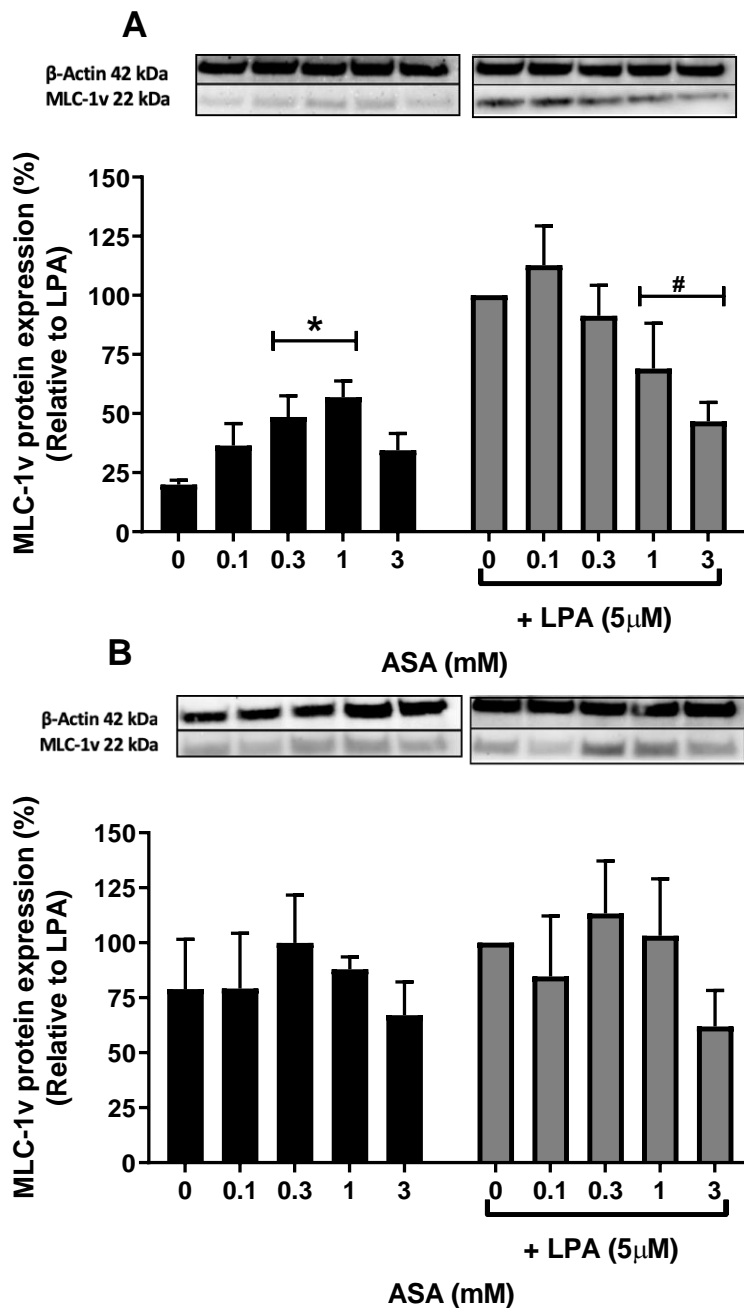


Figure 3.13: Effect of ASA on differentiation of P19 SCs.

Embryoid bodies were grown in ultra-low attachment 96 well-plates and cells were treated with increasing concentrations of ASA alone or in the presence of LPA (5 μM). Cells were grown at 37°C, 95% air and 5% CO₂ and cultured in complete α-MEM medium and left to form EBs over 2 days. In this study, 6-8 EBs were plated into 24 well-plates and cultured for 3 and 6 days and lysed to be probed for MLC-1v expression normalised to β-actin by western blotting. (A) Lysates collected at day 3. (B) Lysates collected at day 6. Statistical comparison was performed using two-way ANOVA with Dunnett's post Hoc test (α=0.05). The data represents the means ± S.E.M. of 7 individual experiments. * Represents statistical comparison relative to control # represents statistical comparison relative to LPA.

3.4 Cell viability assay

3.4.1 MTT assay determining the toxicity of SA

To determine whether SA induced cytotoxicity on P19 stem cell, the MTT assay was carried out as described in the experimental protocol in chapter 2. The data seen in Figure 3.14A shows concentration-dependent cytotoxicity in controls on day 3, in which the lower concentrations (0.1-0.3mM) had little or no cytotoxicity in both LPA and non-LPA treated cells. At 1mM SA there was a significant reduction (40%) of cell viability which increased to 55% with 3mM SA. In the presence of LPA (5 μ M), SA was only found to be cytotoxic at 3mM, reducing viability to nearly 60%. LPA on its own appeared to suppress MTT metabolism when compared to controls, reducing this by about 20%. These trends on MTT metabolism were reflected when total cell count was determined at the end of each experiment. Similar to MTT metabolism SA had no effect on cell number at 0.1-0.3mM but reduced at 1-3mM. This was also seen in LPA treated cells but only reduced at 3mM (Figure 3.14B).

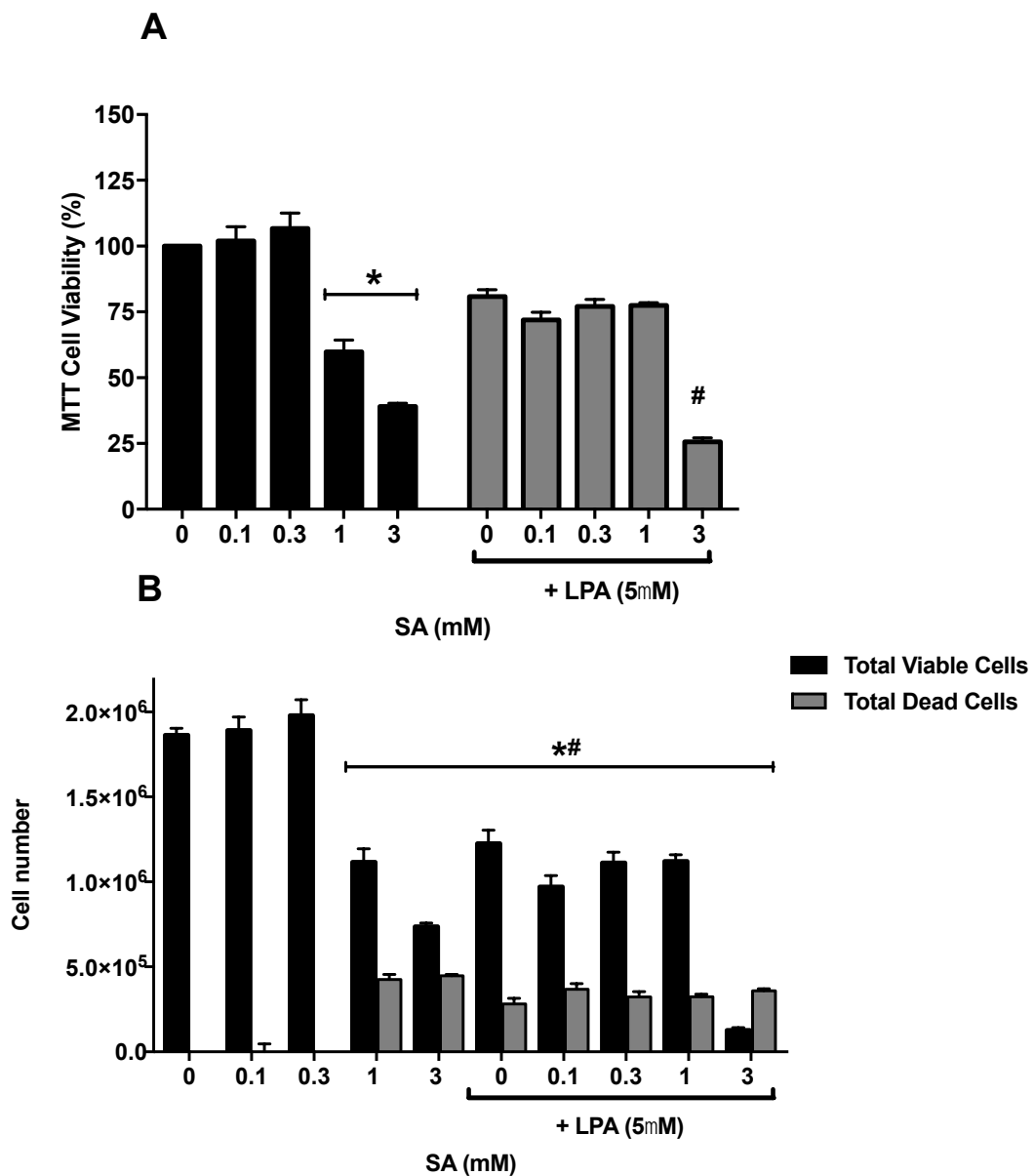


Figure 3.14: Effect of SA on cell viability in the absence and presence of LPA (day 3).

Passage 9, P19 SCs were seeded at 1×10^4 cells/mL in 96 well plates and grown for 3 days. Cells were incubated with LPA ($5\mu\text{M}$) 1-hour post seeding and/or with increasing concentrations of SA. A final concentration of 0.1mg of MTT was incubated 4 hours prior to assessing cell viability as described in materials and method and grown at 37°C , 95% air and 5% CO_2 . (A) Percentage viability assay of treated cells. (B) MTT absorption of treated cells. Graph was derived from a standard curve of cell count vs MTT absorption at 570 nm. Statistical comparison was performed using one-way ANOVA with Dunnett's post Hoc test ($\alpha=0.05$). The data represents the means \pm S.E.M. of 4 individual experiments. (A)* Represents statistical comparison relative to control and # represents statistical comparison relative to LPA. (B) *# represent statistical comparison relative to control.

The data seen in Figure 3.15A shows MTT assays carried out on SA treated cells at day 6 in which most of the concentrations (0.1-1mM) had little or no cytotoxicity in both LPA and non-LPA treated cells. At 3mM SA there was a significant reduction (75%) of cell viability. In the presence of LPA (5 μ M), SA was only found to be cytotoxicity at 3mM, reducing viability to nearly 60%. These trends on MTT metabolism were reflected when total cell count was determined at the end of each experiment. Similar to MTT metabolism SA had no effect on cell number at 0.1-1mM but reduced at 3mM. This was also seen in LPA treated cells, but the cell number was significantly increased at 0.3mM by about 50%.

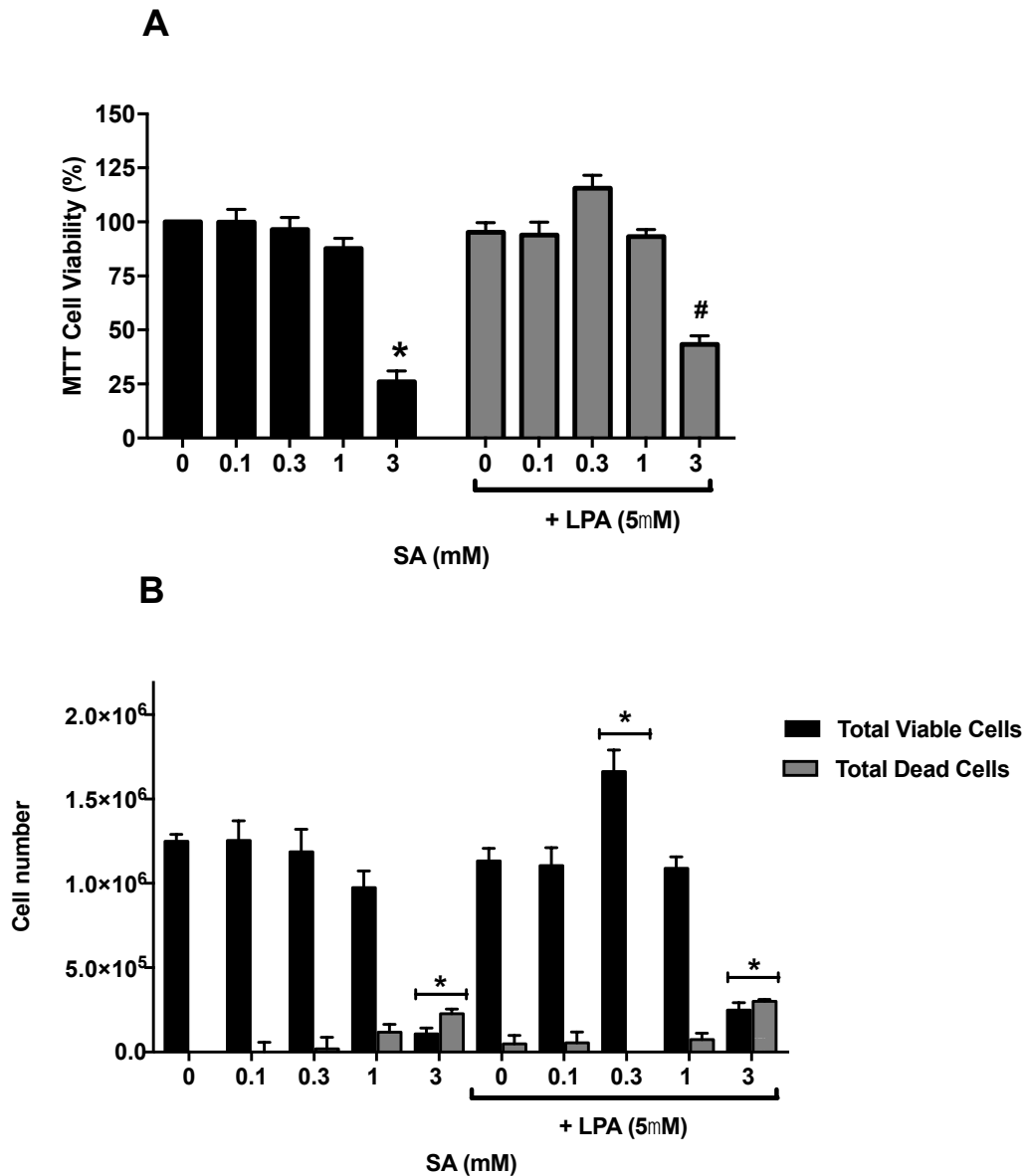


Figure 3.15: Effect of SA on cell viability in the absence and presence of LPA (day 6).

Passage 9, P19 SCs were seeded at 1×10^4 cells/mL in 96 well plates and grown for 6 days. Cells were incubated with LPA ($5\mu\text{M}$) 1-hour post seeding and/or with increasing concentrations of SA. A final concentration of 0.1mg of MTT was incubated 4 hours prior to assessing cell viability as described in materials and method and grown at 37°C , 95% air and 5% CO_2 . (A) Percentage viability assay of treated cells. (B) MTT absorption of treated cells. Graph was derived from a standard curve of cell count vs MTT absorption at 570 nm. Statistical comparison was performed using one-way ANOVA with Dunnett's post Hoc test ($\alpha=0.05$). The data represents the means \pm S.E.M. of 4 individual experiments. (A)* Represents statistical comparison relative to control and # represents statistical comparison relative to LPA. (B) * represent statistical comparison relative to control.

3.4.2 MTT assay determining the toxicity of ASA

To determine whether ASA induced cytotoxicity onto the P19 stem cell, the MTT assay was carried out as described in the experimental protocol in chapter 2. The MTT data for ASA seen at day 3 (Figure 3.16) shows a similar trend in cytotoxicity as seen in SA treated cells in controls levels at day 6 (Figure 3.15), in which most of the concentrations (0.1-1mM) had little or no cytotoxicity in both LPA and non-LPA treated cells. At 3mM ASA there was a significant reduction (70%) of cell viability. In the presence of LPA (5 μ M), ASA was only found to be cytotoxic at 3mM, reducing viability to nearly 90%. These trends on MTT metabolism were reflected when total cell count was determined at the end of each experiment. However, MTT metabolism data showed a significant reduction in cell number at 1-3mM. This was also seen in LPA treated cells.

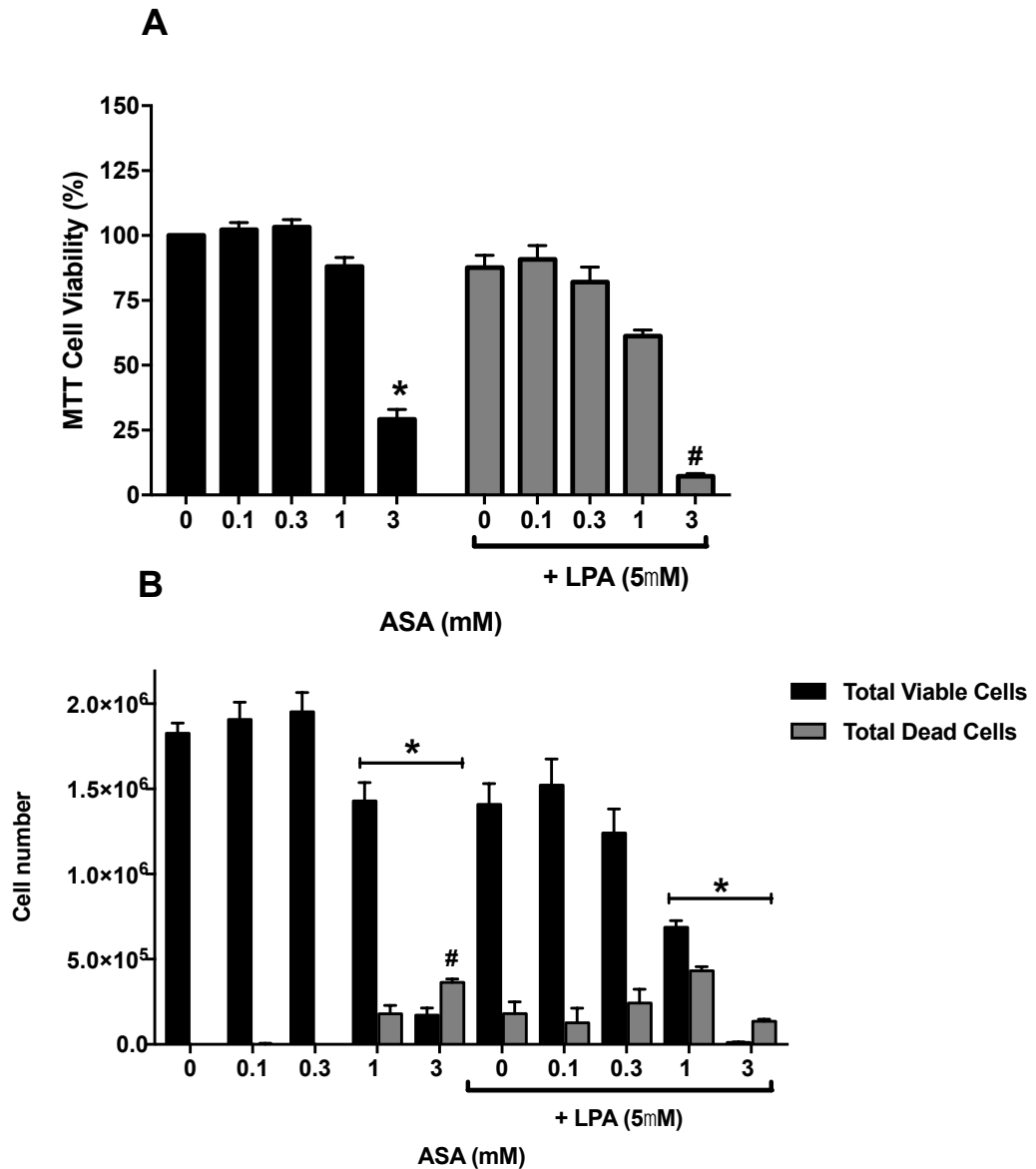


Figure 3.16: Effect of ASA on cell viability in the absence and presence of LPA (day 3).

Passage 9, P19 SCs were seeded at 1×10^4 cells/mL in 96 well plates and grown for 3 days. Cells were incubated with LPA ($5\mu\text{M}$) 1-hour post seeding and/or with increasing concentrations of ASA. A final concentration of 0.1mg of MTT was incubated 4 hours prior to assessing cell viability as described in materials and method and grown at 37°C , 95% air and 5% CO_2 . (A) Percentage viability assay of treated cells. (B) MTT absorption of treated cells. Graph was derived from a standard curve of cell count vs MTT absorption at 570 nm. Statistical comparison was performed using one-way ANOVA with Dunnett's post Hoc test ($\alpha=0.05$). The data represents the means \pm S.E.M. of 4 individual experiments. (A)* Represents statistical comparison relative to control and # represents statistical comparison relative to LPA. (B) *# represent statistical comparison relative to control.

The data seen in Figure 3.17 shows MTT assays carried out on ASA treated cells at day 6 in which most of the concentrations (0.1-1mM) had little or no cytotoxicity in both LPA and non-LPA treated cells as similar to day 3 ASA. At 3mM SA there was a significant reduction (80%) of cell viability. In the presence of LPA (5 μ M), ASA was only found to be cytotoxicity at 3mM, reducing viability to nearly 85%. These trends on MTT metabolism were reflected when total cell count was determined at the end of each experiment. Similar to MTT metabolism, ASA had no effect on cell number at 0.1-1mM but reduced at 3mM. However, in LPA treated cells, cell number was only significantly increased at 1-3mM.

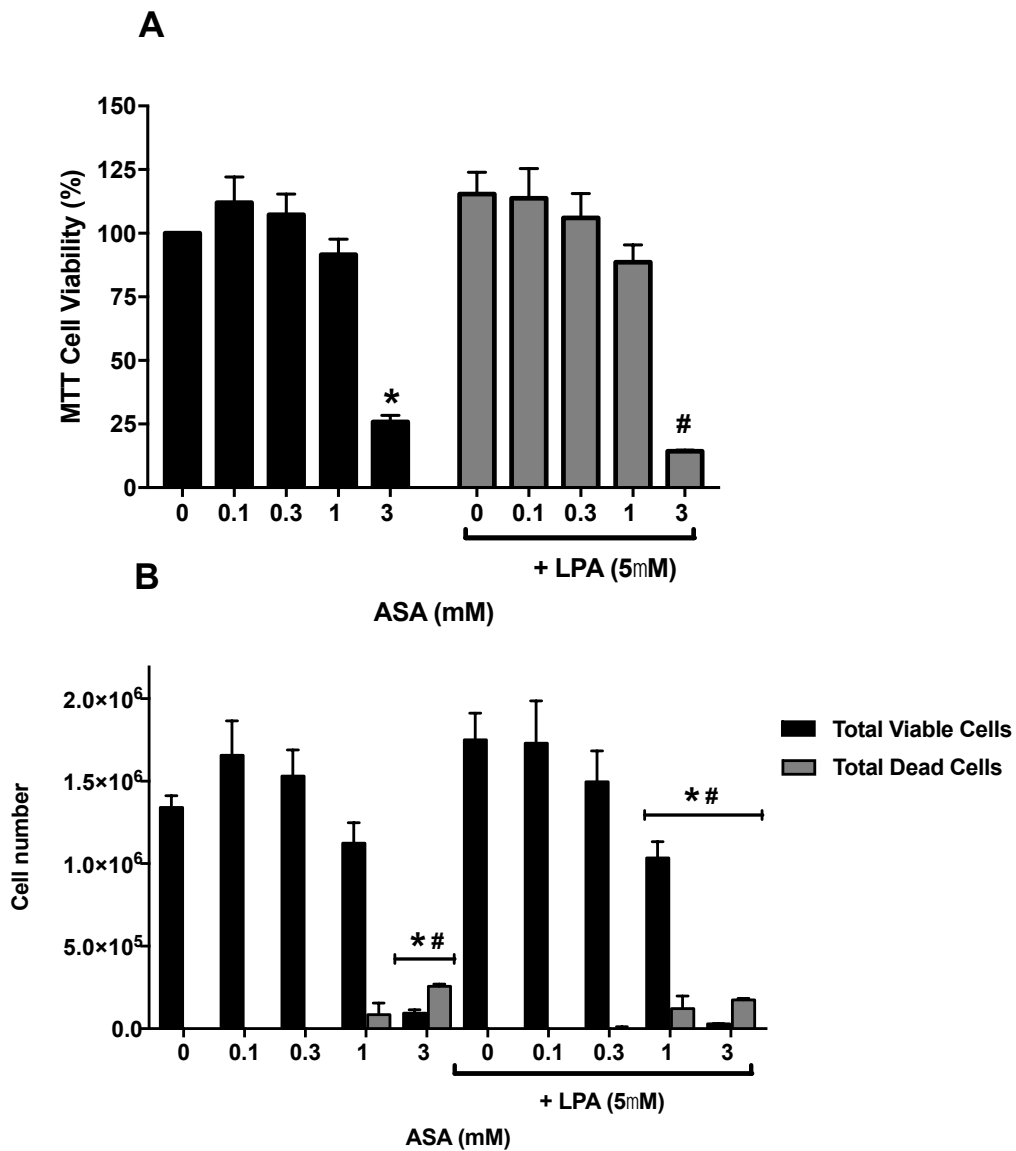


Figure 3.17: Effect of ASA on cell viability in the absence and presence of LPA (day 6).

Passage 9, P19 SCs were seeded at 1×10^4 cells/mL in 96 well plates and grown for 6 days. Cells were incubated with LPA ($5\mu\text{M}$) 1-hour post seeding and/or with increasing concentrations of ASA. A final concentration of 0.1mg of MTT was incubated 4 hours prior to assessing cell viability as described in materials and method and grown at 37°C , 95% air and 5% CO_2 . (A) Percentage viability assay of treated cells. (B) MTT absorption of treated cells. Graph was derived from a standard curve of cell count vs MTT absorption at 570 nm. Statistical comparison was performed using one-way ANOVA with Dunnett's post Hoc test ($\alpha=0.05$). The data represents the means \pm S.E.M. of 4 individual experiments. (A)* Represents statistical comparison relative to control and # represents statistical comparison relative to LPA. (B) *# represent statistical comparison relative to control.

3.5 Effect of LPA, SA and ASA on p65-NFκB expression.

To examine the effects of NFκB in the differentiation process, cells were seeded in suspension in the absence (Figure 3.18A) and presence of LPA (Figure 3.18B), SA (Figure 3.18C) and ASA (Figure 3.18D); lysates were generated at selected time points (5, 10, 15, 30 mins and 1, 3, 6, 9, 24 hours) to examine for the expression of p65-NFκB using western blotting. The results in Figure 3.18A showed no significant change in basal p65-NFκB expression at any of the time points when the densitometric data were compared. In the presence of LPA (5uM), total p65-NFκB expression was stable for the first 6 hours but decreased by more than 50% at 9 and 24 hours (Figure 3.18B). It is not clear why there was this decrease, but it is worth noting that the loading volume (20μg/μL) was greater at these two-time points than the rest of the other time points (data not shown). This would indicate a potential loss of cells which may reflect some degree of cytotoxicity. This was not previously seen in the long-time course studies and needs further investigation. Incubation with SA (1mM) or ASA (1mM) appears to cause time-dependent increases in total p65-NFκB levels, which was significant at 3 hours in SA (Figure 3.18C) and between 30 mins and 3 hours with ASA (Figure 3.18D). With both drugs, levels of p65-NFκB declined from 6 hours onwards back to basal levels. These trends were however only evident when compared within the same experimental group. When compared to trends in cells treated with complete medium alone the changes in p65-NFκB levels did not show much of a significant difference to the latter condition. For ease of comparison, the data has been replotted as seen in Figure 3.19, comparing cells incubated with complete medium alone, with LPA (Figure 3.19A), SA (Figure 3.19B), ASA (Figure 3.19C). These figures show that there was not much of a significant difference as already highlighted above. Where difference was observed, these were isolated and not easily explained. Similar comparisons have been carried out between LPA and SA (Figure 3.20A) and LPA and ASA (Figure 3.20B). In this case, the increasing trends seen with SA and ASA did not appear to be significantly different from the LPA responses. The reduction in p65-NFκB in the presence of LPA was however still evident and appears to be significant when

compared to ASA at 24 hours. The decline in p65-NFκB in the presence of ASA at 6 hours appears to be significantly different from the levels seen in LPA treated cells. These trends would, however, appear random and it is, therefore, difficult to draw any firm conclusions.

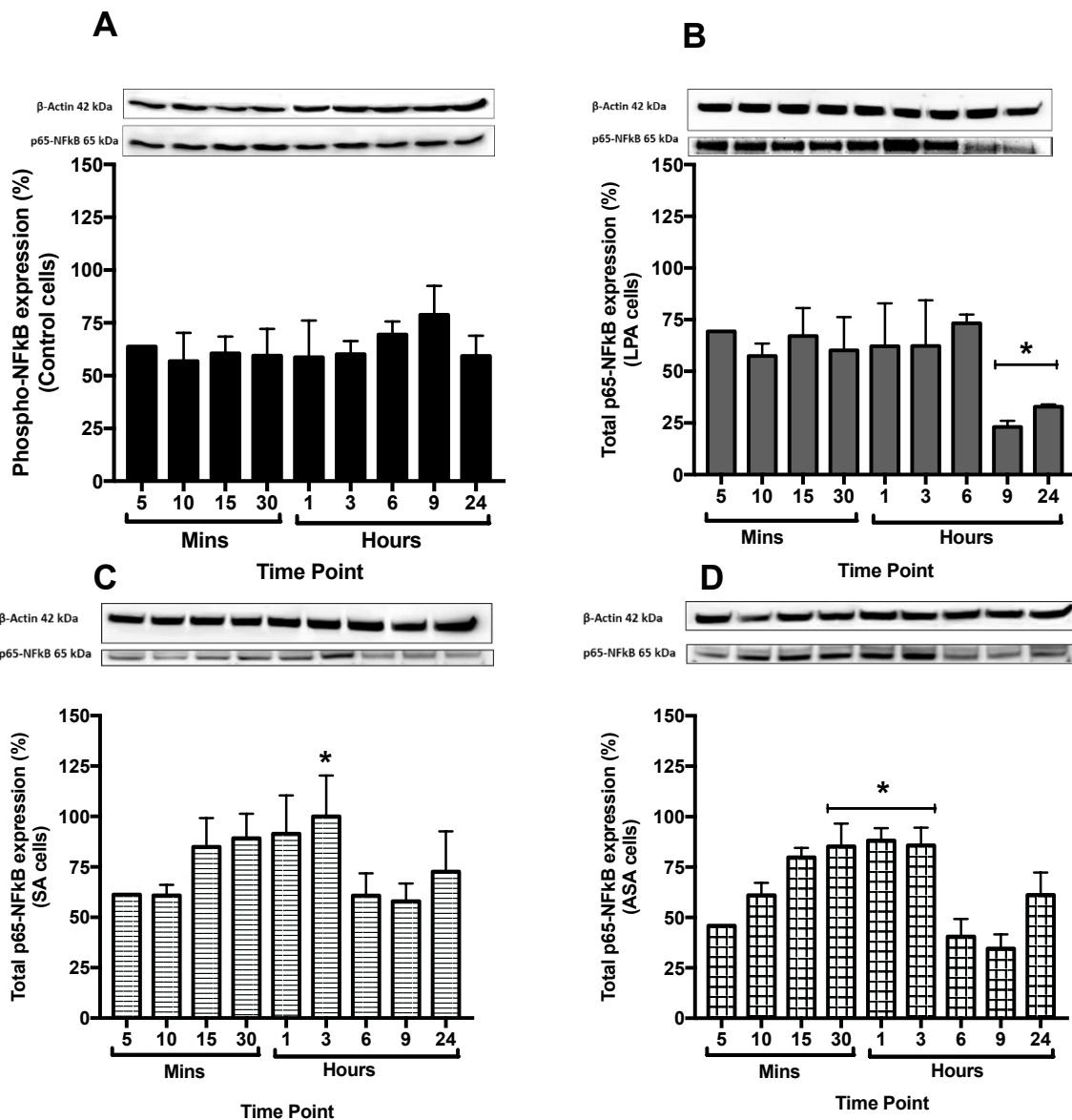


Figure 3.18: Densitometric data for total p65-NFκB protein expression.

Passage 9, P19 SCs were seeded in complete α -MEM at 7×10^7 cells/mL in 1.5 mL microcentrifuge tubes for selected time points at 37°C, 95% air and 5% CO₂. Cells were lysed and probed for p65-NFκB expression normalised to β -actin by western blotting as described in the methods. (A) Control, (B) LPA, (C) SA and (D) ASA treated cells. Statistical comparison was performed using one-way ANOVA with Dunnett's post Hoc test ($\alpha=0.05$). The data represents the means \pm S.E.M. of 4 individual experiments.

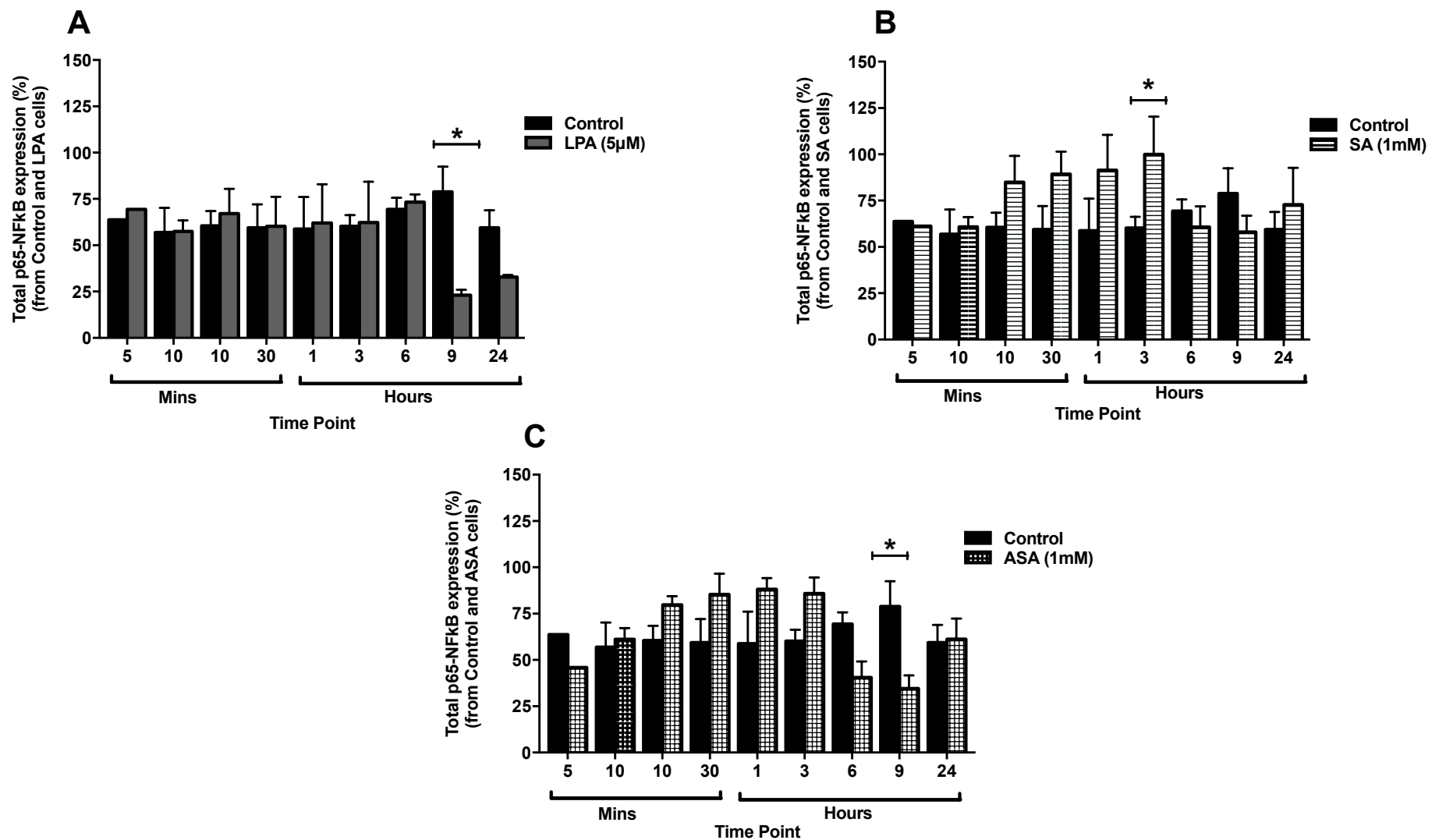


Figure 3.19: Control p65-NFκB densitometric data compared with LPA, SA and ASA p65-NFκB.

Passage 9, P19 SCs were seeded in complete α -MEM at 7×10^7 cells/mL in 1.5 mL microcentrifuge tubes for selected time points at 37°C, 95% air and 5% CO₂. Cells were lysed and probed for p65-NFκB expression normalised to β -actin by western blotting as described in the methods. (A) Control p65-NFκB compared to LPA p65-NFκB levels. (B) Control p65-NFκB compared to SA p65-NFκB levels. (C) Control p65-NFκB compared to ASA p65-NFκB levels. Statistical comparison was performed using two-way ANOVA with Dunnett's post Hoc test ($\alpha=0.05$). The data represents the means \pm S.E.M. of 4 individual experiments.

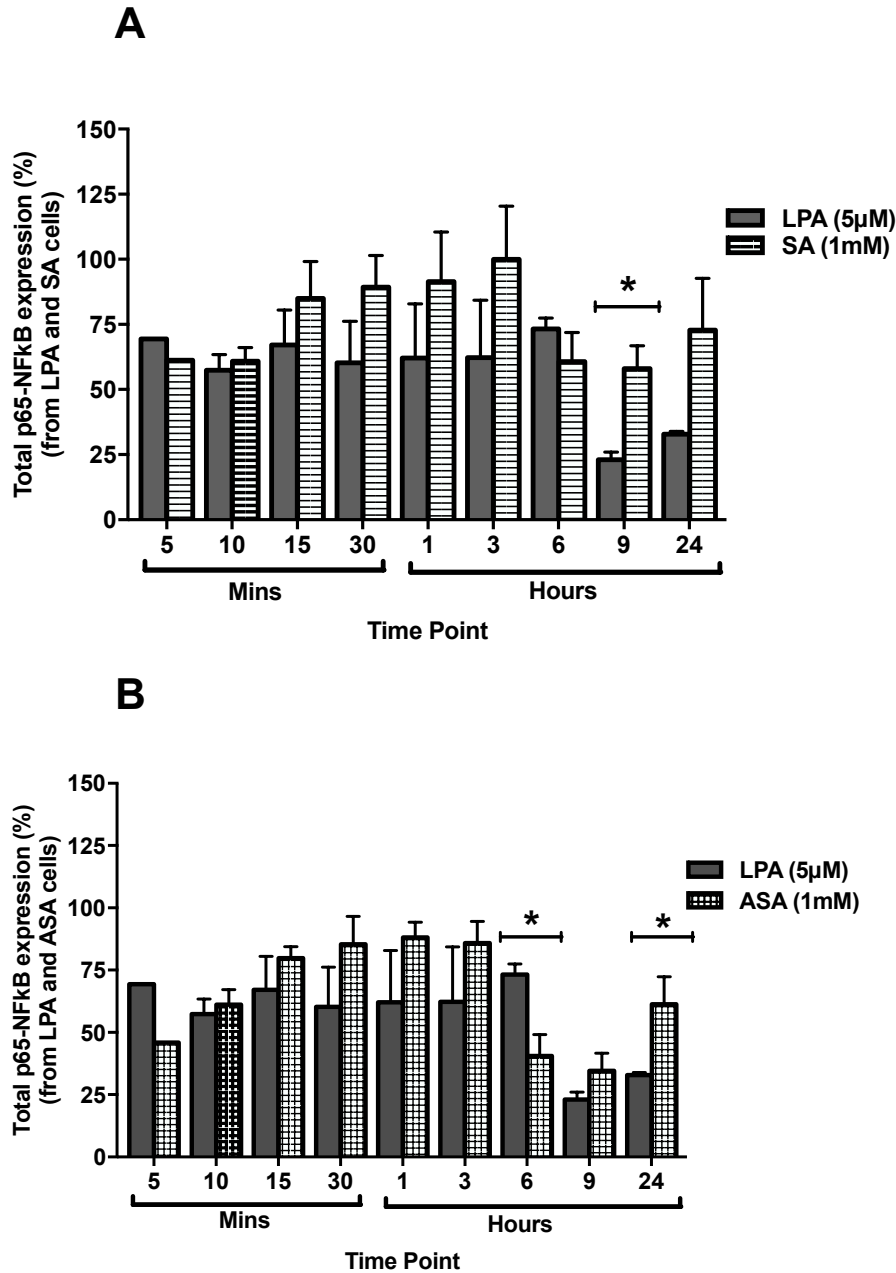


Figure 3.20: LPA p65-NFκB densitometric data compared with SA and ASA p65-NFκB.

Passage 9, P19 SCs were seeded in complete α -MEM at 7×10^7 cells/mL in 1.5 mL microcentrifuge tubes for selected time points at 37°C, 95% air and 5% CO₂. Cells were lysed and probed for p65-NFκB expression normalised to β -actin by western blotting as described in the methods. (A) LPA p65-NFκB compared to SA p65-NFκB levels. (B) LPA p65-NFκB compared to ASA p65-NFκB levels. Statistical comparison was performed using two-way ANOVA with Dunnett's post Hoc test ($\alpha=0.05$). The data represents the means \pm S.E.M. of 4 individual experiments.

3.5.1 Effect of LPA, SA and ASA on phospho NFκB expression.

To further examine the role of NFκB on the differentiation process, cells seeded in suspension were treated for selected time points (5, 10, 15, 30 mins and 1, 3, 6, 9, 24 hours) with complete medium alone, LPA (5μM), SA (1mM) or ASA (1mM) and examined for the expression of phospho NFκB as an index of native NFκB, using western blotting. The results in Figure 3.21A show low basal levels of phospho NFκB which did not change over time in controls. When cells were treated with LPA, a time-dependent, bell-shaped expression in phospho NFκB was observed, becoming evident at 3 hours, peaking at 6 hours and declining at 9 hours, returning to basal levels at 24 hours (Figure 3.21B). Similar trends were seen with SA (Figure 3.21C) and ASA (Figure 3.21D) with the exception that the peak with SA was seen at 9 hours. These results show that NFκB can be phosphorylated on Ser 538 by LPA, SA and ASA independently in a delayed manner. For ease of comparison, the data has been replotted as seen in Figure 3.22, comparing cells incubated with complete medium alone with LPA (Figure 3.22A), SA (Figure 3.22B), ASA (Figure 3.22C). The trends mentioned above were further reflected in these figures, and significance was noted at both 6 and 9 hours in the presence of SA and ASA (Figure 3.22C). Similar comparisons have been carried out between LPA and SA (Figure 3.23A) or LPA and ASA (Figure 3.23B). In this case, significance was seen at both 6 and 9 hours in the presence of SA, where LPA treated cells peaked at 6 hours and delayed phosphorylation of NFκB was seen at 9 hours in SA treated cells. However, there was no significant difference seen in ASA treated cells when compared to LPA, as they shared a similar bell-shaped trend.

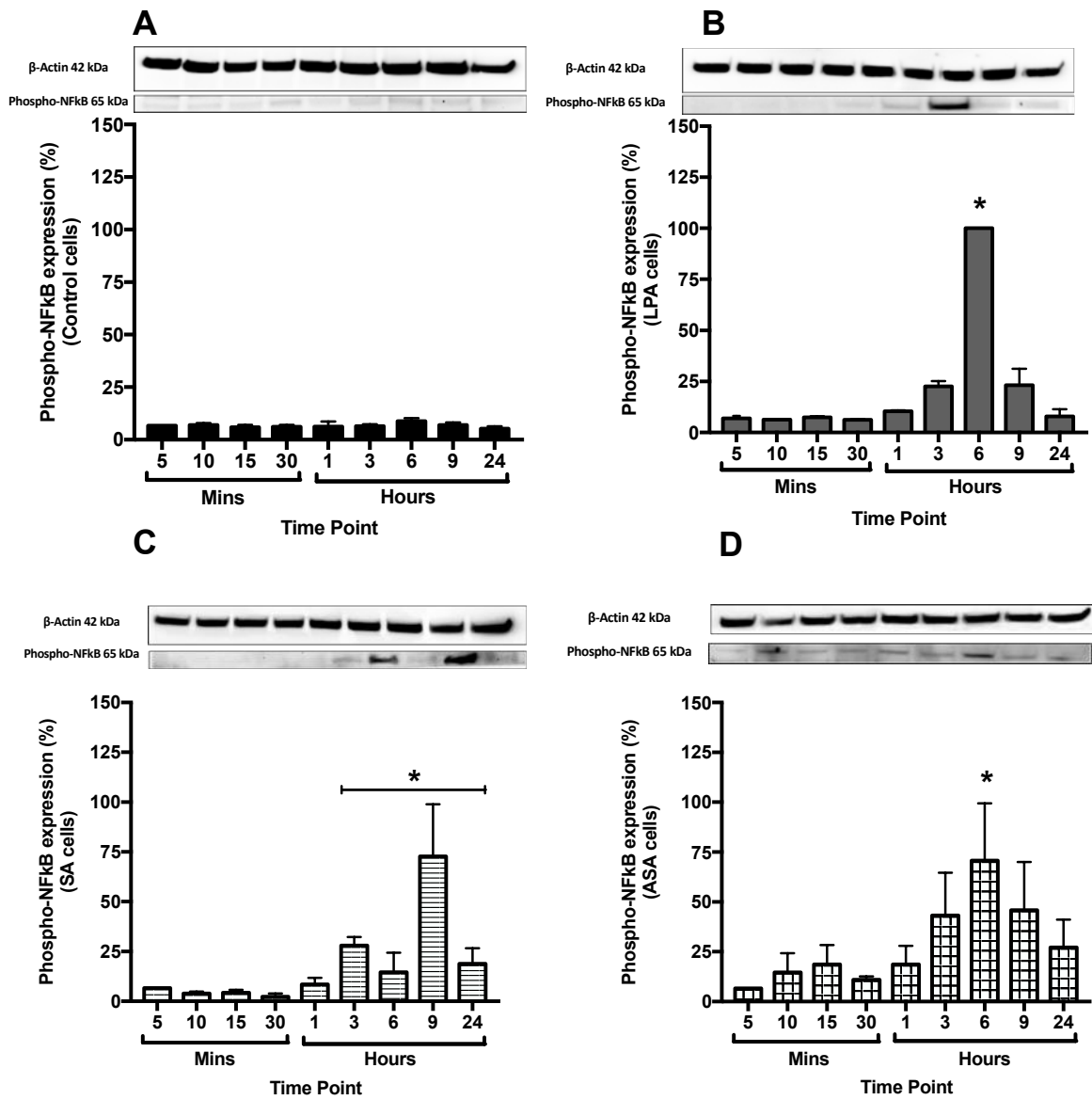


Figure 3.21: Densitometric data for total phospho NFκB protein expression.

Passage 9, P19 SCs were seeded in complete α -MEM at 7×10^7 cells/mL in 1.5 mL microcentrifuge tubes for selected time points at 37°C, 95% air and 5% CO₂. Cells were lysed and probed for phospho NFκB expression normalised to β -actin by western blotting as described in the methods. (A) Control, (B) LPA, (C) SA and (D) ASA treated cells. Statistical comparison was performed using one-way ANOVA with Dunnett's post Hoc test ($\alpha=0.05$). The data represents the means \pm S.E.M. of 4 individual experiments.

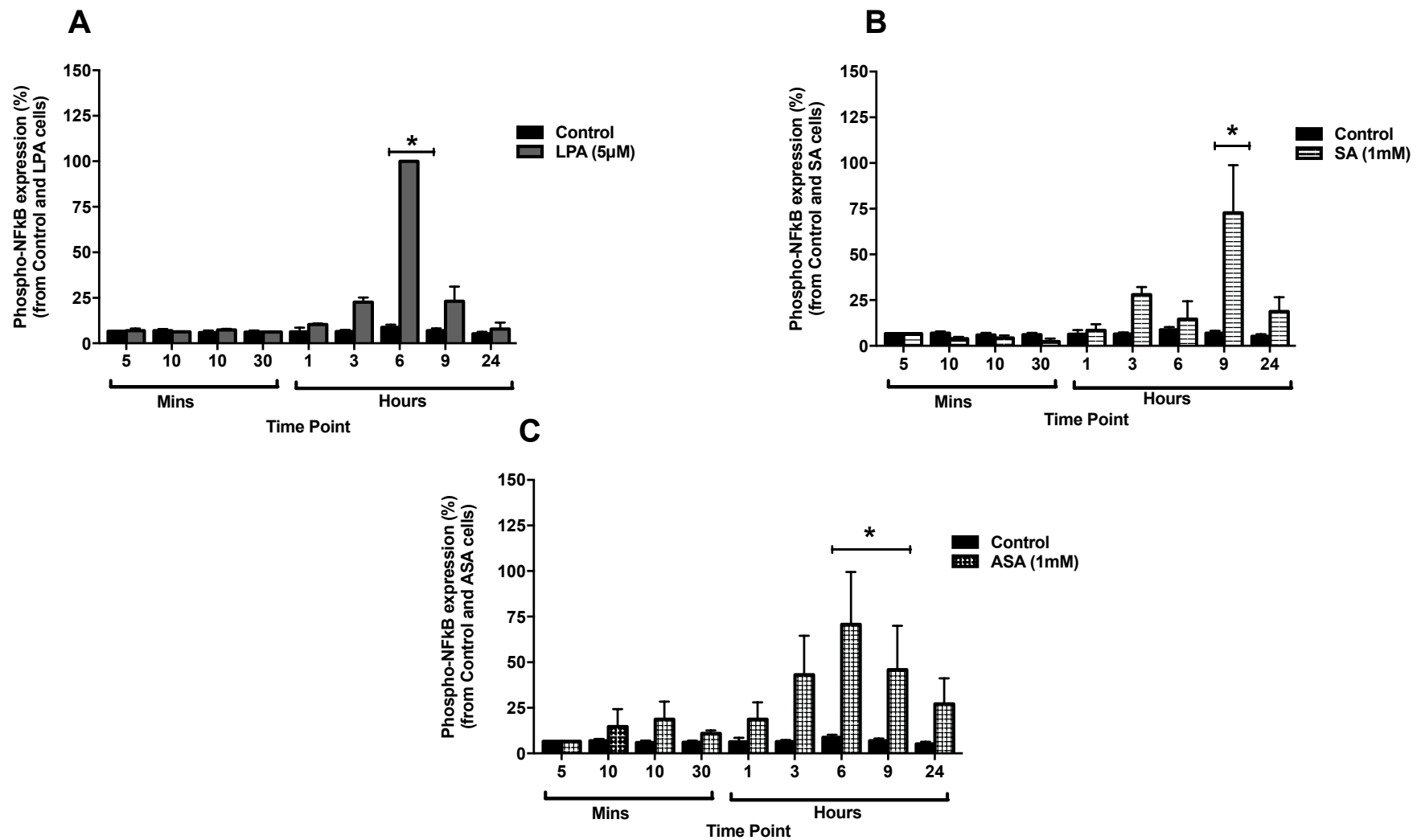


Figure 3.22: Control phospho NFκB densitometric data compared with LPA, SA and ASA phospho NFκB.

Passage 9, P19 SCs were seeded in complete α -MEM at 7×10^7 cells/mL in 1.5 mL microcentrifuge tubes for selected time points at 37°C, 95% air and 5% CO₂. Cells were lysed and probed phospho NFκB expression normalised to β -actin by western blotting as described in the methods. (A) Control phospho NFκB compared to LPA phospho NFκB levels. (B) Control phospho NFκB compared to SA phospho NFκB levels. (C) Control phospho NFκB compared to ASA phospho NFκB levels. Statistical comparison was performed using two-way ANOVA with Dunnett's post Hoc test ($\alpha=0.05$). The data represents the means \pm S.E.M. of 4 individual experiments.

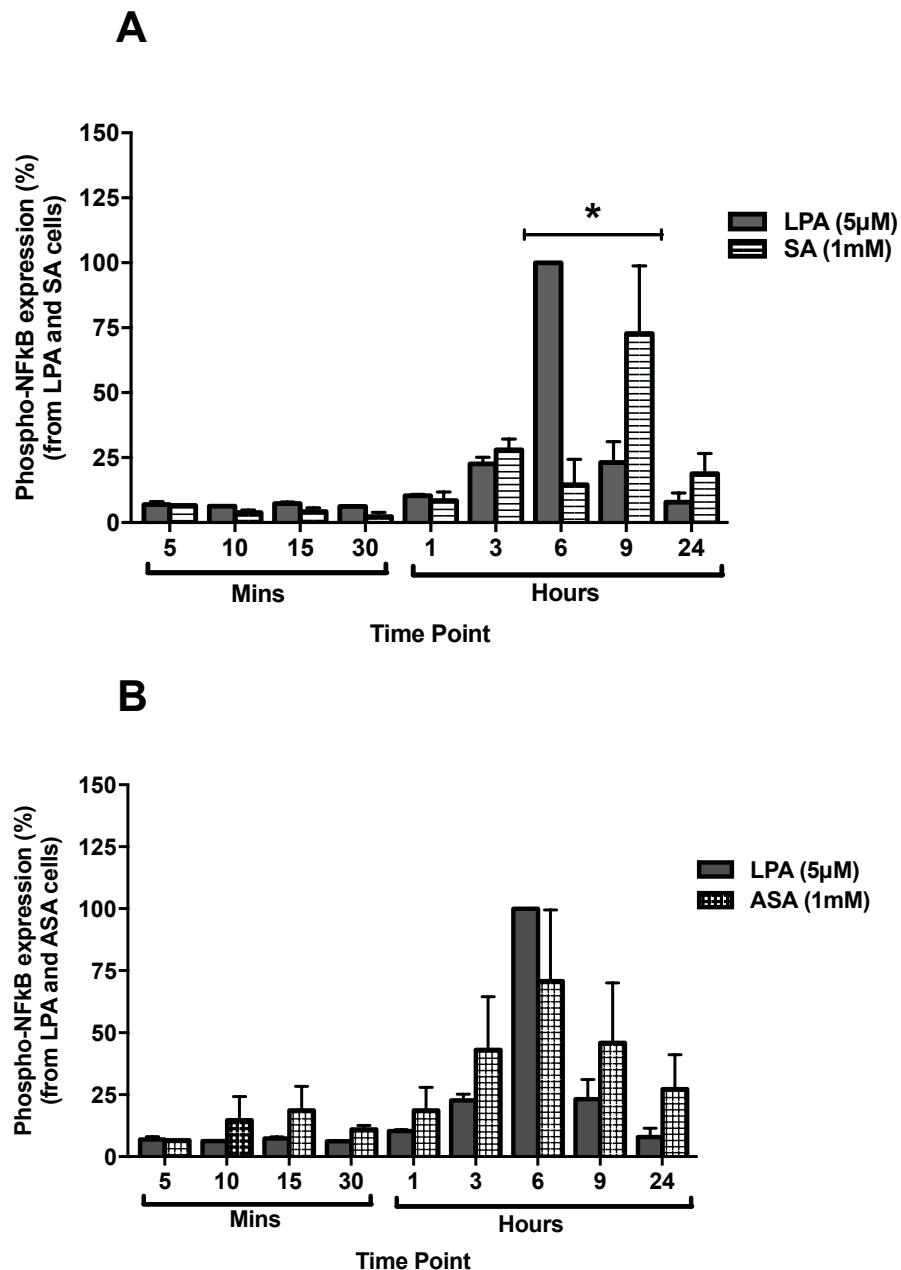


Figure 3.23: Phospho NFκB expression in LPA treated cells compared to SA or ASA treated cells.

Passage 9, P19 SCs were seeded in complete α -MEM at 7×10^7 cells/mL in 1.5 mL microcentrifuge tubes for selected time points at 37°C, 95% air and 5% CO₂. Cells were lysed and probed for phospho NFκB expression normalised to β -actin by western blotting as described in the methods. (A) LPA phospho NFκB compared to SA phospho NFκB levels. (B) LPA phospho NFκB to ASA phospho NFκB levels. Statistical comparison was performed using two-way ANOVA with Dunnett's post Hoc test ($\alpha=0.05$). The data represent the means \pm S.E.M. of 4 individual experiments.

3.5.2 Effect of LPA, SA and ASA on I κ B expression.

In addition to NF κ B, it was critical to examine the role of I κ B; an inhibitory protein that maintains NF κ B at an inactively bound state. Cells were seeded in suspension in the absence (Figure 3.24A) and presence of LPA (Figure 3.24B), SA (Figure 3.24C) and ASA (Figure 3.24D) and lysates were generated at selected time points (5, 10, 15, 30 mins and 1, 3, 6, 9, 24 hours) to examine for the expression of total and phosphorylated I κ B using western blotting. The results in Figure 3.24A showed no significant change in basal I κ B expression at any of the time points when the densitometric data were compared. In the presence of LPA (5 μ M), a time-dependent trend was seen in the expression of I κ B where at 5, 10 and 15 mins I κ B expression was lower than basal levels, returning back to basal levels at 30 mins and 1 hour and exceeding basal levels between 3, 6 and 9 hours but declining at 24 hours (Figure 3.24B). Incubation with SA (1mM) did not show much of a significant change in total I κ B, but this declined at 9 and 24 hours (Figure 3.24). This was also the case following ASA treatment and in the latter I κ B was enhanced at 30 minutes post-treatment (Figure 3.24D). These trends were however only evident when compared within the same experimental group. For ease of comparison, the data has been replotted as seen in Figure 3.25, comparing cells incubated with complete medium alone with LPA (Figure 3.25A), SA (Figure 3.25B), or ASA (Figure 3.25C). These figures show that the changes in I κ B levels did not show much of a significant difference in both drug conditions (SA and ASA). The SA samples did not show any significant difference when compared to controls, but it is worth noting the significance seen at 30 minutes ASA was also seen in Figure 3.25C when compared to control I κ B expression. The LPA treated samples also showed the same significant trend when compared to controls (Figure 3.25A). Similar comparisons have been carried out between LPA and SA (Figure 3.26A) and LPA and ASA (Figure 3.26B). In this case, the trends seen with SA and ASA seem identical, showing significantly higher I κ B expression at 5, 10, 15 mins in SA treated cells; with the addition of 30 mins in ASA treated cells when compared to the LPA samples. The

responses to LPA were however higher than those seen with SA and ASA at 6, 9 and 24 hours for both conditions.

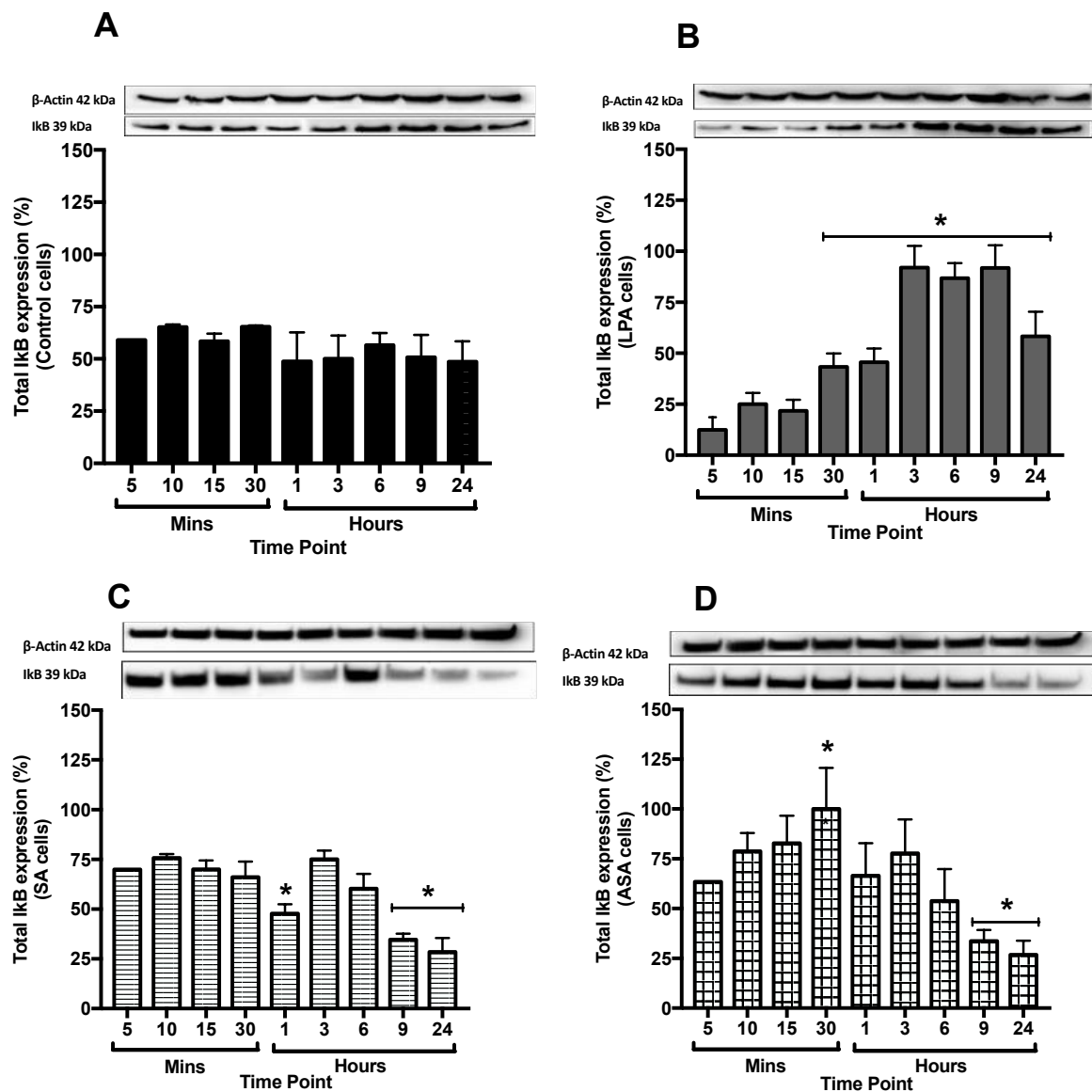


Figure 3.24: Densitometric data for total IκB protein expression.

Passage 9, P19 SCs were seeded in complete α -MEM at 7×10^7 cells/mL in 1.5 mL microcentrifuge tubes for selected time points at 37°C, 95% air and 5% CO₂. Cells were lysed and probed for IκB expression normalised to β -actin by western blotting as described in the methods. (A) Control, (B) LPA, (C) SA and (D) ASA treated cells. Statistical comparison was performed using one-way ANOVA with Dunnett's post Hoc test ($\alpha=0.05$). The data represents the means \pm S.E.M. of 4 individual experiments.

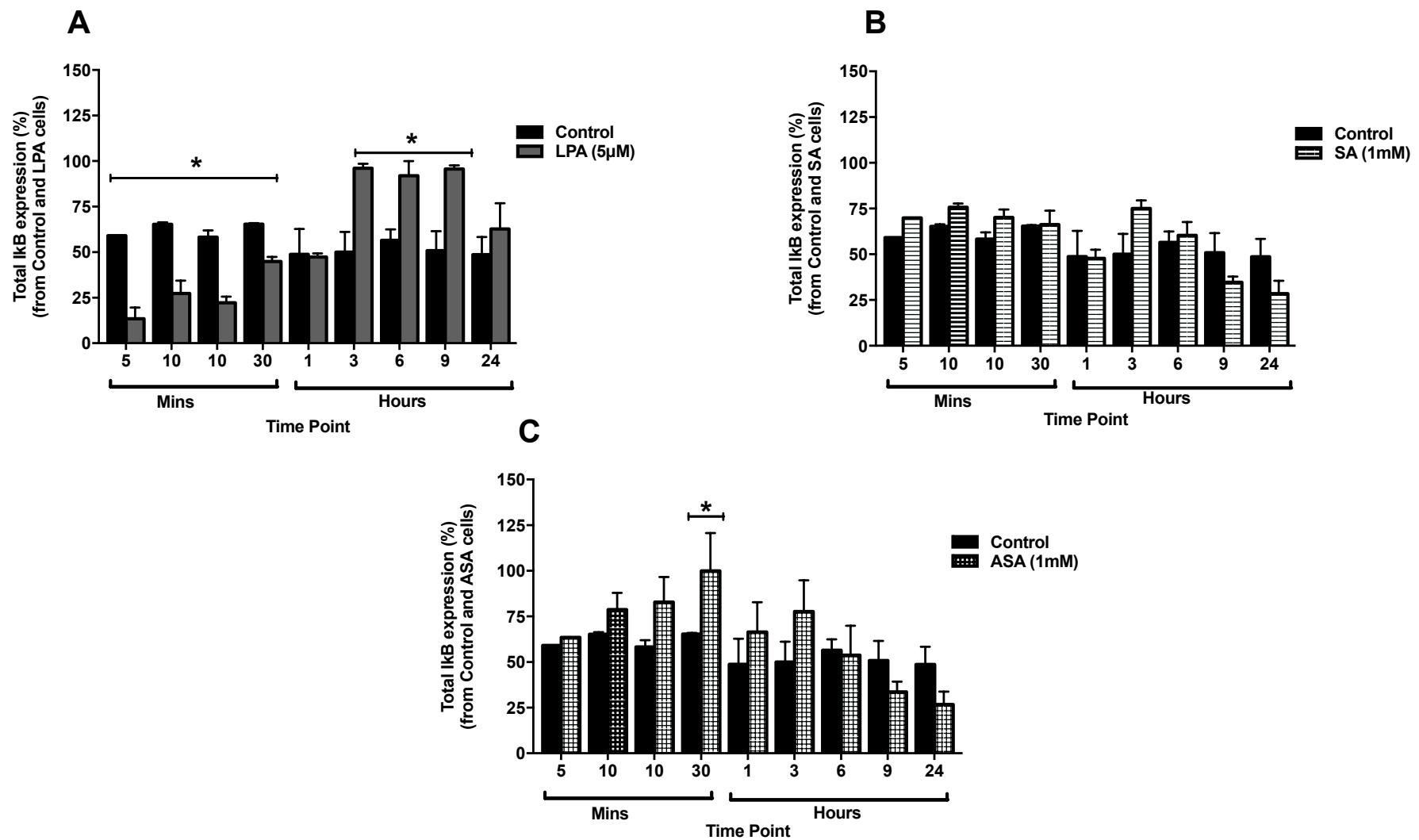


Figure 3.25: Control IκB densitometric data compared with LPA, SA and ASA IκB.

Passage 9, P19 SCs were seeded in complete α -MEM at 7×10^7 cells/mL in 1.5 mL microcentrifuge tubes for selected time points at 37°C, 95% air and 5% CO₂. Cells were lysed and probed for IκB expression normalised to β -actin by western blotting as described in the methods. (A) Control IκB compared to LPA IκB levels. (B) Control IκB compared to SA IκB levels. (C) Control IκB compared to ASA IκB levels. Statistical comparison was performed using two-way ANOVA with Dunnett's post Hoc test ($\alpha=0.05$). The data represents the means \pm S.E.M. of 4 individual experiments.

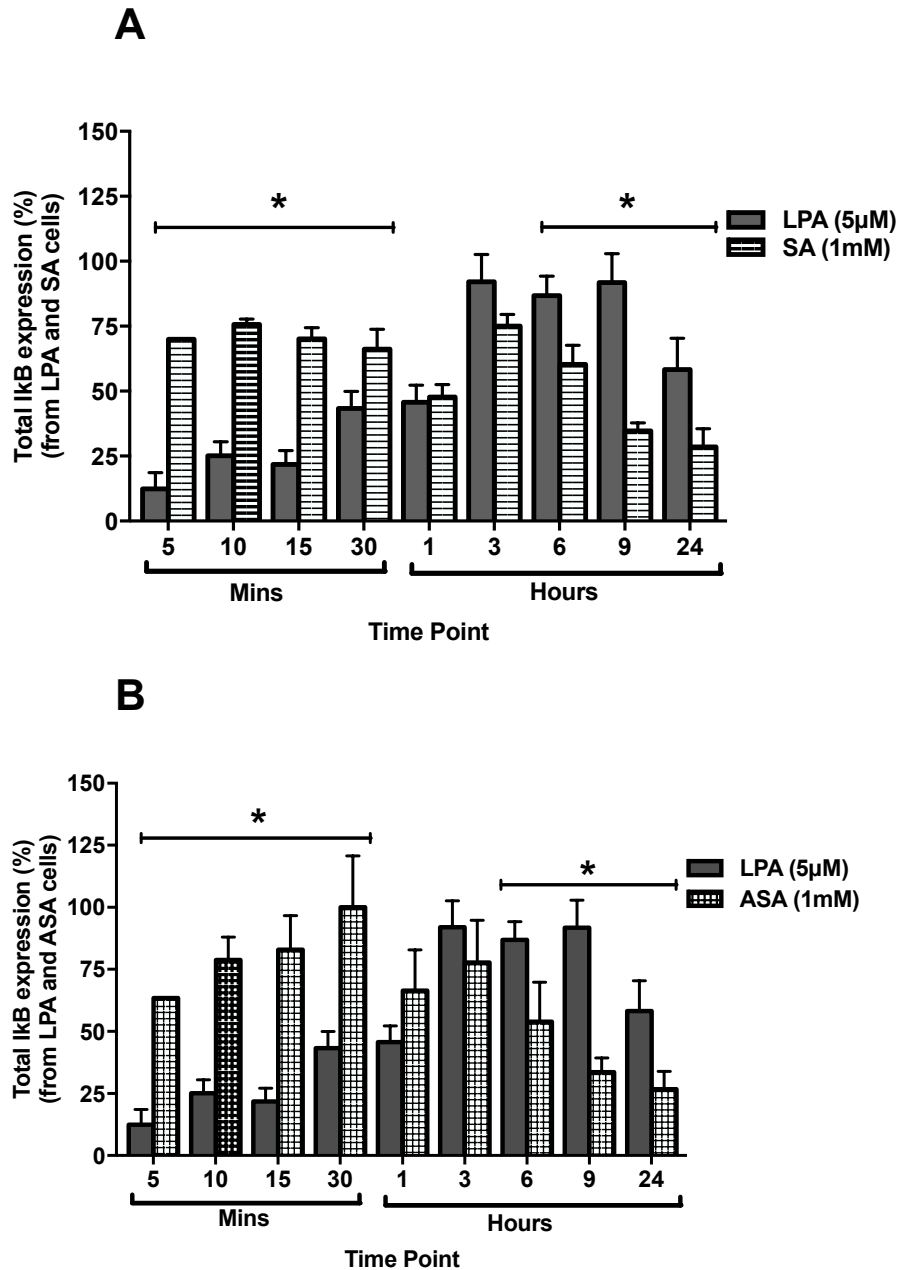


Figure 3.26: IκB expression in LPA treated cells compared to SA or ASA treated cells.

Passage 9, P19 SCs were seeded in complete α -MEM at 7×10^7 cells/mL in 1.5 mL microcentrifuge tubes for selected time points at 37°C, 95% air and 5% CO₂. Cells were lysed and probed for IκB expression normalised to β -actin by western blotting as described in the methods. (A) LPA IκB compared to SA IκB levels. (B) LPA IκB compared to ASA IκB levels. Statistical comparison was performed using two-way ANOVA with Dunnett's post Hoc test ($\alpha=0.05$). The data represents the means \pm S.E.M. of 4 individual experiments.

3.5.3 Effect of LPA, SA and ASA on phospho I κ B expression.

In addition to the experiments conducted above, we further investigated the phosphorylation of I κ B α . Cells were seeded in suspension in the absence (Figure 3.27A) and presence of LPA (Figure 3.27B), SA (Figure 3.27C) and ASA (Figure 3.27D) and lysates were generated at selected time points (5, 10, 15, 30 mins and 1, 3, 6, 9, 24 hours) to examine for the expression of phospho I κ B using western blotting. The results in Figure 3.27A showed a statistically significant change in the overall basal phospho I κ B expression between 1 to 24 hours, presenting a time-dependent bell-shaped change in the densitometric data. These were however small changes, peaking at 6 hours and declining at 9 and 24 hours. In the presence of LPA (5 μ M), high expression of phospho I κ B was seen between 5 and 15 minutes but declined back to basal levels thereafter (Figure 3.27B). Incubation with SA (1mM) (Figure 3.27C) or ASA (1mM) (Figure 3.27D) appeared did not show much of a time-dependent effect although peaks in phospho I κ B were seen with both SA and ASA at 3 hours. However, the overall trends appear random and it is, therefore, difficult to draw any firm conclusions. The trends were also only evident when compared within the same experimental group. For ease of comparison, the data has been replotted as seen in Figure 3.28, comparing cells incubated with complete medium alone with LPA (Figure 3.28A), SA (Figure 3.28B), ASA (Figure 3.28C). Similar comparisons have also been carried out between LPA and SA (Figure 3.29A) and LPA and ASA (Figure 3.29B). The replotted data confirms the trends already highlighted above.

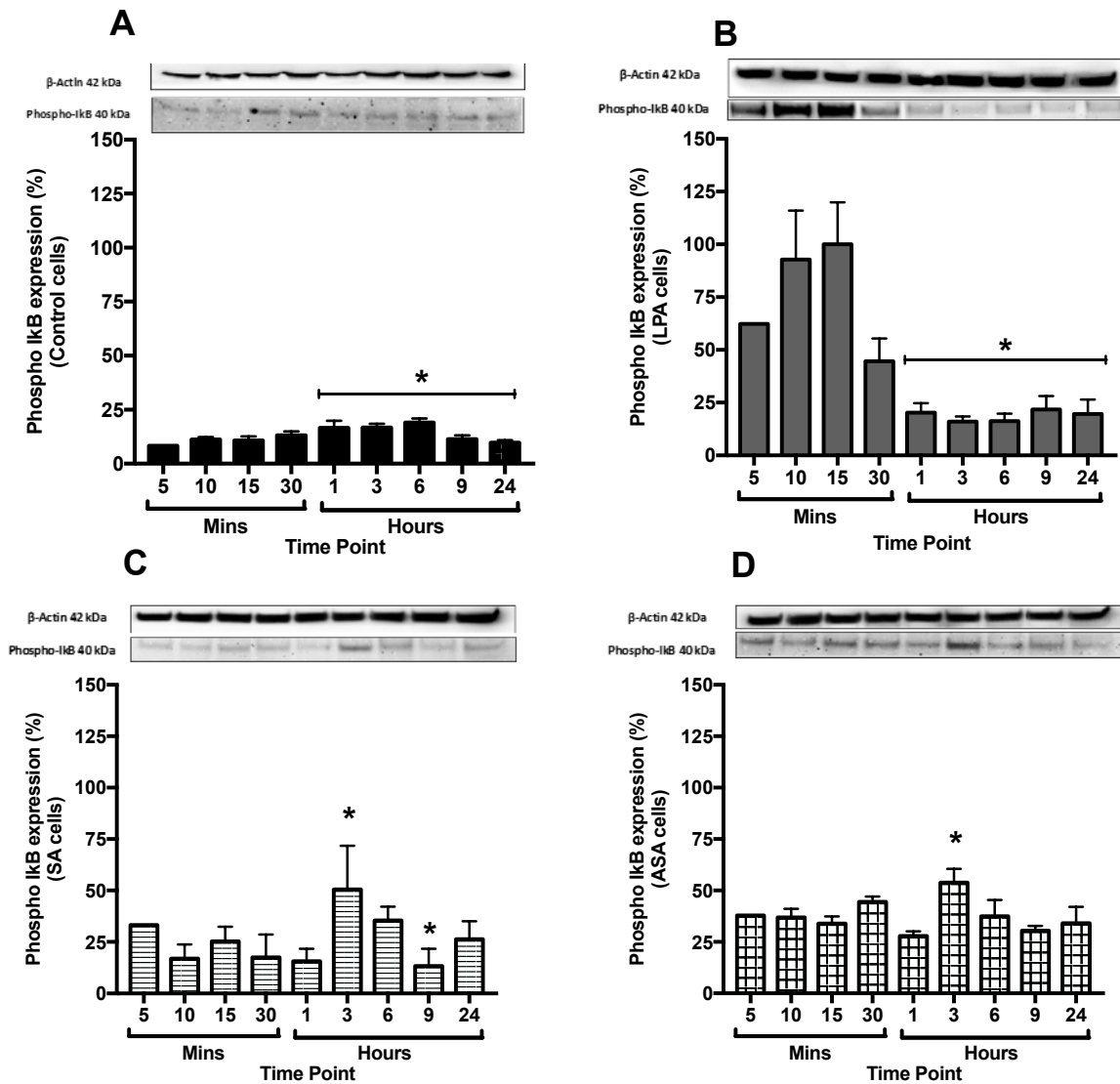


Figure 3.27: Densitometric data for total phospho IκB protein expression.

Passage 9, P19 SCs were seeded in complete α -MEM at 7×10^7 cells/mL in 1.5 mL microcentrifuge tubes for selected time points at 37°C, 95% air and 5% CO₂. Cells were lysed and probed for phospho IκB expression normalised to β -actin by western blotting as described in the methods. (A) Control, (B) LPA, (C) SA and (D) ASA treated cells. Statistical comparison was performed using one-way ANOVA with Dunnett's post Hoc test ($\alpha=0.05$). The data represent the means \pm S.E.M. of 4 individual experiments.

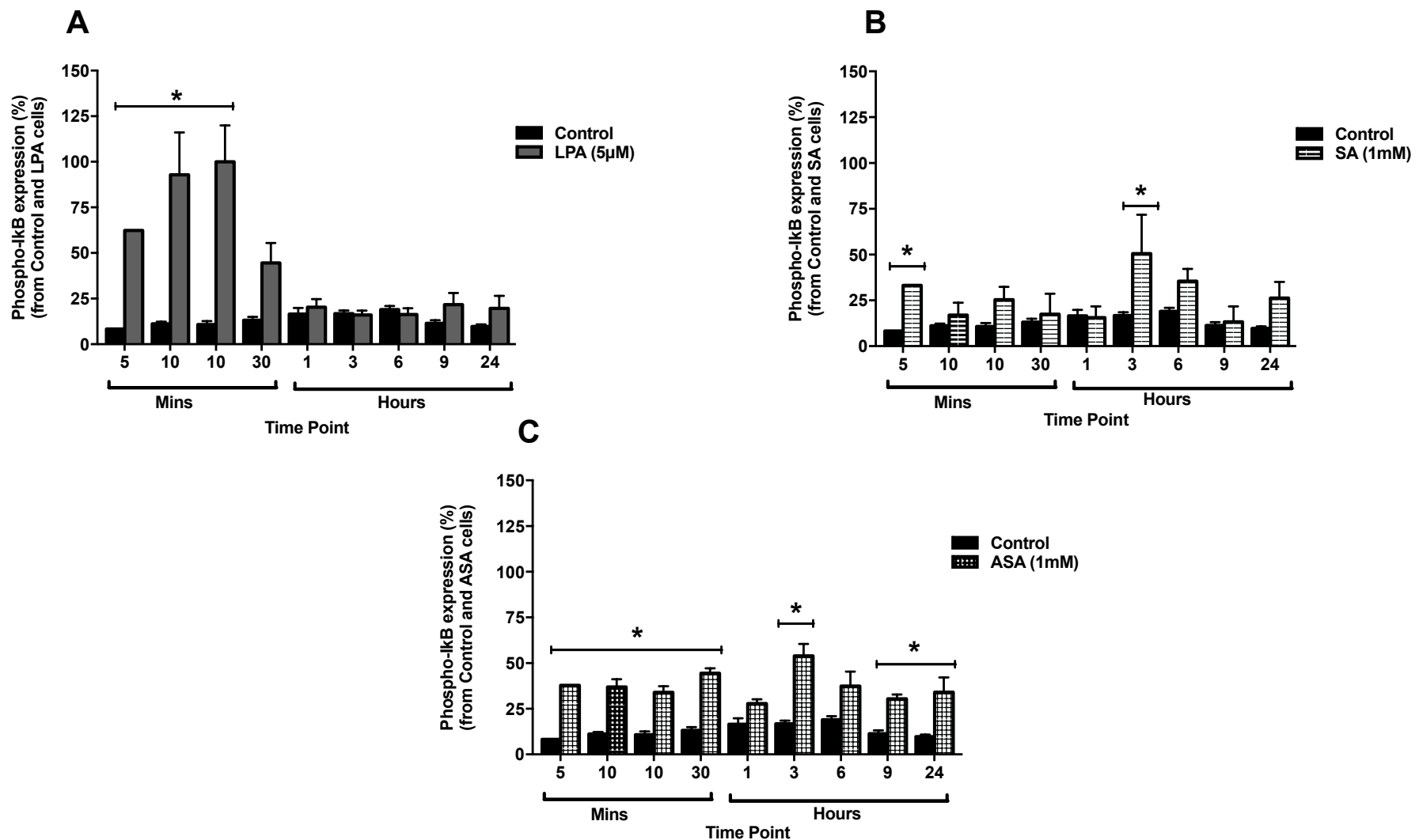


Figure 3.28: Control phospho I κ B densitometric data compared with LPA, SA and ASA phospho I κ B.

Passage 9, P19 SCs were seeded in complete α -MEM at 7×10^7 cells/mL in 1.5 mL microcentrifuge tubes for selected time points at 37°C, 95% air and 5% CO₂. Cells were lysed and probed for phospho I κ B expression normalised to β -actin by western blotting as described in the methods. (A) Control phospho I κ B compared to LPA phospho I κ B levels. (B) Control phospho I κ B compared to SA phospho I κ B levels. (C) Control phospho I κ B compared to ASA phospho I κ B levels. Statistical comparison was performed using two-way ANOVA with Dunnett's post Hoc test ($\alpha=0.05$). The data represents the means \pm S.E.M. of 4 individual experiments.

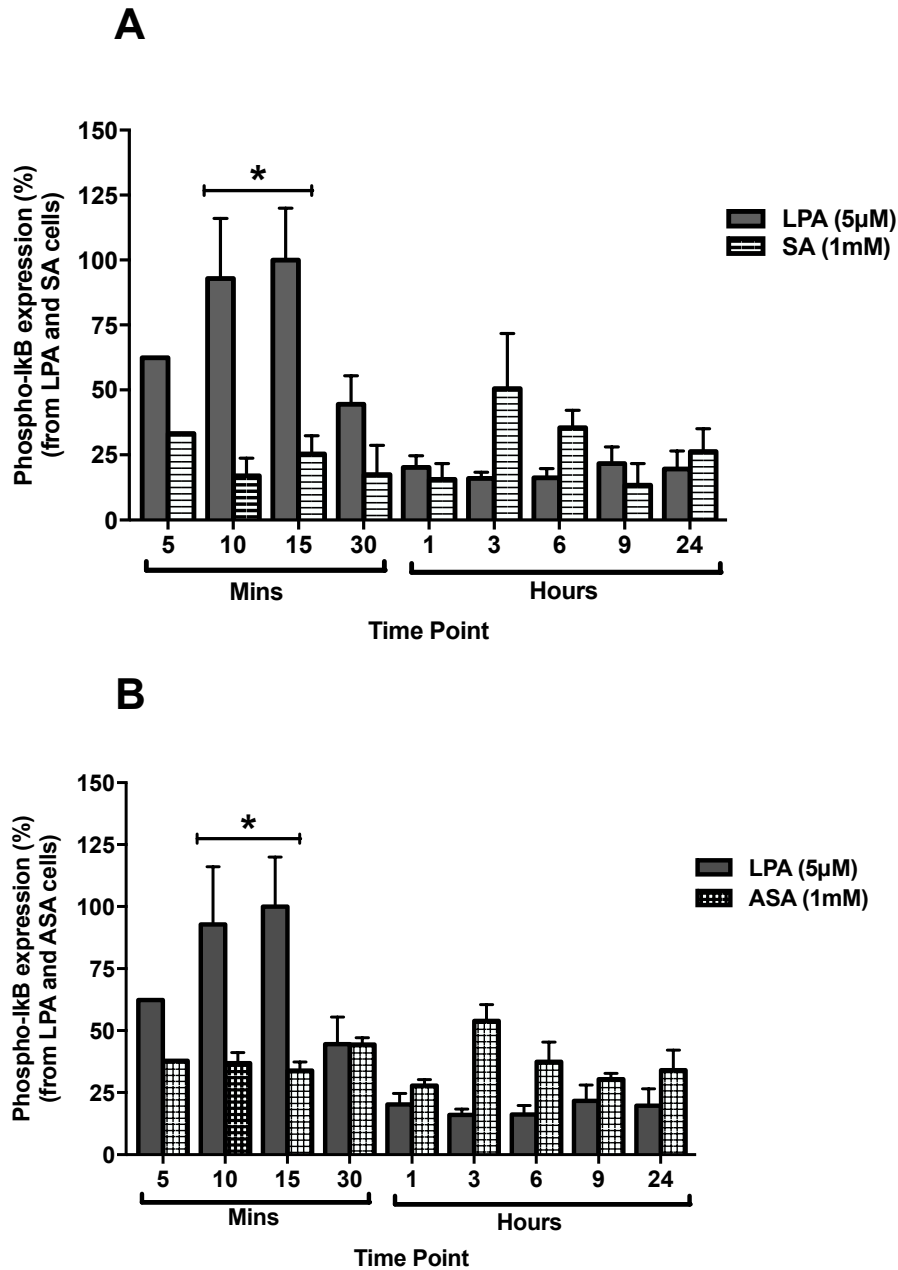


Figure 3.29: Phospho IκB expression in LPA treated cells compared to SA or ASA treated cells.

Passage 9, P19 SCs were seeded in complete α -MEM at 7×10^7 cells/mL in 1.5 mL microcentrifuge tubes for selected time points at 37°C, 95% air and 5% CO₂. Cells were lysed and probed for phospho IκB expression normalised to β -actin by western blotting as described in the methods. (A) LPA phospho IκB compared to SA phospho IκB levels. (B) LPA phospho IκB to ASA phospho IκB levels. Statistical comparison was performed using two-way ANOVA with Dunnett's post Hoc test ($\alpha=0.05$). The data represents the means \pm S.E.M. of 4 individual experiments.

3.5.4 Effect of CAY10470 on LPA-induced MLC-1v expression.

To confirm whether LPA acted on the NF κ B transcription factor in establishing cardiomyocyte differentiation of P19 SCs, CAY10470 was incubated with P19 cell suspension throughout the EB formation phase. CAY10470 showed a concentration-dependent decrease in MLC-1v expression in the presence of LPA (5 μ M), showing significance at 0.01 and 0.1 nM (Figure 3.30).

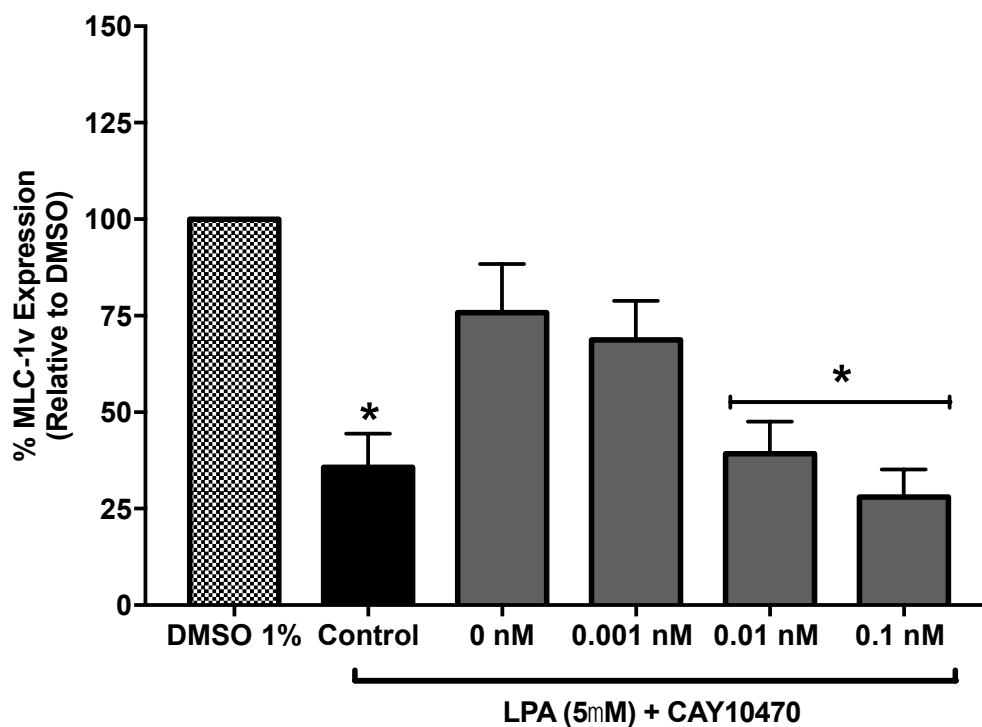


Figure 3.30: Concentration-dependent effects of CAY10470 on MLC-1V expression in LPA activated P19 SCs.

Passage 9, P19 SCs were seeded at 3.5×10^5 cells/mL in P60 microbiology Petri dishes. The cells were treated in the presence and absence of LPA (5 μ M) or LPA (5 μ M) and CAY10470. The latter was added to cells 1-hour post treatment with LPA and grown at 37 $^{\circ}$ C, 95% air and 5% CO $_2$. The cells were cultured in complete α -MEM and left to form EBs over 4 days. In this study, 6-8 EBs were plated into 24 well-plates and cultured for 3 days and lysed to be probed for β -actin and MLC-1v expression by western blotting as described in the methods. Statistical comparison was performed using two-way ANOVA with Dunnett's post Hoc test ($\alpha=0.05$). The data represents the means \pm S.E.M. of 4 individual experiments.

3.5.4.1 MTT assay determining the toxicity of CAY10470

To determine whether the concentrations of CAY10470 used throughout the studies had any cytotoxic effects on the P19 SCs, the MTT assay was carried out as described in the experimental protocol in chapter 2. The data seen in Figure 3.31 shows that CAY10470 was well tolerated with little or no change in cell viability except with 1 nM CAY10470. The inhibition in MTT metabolism at this concentration, although small, was found to be statistically significant (Figure 3.31).

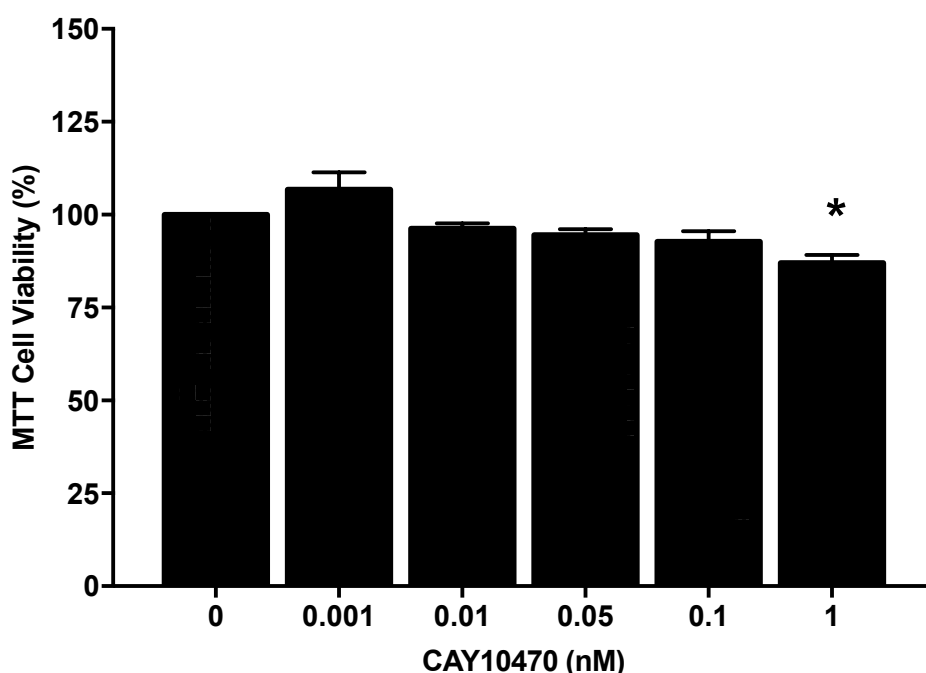


Figure 3.31: Effect of CAY10470 on P19 SC viability.

Passage 10, P19 SCs were seeded at 3.5×10^5 cells/mL and pre-incubated with CAY10470 for 1 hour before adding LPA ($5\mu\text{M}$). Monolayers were then grown until 70% confluency for 3 days. A final concentration of 0.1mg of MTT was added to the monolayers and incubated for 4 hours prior to assessing cell viability as described in materials and methods. Statistical comparison was performed using one-way ANOVA with Dunnett's post Hoc test ($\alpha=0.05$). The data represents the means \pm S.E.M. of 4 individual experiments.

4. Discussion

Coronary artery disease (CAD) related complications pose a significant threat, with high mortality rates across the world. CAD results from atherosclerosis, the build-up of cholesterol-rich lipids and inflammatory cytokines within the arterial wall, leading to major cardiac events such as myocardial infarction. So far, the current and only feasible methods of treatment are management through pharmacological agents, medical interventions (coronary stents and bypass surgery) and heart transplantation.

The increasing interests into stem cell-based research have shown the potential to produce promising alternatives in treating or reversing the damage caused on the myocardium using SCs. The availability of SCs to differentiate into cardiomyocytes has led researchers to gain novel insights into the early development of the heart, one such model widely used experimentally is the murine P19 teratocarcinoma cell line, giving rise to all three primary germ layers (endoderm, mesoderm and ectoderm) (Datta, 2013). Although this model has been widely used for nearly 40 years, examining instrumental signal transduction pathway regulations and the expression of the cardiac-specific transcription factors, that lead onto cardiac differentiation has been the main focus in recent years (van der Heyden & Defize, 2003).

One of the major hurdles in using P19 SCs is the availability of a viable inducing agent for differentiation. Currently, DMSO has been used extensively to initiate consistent differentiation of these P19 cells into cardiomyocytes. However, its toxicity prevents the use of DMSO *in vivo* studies. Our research group has therefore focused on the identification of endogenous bioactive small molecules which could mediate this process and are therefore of clinical relevance. One such molecule investigated by others in the group is LPA; a crucial lipid mediator in key physiological and pathophysiological processes, that has also shown cardioprotective characteristics, including protection against ischaemic injury; regulating the cardiovascular function of cardiac myocytes, endothelial and smooth muscle cells in response to major cardiac events such as myocardial infarction (X. Chen *et al.*, 2003). In addition, research conducted within our group has demonstrated LPA acts on specific receptors (LPAR1/3

and 4) which are in turn coupled to downstream signalling pathways that regulate P19 MSCs differentiation into cardiomyocytes (Pramod, 2015).

The other focus of our research group is to understand how drugs used to treat patients with heart disease might regulate SC differentiation and therefore affect cardiomyocytes generation. One such drug of interest is ASA which is widely given as secondary prevention care for cardiovascular-related complications. Aspirin is a nonsteroidal anti-inflammatory drug (NSAID) that is an effective antithrombotic, antiplatelet and analgesic. The mechanism of action of ASA suppresses the production of prostaglandins and thromboxane through the irreversible inactivation of the cyclooxygenase (COX) enzyme. Aspirin may also regulate cell signalling mechanisms including the NFκB pathway which may play a role in stem cell differentiation. Considering that most patients with heart disease and requiring SC therapy (should this become clinically achievable) may also be on ASA treatment, we have investigated whether ASA and its active metabolite (SA) can regulate the differentiation process either directly or regulate the actions of LPA. Using NSAIDs such as aspirin to condition stem cell for cardiac therapy has been recently proposed, and studies have indicated a modulatory effect on cell proliferation, tissue regeneration and differentiation (Du *et al.*, 2016). This has been thought to be achieved through the control of activating key signalling pathways, receptor modulation and transcriptional factor activity (Massimi *et al.*, 2014). Thus, there is some evidence that ASA may be able to influence SC differentiation. However, it is not clear whether ASA can directly regulate the commitment of SCs into a cardiac lineage. We have therefore examined the effects of aspirin and/or salicylic acid alone and in combination with LPA on cardiomyocyte differentiation. DMSO was also used in some studies as a positive control to confirm differentiation.

A viable cell culture model was first established, inducing P19 SCs from a confluent monolayer to embryoid bodies and then differentiating them into cardiomyocytes. Previously, the methodology used to differentiate P19 SCs into cardiomyocytes used

P60 microbiology non-adherent Petri dishes. This resulted in inconsistent EB growth patterns, in which a concentrated pool of seeded cells could have been exposed to varying concentrations of treatment, resulting in irregular growth morphology and size. Moreover, there were also significant differences in the sizes of the EBs formed which affected their differentiation efficiency, particularly with regards to generating beating cardiomyocyte clusters. In addition, the smaller EBs could have been less viable as they sustained higher cellular toxicity at the selected concentration range, as compared to larger and more pronounced EB sizes. This was exponentially reflected over the course of 4 days during the EB growth period. To minimise these variabilities, cells were grown in ultra-low attachment nunclon sphera 96-well plates, in which each well housed a singular EB. Cells were seeded at increasing concentrations to establish the optimum seeding density in which cells reached the required diameter (350-450 μ m). Studies have shown the morphology and size of EB influenced the efficiency of stem cell differentiation, with smaller EB sizes (150-300 μ m) being more associated with improved endothelial cell differentiation and larger EBs (350-450 μ m) with cardiogenesis (Liyang *et al.*, 2014). Therefore, it was crucial to factor in the size of EB diameter when optimising EB formation and morphology.

It was evident that 10,000 cells per well (300 μ L) was sufficient for experimental use and furthermore, the duration in which EBs were formed and matured, developing the mesoderm was also considered. To examine this, cells were grown for 24 hours and 48 hours. These time points were chosen as studies have established that, at 48 hours, EBs aggregate and form the mesoderm, this was evident by examining the expression of a vascular endothelial growth factor receptor and cell surface marker foetal liver kinase-1(Flk-1) (Dang *et al.*, 2002). The justification of growing EBs for 2-4 days was further emphasised in a study examining multipotent Flk-1+ cardiovascular progenitor in ESC, in which colonies of suspended cells from day 2 onwards, expressed genes associated with cardiac development such as Nkx2.5, MLC2a, Tbx5, and Isl1 b (Kattman *et al.*, 2006). From the results, the combination of seeding 10,000 cells for 48 hours

resulted in reliably consistent sizes of EB that established more defined outer borders characterising the EB morphology.

The two previously stated methods showed a clear difference in their abilities to form EBs. Firstly, the Petri dish protocol required a longer period to develop (4 days) as compared to the optimised ultra-low attachment 96-well plate method (2 days). This longer growth period seen in Petri dishes resulted in hundreds of irregular shaped EB in morphology, making it further complicated to isolate 6-8 individual EB of equal or similar size to be plated. However, the individually grown EBs in ultra-low attachment 96-well plates provided an easier and more reliable use of EBs for resulting experiments. In addition, EB grown in Petri dishes EB required to be grown for a longer time in culture to generate actively beating cardiomyocytes (6-12 days) and occurred with large confluent monolayers. Moreover, beating cardiomyocytes were not always evident showing a lack of consistency. Whereas, ultra-low attachment 96-well plate grown EBs resulted in consistently beating cardiomyocytes from day 3 onwards, with individual fibre shaped cells establishing a network of beating cells.

It is worth noting, the difference seen in monolayers formed by the Petri dish and the individual cells formed by the ultra-low attachment 96-well plate was substantial, as the control cells showed more spontaneous beating cells in the absence of any inducers of differentiation on Petri dish grown EBs. The optimisation of our culture condition has therefore produced a new approach and model for EB formation and enhanced cardiomyocyte differentiation.

In order to examine the effects of SA and ASA in the presence and absence of LPA (5 μ M) on EBs differentiation, cells were also grown in increasing concentrations ranging from 0.01, 0.03, 0.1, 0.3, 1mM. The inconsistency EB size was noticeable, as the effects of SA and ASA in both the presence and absence of LPA conditions showed varying sizes of EBs using the Petri dish method. However, when using the ultra-low attachment 96-well plate methods, EB sizes were consistent and all stayed within 350-450 μ m in diameter.

The next experimental plan focused on establishing and replicating the effects of LPA in inducing MLC-1v expression on P19 SCs. Initial studies that were conducted, examined increasing non-cytotoxic concentrations of LPA (1, 5, 10, 20 μ M) and were compared to a positive control (DMSO 1%). It was evident that cardiac differentiation was presented at all concentrations, however, maximal induction was achieved at 5 μ M and mirrored that of DMSO 1%. These results imply LPA can consistently induce differentiation of cells into cardiomyocytes. In most studies, LPA was used at a concentration of 5 μ M which was within the group. This concentration was selected because it induces differentiation reproducibly and is well within the physiological range found in plasma concentrations (X. Chen *et al.*, 2003). Using this concentration, P19 SCs were examined at days 3 and 6 in the plated phase to examine for the evidence of these cells differentiating into cardiomyocytes.

In addition to LPA, increasing concentrations of SA and ASA were used (0.1, 0.3, 1, 3 mM) and lysates were collected at days 3 and day 6. Western blot analysis was subsequently undertaken, examining the differentiation of P19 SCs through the expression of a cardiac-specific marker (MLC-1v) and a commonly used housekeeping gene (β -actin). Findings indicated differentiation was induced at selected concentrations of ASA (0.3 -1mM, at day 3) and SA (1mM, at day 3). However, maximal induction was achieved at 1mM on day 3, which declined in response to an increase in SA and ASA concentration (3mM), implying SA and ASA can enhance EB differentiation individually, but the decrease in MLC-1v expression levels could be attributed to cytotoxicity, which was represented with higher loading volumes to achieve a consistent loading content (20 μ g/ μ L) at higher concentrations of SA and ASA. This is further supported by the MTT assay for cell viability and cell number; undertaken at days 3 and day 6. As MTT is primarily a cell viability assay, it could also be used to indicate cell proliferation, which was significantly reduced, indicating why the maximal expression of MLC-1v was only reached at 1mM.

For the first time, we have shown aspirin (ASA) and its active molecule (SA) are able to potentiate cardiomyocyte differentiation in a concentration-dependent manner on P19 ESCs. From this finding, further work would be required to understand the mechanism of the effect of SA on differentiation. Possible mechanisms include the canonical Wnt/ β -catenin signalling pathway. Studies (Naito *et al.*, 2006; Ueno *et al.*, 2007) have shown manipulation of this pathway can result in a biphasic response. Activation during the EB formation phase, in which the formation of the germ layer is yet to be developed, leading to the promotion of embryonic stems cell to differentiate. Contrastingly, the latter phases (post EB formation) results in the inhibition of cardiomyocyte formation, as programmed cardiomyocytes are redirected toward an alternate mesoderm fate. It is possible that SA and ASA may be involved in the manipulation of the canonical Wnt/ β -catenin signalling pathway mediated cardiac differentiation of P19 cells (Naito *et al.*, 2006; Ueno *et al.*, 2007). This, however, needs to be confirmed in our studies.

Although SA and ASA were able to induce differentiation individually, when introduced with LPA (5 μ M) the effect of SA/ASA seem to inhibit the effectiveness of LPA to induce differentiation, acting as an antagonist. Interestingly, from the result, SA at 0.1mM in the presence LPA showed an increase in MLC-1v expression, it could be assumed low levels of SA could enhance LPA induced differentiation. Contrastingly, higher concentrations produce an inhibitory function. This hypothesis needs to be investigated in future studies, where a lower concentration range is used in combination with LPA to examine differentiation.

Previous research from our group has established that LPA initiates differentiation through downstream signalling pathways involving the Rho-associated protein kinase (ROCK), PI3K, phosphoinositide 3-kinase (PKC), that converge on extracellular signal-regulated kinase-1 and 2 (ERK1/2) (Maan, 2018; Pramod, 2015). A mechanism in which SA/ASA blocks the ability of LPA to induce differentiation could be explained by blocking the transient activation of the mitogen-activated protein kinase

(MAPK)/Erk1/2. Studies have shown by blocking the upstream kinase MEK and the subsequent inhibition of p-ERK 1/2 activation, prevented the differentiation of neuronal cells from cultured ES cells (Li *et al.*, 2006). This is supported by another study examining rat spinal cord mixed culture, in which ASA was used to treat hypoxia/reoxygenation (H/R) damage. Results indicated ASA strongly inhibits ERK1/2 activation (Vartiainen *et al.*, 2003).

An alternative mechanism could be presented by examining whether the PI3K/AKT pathway is inhibited by SA/ASA. Research using a specific PI3K inhibitor (LY294002) has shown to reduce LPA's effect on neuronal differentiation by roughly 53%. This suggests that the involvement of the PI3K/Akt pathway plays a vital role in inducing differentiation and subsequent inhibition could result in the loss of differentiation potential (Dottori *et al.*, 2008). To further substantiate this hypothesis, studies examining lung tissues have shown ASA at varying concentrations resulted in the decreased expression of ERK, PI3K and Akt, indicating ASA downregulate the expression of these intracellular signalling pathways in rat lungs (Wang *et al.*, 2013).

It is crucial to note, at day 6 both SA and ASA conditions showed high control levels of MLC-1v expression, indicating the cells were already committed to a cardiomyocyte fate at this time point. To exclude this variability, cells batches were routinely changed to confirm spontaneous differentiation was not established due to poor cell line, anomalies or user error. To further substantiate this examination, each batch of cells were spot checked and probed for MLC-1v using western blotting to determine if the cells were already predisposed to a cardiac lineage in the absence of any treatments or inducers of cardiomyocyte differentiation. Batches of cells thought to be unsuitable for use were discarded.

Following the studies examining the differentiated state of P19 SCs, our research focused on whether these drugs could mediate their effects through activation of NFκB as a target downstream of key upstream signalling pathways including ERK1/2. NFκB is often found in the variants p65 (RelA), p105/p50 (NF-κB1), p100-p52 (NFκB2),

c-Rel (Rel), and RelB is a multi-functional transcription factor involved in various biological processes including apoptosis, inflammation and more relevantly the differentiation and proliferation of stem cells. In the resting state of mammalian cells, NFκB exists within the cytosol in an inactively bound state, preventing its nuclear localisation and transcriptional function, mediated through the inhibitory IκB kinase (IKK) complex. Upon activation, the degradation of IκBα is regulated by various signals such as phosphorylation of MAPK, similar upstream signalling pathways and IκB kinase (IKK); freeing the NFκB complex. NFκB is then able to translocate from the cytosol into the nucleus, enabling activated NFκB to bind to DNA-binding sites on specific genes, and regulating their expression.

Studies have shown that aspirin potentiates the activation of NFκB, this can be seen in the research conducted by Stark *et al.*, in which a time-dependent and dose-dependent increase of nuclear p65 was seen when treated with aspirin. Subsequently activating the NFκB pathway to induce apoptosis of the HT-29 colorectal cancer cell line (Stark *et al.*, 2001). Alternatively, aspirin is also seen to mediate inhibition of NFκB activation, which is reflected in various studies. These studies concluded that aspirin inhibited the degradation of the IκBα from the NFκB complex, preventing NFκB from translocating from the cytosol to the nucleus (Kopp & Ghosh, 1994; McCarty & Block, 2006). Although the role of aspirin within the NFκB pathway, portray both inhibitory and stimulatory functions, its potential effect on NFκB in mediating cardiomyocyte differentiation is a topic of interest. Therefore, we examined the role of native p65 NFκB variant, one of the central regulators of the transcriptional responses. Studies have also shown that NFκB plays a major cardioprotective role during acute hypoxia and reperfusion injury (Tranter *et al.*, 2010). Our results indicated the native levels of NFκB remained relatively constant between control and LPA but appear to be potentiated by SA and ASA which increases total NFκB within 30 mins of incubation. It is not known why this occurred and appears too rapid a time course to see such a significant change in total NFκB protein expression. This may be a random effect but clearly needs further investigation. Worth noting also is the observation that native

levels of NFκB in LPA treatment seemed to unexpectedly drop at the later time points (9 and 24 hours). Again, it is not clear why this occurred but may be a result of potential cytotoxicity on the cells. Cytotoxicity assays were not carried out on this occasion because of time constraints but previous studies have shown that LPA was well tolerated at concentrations of up to 20 μM. The fact that the loading volume had to be increased in the more recent studies would suggest potential cytotoxicity leading to cell loss and therefore lower total cell protein.

Although native NFκB was widely expressed in all conditions, it is the phosphorylation of the p65 NFκB subunit that is crucial as it regulates the transcriptional activity, enabling the translocation of activated NFκB from the cytosol into the nucleus. To further examine the role of NFκB in detail, experiments were carried out examining the time-dependent phosphorylation of NFκB in control, LPA, SA and ASA conditions. Results indicated control conditions had no variation across all time points and showed low levels of phosphorylated NFκB expression when examined by western blot, which indicates our cell line did not spontaneously phosphorylate NFκB. In contrast, LPA, SA and ASA appeared to induce substantial expression of phospho NFκB at the 6-9-hour time points. It could be assumed initiation of cardiomyocyte differentiation could be triggered as early as these time points resulting from phosphorylation of NFκB through various cell signalling pathways. Our findings are similar to studies conducted on fibroblasts isolated from p65 S276A knock-in mice, which showed inhibition of p65-NFκB phosphorylation severely impaired the transcription of many tested genes (Hochrainer *et al.*, 2013). This is also supported in *Drosophila* Rel protein studies, where signal-dependent dorsal phosphorylation occurs in the cytoplasm, rendering the process of phosphorylation essential in nuclear import from the cytoplasm to the nucleus (Drier *et al.*, 1999). More substantially studies have implicated the upregulation of p65 NFκB in differentiation, as activation synergistically regulate TGF-β induced differentiation of lung fibroblast, resulting from the translocation of p65 NFκB into the nucleus and inducing gene expression (Sun *et al.*, 2015).

The first identified IKK complex, is the initiating factor in the degradation of the NFκB complex, containing two catalytic subunits (IKKα and IKKβ), and a structural regulatory component named NEMO (IKKγ). This complex has been thought to promote assembly of the IKK by relaying upstream signals to IKK. Thereby, leading to the phosphorylation of IκB and subsequent activation of NFκB. To investigate this, western blot analysis was conducted on cell lysates collected at defined time points and probed for both native and phospho-IκB. Results indicate, in control conditions, native IκB levels were consistent throughout, as expected. This was further reflected in phospho-IκB data sets. However, in the presence of LPA; a known biological inducer of cardiomyocyte differentiation, the native IκB decreased as phospho-IκB levels increased, implying phosphorylation of IκB is undertaken at earlier time points (5 to 30 mins), native IκB levels are proportionally lower and the opposite is seen. When the levels of phosphorylation are reduced, native IκB levels are overcome. Evidence of this is also seen in studies examining terminal differentiation of neural stem cells (NSCs); the results presented confirmed the activation of the canonical IKKβ/IκBα/p65 pathway during initial stages of neural differentiation induced by collagenase II treatment with TNF (Zhang *et al.*, 2012). In addition, phorbol 12-myristate 13-acetate (PMA)-induced macrophage-differentiation was examined in U937 cells, by investigating the role of IκBα phosphorylation and the activity of NFκB. Results from this study indicated prolonged phosphorylation of IκBα enhanced differentiation by potentially regulating other molecules that initiate differentiation (Hu *et al.*, 2000). This trend seen in our LPA studies is also partially seen in our studies examining SA and ASA condition, whereby levels of phosphorylation seem to occur at the later time point (3 hours) and native IκB levels reduce overtime. This indicates, although SA/ASA conditions seemed to show a similar pattern to that of LPA seen in NFκB studies, the results here examining the phosphorylation of IκB were dissimilar, suggesting that SA and ASA act on different signalling pathways in the process of NFκB-IκB degradation. Further studies are however needed to fully confirm the trends we have seen. In summary, NFκB transcriptional activity is regulated at multiple events, and the phosphorylation

of the p-65 NFκB dimer may play a vital role in both upstream and downstream related signalling pathways in activating the cascade, following the degradation of IκB proteins. These preliminary studies targeting the native NFκB and IκB complex with our selected treatments successfully investigate the appropriate time in which differentiation initiates, represented by the detection of phosphorylated NFκB and IκB.

To further substantiate the role NFκB plays in mediating the actions of LPA in P19 cells differentiation, NFκB activity was inhibited using increasing concentrations of CAY10470, a highly potent and selective NFκB inhibitor (Wen *et al.*, 2011). These experiments were undertaken in parallel with changes in MLC-1v expression. The expression in MLC-1v showed a dose-dependent reduction in the presence of CAY10470, where maximal inhibition was reached at 0.1 nM. Cell viability assays (MTT) were carried out to rule out any effects of cytotoxicity caused by CAY10470. These studies showed no cytotoxicity at the concentrations of CAY10470 used, confirming the role of NFκB in cardiomyocyte differentiation. Thus, the link between NFκB and cardiomyocyte differentiation is vital, as the regulation of this transcription factor may be the key in identifying the mechanism and signalling pathways in which induction of differentiation can be established.

5. Conclusion

In conclusion, we have developed a new protocol for generating EBs by optimising the differentiation of P19 SCs into cardiomyocytes. This work highlighted the importance of EB growth and size, demonstrating that they both play a critical role in the efficiency and potential for cells to differentiate into cardiomyocytes. Furthermore, we were able to confirm that LPA is an inducer for cardiomyocyte differentiation. Thus, the introduction of LPA as a biological inducer for differentiation at low physiological concentrations provides a potential for future treatment plans. In addition, SA and ASA were partially able to replicate the results seen in LPA conditions individually, however, when subjected to combination treatment with LPA (5 μ M), both SA and ASA presented antagonistic characteristics. It is therefore assumed that although SA and ASA do possess the ability to induce differentiation independently, they may do so by mechanisms independent of those activated by LPA. In parallel studies, we were successfully able to analyse phospho and native proteins associated with the NF κ B complex. These preliminary studies indicated that in SA and ASA conditions, expressed phospho NF κ B levels that were similar in trend to LPA treated cells, implying a shared mechanism. However, the phosphorylated and non-phosphorylated I κ B levels of ASA/SA did not share the same trend to LPA treatment. This supports the implication that SA and ASA work on independent signalling pathways to that of LPA in the NF κ B activation cascade.

In conclusion, the findings from this thesis make a case to critically evaluate patients undergoing SC therapy who are using aspirin for their underlying heart disease. Aspirin may suppress the efficiency and viability of repairing the heart by inhibiting the activation of vital signalling pathways. Its potential to induce the process cannot, however, be ruled out and therefore needs further investigation.

6. Future Works

- 1) Our research has indicated, both SA and ASA independently initiate differentiation, however in the presence of LPA treatment, it has shown antagonistic characteristics. Studies from other groups have shown, aspirin has opposing characteristics at low and high concentrations, therefore future experiments could examine if concentrations beyond our selected range could prevent the antagonistic tendencies associated with SA/ASA + LPA treatments.
- 2) Studies could also aim towards, examining the importance of prostaglandin synthesis and/or enhanced adenylyl cyclase activation on NFκB activation. Therefore, by blocking with aspirin, we could investigate the potential depletion of cyclic adenosine monophosphate (cAMP) levels, enhancing NFκB activation.
- 3) Selective inhibition of the proteins MLC-1v and phospho-NFκB were seen in LPA treated cells, when treated with CAY10470. Due to the limited time and nature of this project, we were unable to examine the effect of CAY10470 on SA and ASA in the presence and absence of LPA (5μM). Therefore, experiments undertaking these investigations would present a better understanding that links SA and ASA to LPA's mechanism of action.
- 4) The studies examining the early differentiation time points of embryoid bodies showed a generic time range in which either phospho-NFκB or phospho-IκB peaked. However, a more refined time course is needed to provide a more accurate set of results to pinpoint the time in which the phosphorylation of the selected transcription factor is initiated.
- 5) The conclusion gained from western blot studies are limited, therefore PCR studies would further support our research by examining the expression of selected genes such as MLC, GATA4, NFκB.

6) It is generally accepted that LPA may act through Mitogen-activated kinases (MAPKs) and PI3K which induces differentiation. However, it is not clear whether SA and ASA act in a similar manner. Experiments could be carried out examining whether SA and ASA regulate phosphorylation of targeted signalling pathways including MAPKs and PI3K.

7) Studies conducted by our research group have implicated GATA4 in playing a crucial role in the differentiation of P19 SCs into cardiomyocytes. Consequently, a potential experimental plan could be initiated in examining how SA/ASA and SA/ASA + LPA interact with the expression of GATA4.

7. References

- Abd Rahman, F., Mohd Ali, J., Abdullah, M., Abu Kasim, N. H., & Musa, S. (2016). Aspirin Enhances Osteogenic Potential of Periodontal Ligament Stem Cells (PDLSCs) and Modulates the Expression Profile of Growth Factor–Associated Genes in PDLSCs. *Journal of Periodontology*, 87(7), 837-847. doi: 10.1902/jop.2016.150610
- Assmann, G., Cullen, P., Jossa, F., Lewis, B., & Mancini, M. (1999). Coronary Heart Disease: Reducing the Risk. *The Scientific Background to Primary and Secondary Prevention of Coronary Heart Disease A Worldwide View*, 19(8), 1819-1824. doi: 10.1161/01.atv.19.8.1819
- Bertero, A., & Murry, C. E. (2018). Hallmarks of cardiac regeneration. *Nature Reviews Cardiology*, 15(10), 579-580. doi: 10.1038/s41569-018-0079-8
- Campregher, C., Luciani, M. G., & Gasche, C. (2007). Aspirin blocks proliferation in colon cells by inducing a G 1 arrest and apoptosis through activation of the checkpoint kinase ATM. *Carcinogenesis*, 28(10), 2207-2217. doi: 10.1093/carcin/bgm101 %J Carcinogenesis
- Cao, Y., Xiong, J., Mei, S., Wang, F., Zhao, Z., Wang, S., et al. (2015). Aspirin promotes bone marrow mesenchymal stem cell-based calvarial bone regeneration in mini swine. *Stem Cell Research & Therapy*, 6, 210. doi: 10.1186/s13287-015-0200-4
- Caspi, O., Lesman, A., Basevitch, Y., Gepstein, A., Arbel, G., Habib, I. H. M., et al. (2007). Tissue Engineering of Vascularized Cardiac Muscle From Human Embryonic Stem Cells. *Circulation Research*, 100(2), 263-272. doi: 10.1161/01.RES.0000257776.05673.ff
- Castaño, E., Dalmau, M., Barragán, M., Pueyo, G., Bartrons, R., & Gil, J. (1999). Aspirin induces cell death and caspase-dependent phosphatidylserine externalization in HT-29 human colon adenocarcinoma cells. *British Journal of Cancer*, 81(2), 294-299. doi: 10.1038/sj.bjc.6690690
- Cha, J. M., Bae, H., Sadr, N., Manoucheri, S., Edalat, F., Kim, K., et al. (2015). Embryoid body size-mediated differential endodermal and mesodermal differentiation using polyethylene glycol (PEG) microwell array. *Macromolecular Research*, 23(3), 245-255. doi: 10.1007/s13233-015-3034-0
- Chen, L.-F., & Greene, W. C. (2004). Shaping the nuclear action of NF-κB. *Nature Reviews Molecular Cell Biology*, 5, 392. doi: 10.1038/nrm1368
- Chen, X., Yang, X. Y., Wang, N. D., Ding, C., Yang, Y. J., You, Z. J., et al. (2003). Serum lysophosphatidic acid concentrations measured by dot immunogold filtration assay in patients with acute myocardial infarction. *Scandinavian Journal of Clinical and Laboratory Investigation*, 63(7-8), 497-504. doi: 10.1080/00365510310003265

- Chien, K. R., Frisen, J., Fritsche-Danielson, R., Melton, D. A., Murry, C. E., & Weissman, I. L. (2019). Regenerating the field of cardiovascular cell therapy. *Nat Biotechnol*, *37*(3), 232-237. doi: 10.1038/s41587-019-0042-1
- Choi, J. W., Herr, D. R., Noguchi, K., Yung, Y. C., Lee, C.-W., Mutoh, T., et al. (2010). LPA Receptors: Subtypes and Biological Actions. *Annual Review of Pharmacology and Toxicology*, *50*(1), 157-186. doi: 10.1146/annurev.pharmtox.010909.105753
- Chong, J. J. H., Yang, X., Don, C. W., Minami, E., Liu, Y.-W., Weyers, J. J., et al. (2014). Human embryonic-stem-cell-derived cardiomyocytes regenerate non-human primate hearts. *Nature*, *510*(7504), 273-277. doi: 10.1038/nature13233
- Cros, C., Sallé, L., Warren, D. E., Shiels, H. A., & Brette, F. (2014). The calcium stored in the sarcoplasmic reticulum acts as a safety mechanism in rainbow trout heart. *American journal of physiology. Regulatory, integrative and comparative physiology*, *307*(12), R1493-R1501. doi: 10.1152/ajpregu.00127.2014
- Dang, S. M., Kyba, M., Perlingeiro, R., Daley, G. Q., & Zandstra, P. W. (2002). Efficiency of embryoid body formation and hematopoietic development from embryonic stem cells in different culture systems. *Biotechnology and Bioengineering*, *78*(4), 442-453. doi: doi:10.1002/bit.10220
- Datta, P. K. (2013). Murine teratocarcinoma-derived neuronal cultures. *Methods in molecular biology (Clifton, N.J.)*, *1078*, 35-44. doi: 10.1007/978-1-62703-640-5_4
- De Luna-Bertos, E., Ramos-Torrecillas, J., García-Martínez, O., Díaz-Rodríguez, L., & Ruiz, C. (2012). Effect of Aspirin on Cell Growth of Human MG-63 Osteosarcoma Line. *The Scientific World Journal*, *2012*, 834246. doi: 10.1100/2012/834246
- Dottori, M., Leung, J., Turnley, A. M., & Pébay, A. (2008). Lysophosphatidic Acid Inhibits Neuronal Differentiation of Neural Stem/Progenitor Cells Derived from Human Embryonic Stem Cells. *Stem Cells*, *26*(5), 1146-1154. doi: 10.1634/stemcells.2007-1118
- Drier, E. A., Huang, L. H., & Steward, R. (1999). Nuclear import of the Drosophila Rel protein Dorsal is regulated by phosphorylation. *Genes & Development*, *13*(5), 556-568.
- Du, M., Pan, W., Duan, X., Yang, P., & Ge, S. (2016). Lower dosage of aspirin promotes cell growth and osteogenic differentiation in murine bone marrow stromal cells. *Journal of Dental Sciences*, *11*(3), 315-322. doi: <https://doi.org/10.1016/j.jds.2016.03.009>

- Eaves, C. (2002). Stem Cells and the Future of Regenerative Medicine. *Nature Medicine*, 8, 326. doi: 10.1038/nm0402-326
- Eroles, P., Perez-Fidalgo, J. A., & Lluch, A. (2014). *Stem Cells in Cancer: Should We Believe or Not?*
- Evans, M. J., & Kaufman, M. H. (1981). Establishment in culture of pluripotential cells from mouse embryos. *Nature*, 292, 154. doi: 10.1038/292154a0
- Gudjonsson, T., & Magnusson, M. K. (2005). Stem cell biology and the cellular pathways of carcinogenesis. *Apmis*, 113(11-12), 922-929. doi: 10.1111/j.1600-0463.2005.apm_371.x
- Hao, W., Shi, S., Zhou, S., Wang, X., & Nie, S. (2018). Aspirin inhibits growth and enhances cardiomyocyte differentiation of bone marrow mesenchymal stem cells. *European Journal of Pharmacology*, 827, 198-207. doi: <https://doi.org/10.1016/j.ejphar.2018.03.016>
- Hochrainer, K., Racchumi, G., & Anrather, J. (2013). Site-specific phosphorylation of the p65 protein subunit mediates selective gene expression by differential NF- κ B and RNA polymerase II promoter recruitment. *The Journal of Biological Chemistry*, 288(1), 285-293. doi: 10.1074/jbc.M112.385625
- Hopper, D. W., Ragan, S. P., Hooks, S. B., Lynch, K. R., & Macdonald, T. L. (1999). Structure–Activity Relationships of Lysophosphatidic Acid: Conformationally Restricted Backbone Mimetics. *Journal of Medicinal Chemistry*, 42(6), 963-970. doi: 10.1021/jm970809v
- Hu, T., Janssen, W., Dangsupa, A., & Zuckerman, K. (2000). *Phosphorylation of I kappa B alpha and NK-kappa B activation are required for macrophage-differentiation of U937 cells* (Vol. 28).
- Isao Ishii, Nobuyuki Fukushima, Xiaoqin Ye, a., & Chun, J. (2004). Lysophospholipid Receptors: Signaling and Biology. *Annual Review of Biochemistry*, 73(1), 321-354. doi: 10.1146/annurev.biochem.73.011303.073731
- Jackson, R., Tilokee, E. L., Latham, N., Mount, S., Rafatian, G., Strydhorst, J., et al. (2015). Paracrine Engineering of Human Cardiac Stem Cells With Insulin-Like Growth Factor 1 Enhances Myocardial Repair. *Journal of the American Heart Association*, 4(9). doi: 10.1161/jaha.115.002104
- Karantalis, V., DiFede, D. L., Gerstenblith, G., Pham, S., Symes, J., Zambrano, J. P., et al. (2014). Autologous Mesenchymal Stem Cells Produce Concordant Improvements in Regional Function, Tissue Perfusion and Fibrotic Burden when Administered to Patients Undergoing Coronary Artery Bypass Grafting – The

- PROMETHEUS Trial. *Circulation Research*, 114(8), 1302-1310. doi: 10.1161/CIRCRESAHA.114.303180
- Kattman, S. J., Huber, T. L., & Keller, Gordon M. (2006). Multipotent Flk-1+ Cardiovascular Progenitor Cells Give Rise to the Cardiomyocyte, Endothelial, and Vascular Smooth Muscle Lineages. *Developmental Cell*, 11(5), 723-732. doi: <https://doi.org/10.1016/j.devcel.2006.10.002>
- Kohli, S., Ahuja, S., & Rani, V. (2011). Transcription Factors in Heart: Promising Therapeutic Targets in Cardiac Hypertrophy. *Current Cardiology Reviews*, 7(4), 262-271. doi: 10.2174/157340311799960618
- Kopp, E., & Ghosh, S. (1994). Inhibition of NF-kappa B by sodium salicylate and aspirin. 265(5174), 956-959. doi: 10.1126/science.8052854 %J Science
- Lanza, R. P. (2006). *Essentials of stem cell biology*: Amsterdam ; Boston : Elsevier/Academic Press.
- Lawrence, T. (2009). The nuclear factor NF-kappaB pathway in inflammation. *Cold Spring Harbor perspectives in biology*, 1(6), a001651-a001651. doi: 10.1101/cshperspect.a001651
- Leon, B. M., & Maddox, T. M. (2015). Diabetes and cardiovascular disease: Epidemiology, biological mechanisms, treatment recommendations and future research. *World Journal of Diabetes*, 6(13), 1246-1258. doi: 10.4239/wjd.v6.i13.1246
- Li, Z., Theus, M. H., & Wei, L. (2006). Role of ERK 1/2 signaling in neuronal differentiation of cultured embryonic stem cells. 48(8), 513-523. doi: doi:10.1111/j.1440-169X.2006.00889.x
- Lim, W. F., Inoue-Yokoo, T., Tan, K. S., Lai, M. I., & Sugiyama, D. (2013). Hematopoietic cell differentiation from embryonic and induced pluripotent stem cells. *Stem Cell Research & Therapy*, 4(3), 71-71. doi: 10.1186/scrt222
- Lin, M.-E., Herr, D. R., & Chun, J. (2010). Lysophosphatidic acid (LPA) receptors: signaling properties and disease relevance. *Prostaglandins & other lipid mediators*, 91(3-4), 130-138. doi: 10.1016/j.prostaglandins.2009.02.002
- Liu, Y., Peterson, D. A., Kimura, H., & Schubert, D. (1997). Mechanism of Cellular 3-(4,5-Dimethylthiazol-2-yl)-2,5-Diphenyltetrazolium Bromide (MTT) Reduction. *Journal of Neurochemistry*, 69(2), 581-593. doi: doi:10.1046/j.1471-4159.1997.69020581.x

- Liyang, G., Abdullah, S., Rosli, R., & Nordin, N. (2014). Neural Commitment of Embryonic Stem Cells through the Formation of Embryoid Bodies (EBs). *The Malaysian journal of medical sciences : MJMS*, 21(5), 8-16.
- Luciani, M. G., Campregher, C., & Gasche, C. (2007). Aspirin blocks proliferation in colon cells by inducing a G 1 arrest and apoptosis through activation of the checkpoint kinase ATM. *Carcinogenesis*, 28(10), 2207-2217. doi: 10.1093/carcin/bgm101 %J Carcinogenesis
- Maan, G. (2018). *Signal Transduction Mechanisms for Lysophosphatidic Acid Mediated Cardiac Differentiation of P19 Stem Cells*. (PhD), University of Hertfordshire.
- Marshak, D. R., Gardner, R. L., & Gottlieb, D. (2008). *Stem Cell Biology* (1 ed. Vol. 73). New York: Cold Spring Harbor Laboratory Press,U.S.
- Martinez-Agosto, J. A., Mikkola, H. K. A., Hartenstein, V., & Banerjee, U. (2007). The hematopoietic stem cell and its niche: a comparative view. *Genes & Development*, 21(23), 3044-3060. doi: 10.1101/gad.1602607
- Massimi, I., Guerriero, R., Lotti, L. V., Lulli, V., Borgognone, A., Romani, F., et al. (2014). Aspirin influences megakaryocytic gene expression leading to up-regulation of multidrug resistance protein-4 in human platelets. *British journal of clinical pharmacology*, 78(6), 1343-1353. doi: 10.1111/bcp.12432
- McCarty, M. F., & Block, K. I. (2006). Preadministration of High-Dose Salicylates, Suppressors of NF-κB Activation, May Increase the Chemosensitivity of Many Cancers: An Example of Proapoptotic Signal Modulation Therapy. *Integrative Cancer Therapies*, 5(3), 252-268. doi: 10.1177/1534735406291499
- Metzele, R., Alt, C., Bai, X., Yan, Y., Zhang, Z., Pan, Z., et al. (2011). Human adipose tissue-derived stem cells exhibit proliferation potential and spontaneous rhythmic contraction after fusion with neonatal rat cardiomyocytes. *FASEB journal : official publication of the Federation of American Societies for Experimental Biology*, 25(3), 830-839. doi: 10.1096/fj.09-153221
- Mezey, E., Chandross, K. J., Harta, G., Maki, R. A., & McKercher, S. R. (2000). Turning blood into brain: cells bearing neuronal antigens generated in vivo from bone marrow. *Science*, 290(5497), 1779-1782.
- Michaels, A. D., & Chatterjee, K. (2002). Angioplasty Versus Bypass Surgery for Coronary Artery Disease. *Circulation*, 106(23), e187.
- Mohsin, S., Avitabile, D., & Khan, M. (2015). Stem Cells and Cardiac Repair. *Stem Cells International*, 2015, 153627. doi: 10.1155/2015/153627

- Mummery, C. L., Stolpe, A. v. d., Roelen, B. A. J., & Clevers, H. (2011). *Stem cells : scientific facts and fiction* (First edit ed.). London: Elsevier/Academic Press.
- Nagelschmitz, J., Blunck, M., Kraetzschmar, J., Ludwig, M., Wensing, G., & Hohlfeld, T. (2014). Pharmacokinetics and pharmacodynamics of acetylsalicylic acid after intravenous and oral administration to healthy volunteers. *Clinical pharmacology : advances and applications*, *6*, 51-59. doi: 10.2147/CPAA.S47895
- Naito, A. T., Shiojima, I., Akazawa, H., Hidaka, K., Morisaki, T., Kikuchi, A., et al. (2006). Developmental stage-specific biphasic roles of Wnt/ β -catenin signaling in cardiomyogenesis and hematopoiesis. *Proceedings of the National Academy of Sciences*, *103*(52), 19812-19817. doi: 10.1073/pnas.0605768103
- Norman, D. A. M., Yacoub, M. H., & Barton, P. J. R. (1998). Nuclear factor NF-kappa B in myocardium: developmental expression of subunits and activation by interleukin-1 beta in cardiac myocytes in vitro. *Cardiovascular Research*, *39*, 434-441. doi: 10.1016/S0008-6363(98)00118-7
- Novella, S., & Hermenegildo, C. (2011). Estradiol Regulation of Prostanoids Production in Endothelium.
- Nowbar, A. N., Mielewczik, M., Karavassilis, M., Dehbi, H.-M., Shun-Shin, M. J., Jones, S., et al. (2014). Discrepancies in autologous bone marrow stem cell trials and enhancement of ejection fraction (DAMASCENE): weighted regression and meta-analysis. *BMJ : British Medical Journal*, *348*, g2688. doi: 10.1136/bmj.g2688
- Orsó, E., & Schmitz, G. (2017). Lipoprotein(a) and its role in inflammation, atherosclerosis and malignancies. *Clinical Research in Cardiology Supplements*, *12*(Suppl 1), 31-37. doi: 10.1007/s11789-017-0084-1
- Pagès, C., Simon, M.-F., Valet, P., & Saulnier-Blache, J. S. (2001). Lysophosphatidic acid synthesis and release. *Prostaglandins & Other Lipid Mediators*, *64*(1), 1-10. doi: [https://doi.org/10.1016/S0090-6980\(01\)00110-1](https://doi.org/10.1016/S0090-6980(01)00110-1)
- Perán, M., Marchal, J. A., López, E., Jiménez-Navarro, M., Boulaiz, H., Rodríguez-Serrano, F., et al. (2010). Human cardiac tissue induces transdifferentiation of adult stem cells towards cardiomyocytes. *Cytotherapy*, *12*(3), 332-337. doi: <https://doi.org/10.3109/14653240903548202>
- Phillips, T., & Hoopes, L. (2008). Transcription Factors and Transcriptional Control in Eukaryotic Cells. *Nature Education*, *1*(1), 119.
- Pramod, H. (2015). *Regulation of stem cell differentiation into cardiomyocytes by lysophosphatidic acid*. (PhD PhD), University of Hertfordshire.

- Rinkenbaugh, A. L., & Baldwin, A. S. (2016). The NF- κ B Pathway and Cancer Stem Cells. *Cells*, 5(2), 16. doi: 10.3390/cells5020016
- Schrör, K. (2016). *Pharmacology Acetylsalicylic Acid* (pp. 51-166): Wiley-VCH Verlag GmbH & Co. KGaA.
- Sheng, X., Yung, Y. C., Chen, A., & Chun, J. (2015). Lysophosphatidic acid signalling in development. *Development*, 142(8), 1390-1395. doi: 10.1242/dev.121723
- Stark, L. A., Din, F. V., Zwacka, R. M., & Dunlop, M. G. (2001). Aspirin-induced activation of the NF- κ B signaling pathway: a novel mechanism for aspirin-mediated apoptosis in colon cancer cells. *The FASEB Journal*, 15(7), 1273-1275.
- Sultana, N., Zhang, L., Yan, J., Chen, J., Cai, W., Razzaque, S., et al. (2015). Resident c-kit(+) cells in the heart are not cardiac stem cells. *Nature Communications*, 6, 8701-8701. doi: 10.1038/ncomms9701
- Sun, X., Chen, E., Dong, R., Chen, W., & Hu, Y. (2015). Nuclear factor (NF)- κ B p65 regulates differentiation of human and mouse lung fibroblasts mediated by TGF- β . *Life Sciences*, 122, 8-14. doi: <https://doi.org/10.1016/j.lfs.2014.11.033>
- Takahashi, K., & Yamanaka, S. (2006). Induction of Pluripotent Stem Cells from Mouse Embryonic and Adult Fibroblast Cultures by Defined Factors. *Cell*, 126(4), 663-676. doi: <https://doi.org/10.1016/j.cell.2006.07.024>
- Takase, O., Yoshikawa, M., Idei, M., Hirahashi, J., Fujita, T., Takato, T., et al. (2013). The Role of NF- κ B Signaling in the Maintenance of Pluripotency of Human Induced Pluripotent Stem Cells. *PLoS ONE*, 8(2), e56399. doi: 10.1371/journal.pone.0056399
- Townsend, N., Wilson, L., Bhatnagar, P., Wickramasinghe, K., Rayner, M., & Nichols, M. (2016). Cardiovascular disease in Europe: epidemiological update 2016. *European Heart Journal*, 37(42), 3232-3245. doi: 10.1093/eurheartj/ehw334
- Tranter, M., Ren, X., Forde, T., Wilhide, M. E., Chen, J., Sartor, M. A., et al. (2010). NF- κ B driven cardioprotective gene programs; Hsp70.3 and cardioprotection after late ischemic preconditioning. *Journal of molecular and cellular cardiology*, 49(4), 664-672. doi: 10.1016/j.yjmcc.2010.07.001
- Ueno, S., Weidinger, G., Osugi, T., Kohn, A. D., Golob, J. L., Pabon, L., et al. (2007). Biphasic role for Wnt/ β -catenin signaling in cardiac specification in zebrafish and embryonic stem cells. *Proceedings of the National Academy of Sciences*, 104(23), 9685-9690. doi: 10.1073/pnas.0702859104
- van der Heyden, M. A. G., & Defize, L. H. K. (2003). Twenty one years of P19 cells: what an embryonal carcinoma cell line taught us about cardiomyocyte

differentiation. *Cardiovascular Research*, 58(2), 292-302. doi: 10.1016/S0008-6363(02)00771-X

Vartiainen, N., Goldsteins, G., Keksa-Goldsteine, V., Chan Pak, H., & Koistinaho, J. (2003). Aspirin Inhibits p44/42 Mitogen-Activated Protein Kinase and Is Protective Against Hypoxia/Reoxygenation Neuronal Damage. *Stroke*, 34(3), 752-757. doi: 10.1161/01.STR.0000057813.31798.1F

Wang, L., Wu, J., Zhang, W., Zhi, Y., Wu, Y., Jiang, R., et al. (2013). Effects of aspirin on the ERK and PI3K/Akt signaling pathways in rats with acute pulmonary embolism. *Mol Med Rep*, 8(1), 1465-1471.

Wen, J., Ribeiro, R., & Zhang, Y. (2011). Specific PKC isoforms regulate LPS-stimulated iNOS induction in murine microglial cells. *Journal of neuroinflammation*, 8, 38-38. doi: 10.1186/1742-2094-8-38

Willey, S., Ayuso-Sacido, A., Zhang, H., Fraser, S. T., Sahr, K. E., Adlam, M. J., et al. (2006). Acceleration of mesoderm development and expansion of hematopoietic progenitors in differentiating ES cells by the mouse Mix-like homeodomain transcription factor. *Blood*, 107(8), 3122-3130. doi: 10.1182/blood-2005-10-4120

Xiao, Y., Chen, Y., Kennedy, A. W., Belinson, J., & Xu, Y. A. N. (2000). Evaluation of Plasma Lysophospholipids for Diagnostic Significance Using Electrospray Ionization Mass Spectrometry (ESI-MS) Analyses. *Annals of the New York Academy of Sciences*, 905(1), 242-259. doi: 10.1111/j.1749-6632.2000.tb06554.x

Young-Eun, K., It, sup, gt, It, sup, et al. (2008). Upregulation of NF- κ B upon differentiation of mouse embryonic stem cells. *BMB Rep.*, 41(10), 705-709.

Yu, J., & Thomson, J. A. (2008). Pluripotent stem cell lines. *Genes & Development*, 22(15), 1987-1997. doi: 10.1101/gad.1689808

Zhang, Y., Liu, J., Yao, S., Li, F., Xin, L., Lai, M., et al. (2012). Nuclear factor kappa B signaling initiates early differentiation of neural stem cells. *Stem Cells*, 30(3), 510-524. doi: 10.1002/stem.1006

Zhao, S., Xu, Z., Wang, H., Reese, B. E., Gushchina, L. V., Jiang, M., et al. (2016). Bioengineering of injectable encapsulated aggregates of pluripotent stem cells for therapy of myocardial infarction. *Nature Communications*, 7, 13306. doi: 10.1038/ncomms13306